

NOISE OPTIMIZATION TECHNIQUES FOR LINEAR
TRANSISTOR AMPLIFIERS

Thesis by
Aldo Gene DiLoreto

In Partial Fulfillment of the Requirements
For the Degree of
Doctor of Philosophy

California Institute of Technology
Pasadena, California

1962

ACKNOWLEDGMENTS

The author is particularly grateful to Dr. R. D. Middlebrook for his guidance and continual encouragement in the preparation and completion of this work. Gratitude is also extended to Drs. H. Martel and C. Wilts for their assistance in the preparation of the final text.

Personnel of R. C. A. Laboratories, Raytheon, and Telefunken generously donated the transistors used in this investigation; Aerojet-General Corporation loaned the test equipment used in the low-frequency studies. Appreciation is expressed to them for this invaluable assistance.

Thanks are also due the Naval Ordnance Test Station for financial aid and use of the test equipment required to perform the high-frequency studies, to Lloyd Maudlin who was instrumental in obtaining this aid, and to Mrs. Anna A. Haynes for her typing skills.

ABSTRACT

Methods of minimizing the effects of internally generated noise in transistor amplifiers are described. The study is both theoretical and experimental in nature, the greater part of the theoretical portion being based on van der Ziel's transistor noise model. From this model, analytical expressions are formulated giving (in terms of easily measurable transistor parameters) the operating point and source resistance that will optimize the noise performance of the amplifier. The derived equations are substantiated by an experimental study. Both audio and radio frequency amplifiers are considered. At audio frequencies, the work is primarily experimental in nature. Here, attention is focused on developing a simplified optimization procedure. For the radio frequency amplifier, formulas are also derived that describe the effect of source reactance on the amplifier's noise performance.

Formulas giving the noise figures of the transformer-coupled transistor amplifier are included. From these equations, analytical expressions are formulated that describe the emitter current and transformer turns ratio which will minimize the effects of internally generated noise. An experimental investigation verified the results.

A portion of the work is devoted to a theoretical and experimental study of temperature and its effect on the noise performance of transistor amplifiers. This study, which considers temperatures from 77 to 320°K, differs from those previously conducted in that a wide range of source resistances are used.

Equations describing the degradation in noise performance produced by resistive stabilizing components are given.

Also included is an analytical description of the methods used to obtain noise-factor measurements.

TABLE OF CONTENTS

| | PAGE |
|---|------|
| INTRODUCTION | 1 |
| Concept of Noise Performance | 3 |
| Definitions of Noise Performance | 4 |
| Optimum Noise Performance | 7 |
| The Optimization Problem | 9 |
| Explicit Parameter Dependence | 11 |
| Effect of Source Impedance on Noise Performance | 11 |
| Frequency Dependence of Noise Factor Parameters | 15 |
| Brief Resume of the Remaining Controllable and Uncontrollable Parameters | 18 |
| Example of an Optimization Problem | 19 |
| The Three Frequency Regions | 23 |
| A BRIEF DESCRIPTION OF THE THESIS | 25 |
| Mean Frequency Region | 25 |
| 1/f Frequency Region | 25 |
| High Frequency Region | 26 |
| Transformer Coupling | 27 |
| Temperature | 27 |
| Emitter Degeneration, Bias Stabilization | 27 |
| Load Resistance and Multistaging | 27 |
| Measuring Methods | 28 |
| 1. MEAN-FREQUENCY REGION | 29 |
| Mean-Frequency Noise Model | 30 |
| Common-Base and Common-Emitter Amplifiers | 32 |
| Common-Collector Amplifier | 35 |
| Experimental Measurements | 36 |
| Source Resistance as an Uncontrollable Parameter | 37 |
| Equivalent Noise Resistance | 41 |
| Collector Voltage and Its Effects on Mean-Frequency Noise Performance | 41 |
| Conclusions | 44 |
| 2. 1/f FREQUENCY REGION | 48 |
| 1/f and Transition-Frequency Noise Models | 51 |
| Simplified Optimization Procedure | 59 |
| Experimental Confirmation of Simplified Method | 62 |
| Source Resistance as an Uncontrollable Parameter | 73 |
| The Collector Voltage as an Optimization Parameter | 76 |
| Conclusions | 76 |

| | PAGE |
|--|------|
| 3. HIGH FREQUENCY REGION | 79 |
| van der Ziel's Noise Model | 80 |
| Common-Base and Common Emitter Amplifier | 82 |
| Common-Collector Transistor Amplifier | 89 |
| Experimental Technique | 91 |
| Conclusions | 96 |
| 4. TRANSFORMER COUPLING | 97 |
| Transformer-Coupled Common-Base and Common-Emitter Amplifier | 97 |
| Transformer-Coupled Common-Collector Amplifier | 101 |
| Experimental Verification of the Derived Results | 101 |
| 5. TEMPERATURE. | 106 |
| Experimental Study | 106 |
| Mean-Frequency Theoretical Study | 111 |
| Conclusions | 119 |
| 6. BIAS STABILIZATION AND Emitter DEGENERATION | 120 |
| Effect of Bias Stabilization on Noise Performance of Transistor Amplifier | 120 |
| Emitter Degeneration | 123 |
| Conclusions | 125 |
| 7. LOAD RESISTANCE AND MULTISTAGING | 126 |
| Effect of Load Resistance on Noise Performance | 126 |
| Multistaging | 128 |
| 8. MEASURING METHODS | 131 |
| Transistor Noise Factor Measurements | 131 |
| Continuous-Wave Method | 131 |
| Noise Injection Method | 133 |
| Effects of Equipment Noise on Noise Factor Measurements | 135 |
| Indicating Device Error | 138 |
| 9. CONCLUSIONS | 141 |
| APPENDIX | 145 |

INTRODUCTION

In the 14 years that have elapsed since the development of the first experimental transistors, several investigations have been conducted in an effort to formulate models that would describe the mean-square magnitude of noise fluctuations observed at the output terminals of a semiconductor diode or transistor. Owing to the spectral character of the observed noise, universal models have not yet been forthcoming. However, van der Ziel (Ref. 1) and Guggenbuehl (Ref. 2), utilizing results obtained by Johnson (Ref. 3) and Schottky (Ref. 4), independently formulated equations that describe (for a limited portion of the frequency spectrum) the mean-square magnitude of fluctuations produced by current flow across a semiconductor diode junction. The diode equations were later extended by van der Ziel to include the effect of random diffusion and recombination-regeneration which occurs in the base region of a semiconductor triode.

Van der Ziel's triode model, while subject to restrictions not often met in design practice (and restricted to the frequency region where $1/f$ noise can be neglected) forms a basis from which operating parameters can be found that will minimize the effects of internally generated amplifier noise.

The triode model has been extensively used in other experimental investigations. These studies, however, were conducted primarily to corroborate the validity of the model. In this dissertation the model is assumed valid. Here, analytical expressions are formulated that describe parameters which will minimize the effects of transistor amplifier noise. The problem involves:

Formulating equations that describe the source resistance and emitter current that will minimize the effect of noise in the unconstrained amplifier.

Formulating equations that describe the optimum emitter current in an amplifier constrained by a fixed-source resistance.

Formulating equations that describe the optimum turns ratio and emitter current in a transformer-coupled amplifier.

Formulating equations that describe the effect of source reactance on the high-frequency amplifier.

Formulating equations that describe the effect of temperature on the noise performance of the amplifier.

Formulating equations that describe the degradation in noise performance produced by resistive stabilizing components.

At low audio frequencies, the spectral density of the noise observed at the output terminals of a transistor amplifier follows a phenomenological inverse frequency dependence. This noise, called $1/f$ or excess noise, is caused by a yet-undetermined surface phenomenon. Hence, an analytical model that accounts for the mean-square magnitude of the observed noise has not been formulated. However, Fonger (Ref. 5) in his investigation of excess noise proposes an empirical noise model for the transistor amplifier in which each of the noise generators contained in the model has a mean-square value, K_n/f . Each of the constants but one is determined from direct current transistor measurements; the last constant is obtained from a noise measurement. The measurement technique required to fix values to the constants contained in Fonger's model renders it unwieldy as a tool for obtaining operating-point parameters (e.g., emitter current, source resistance) that will minimize the effect

of $1/f$ noise in a transistor amplifier). It does become possible, however, with the assumption that the noise sources contained in the amplifier have a $1/f$ frequency dependence, and with the further assumption that the noise sources are not functions of the driving-point impedance, to obtain optimization parameters from a limited number of noise measurements.

Yajimi (Ref. 6), utilizing the results of both Fonger and van der Ziel, has developed an empirical noise model for the predominant $1/f$ noise generator. From the results of an experimental investigation contained in this dissertation, it was found that Yajimi's model can be used to obtain an optimization procedure whereby the values of emitter current and source resistance which will minimize the effect of $1/f$ noise can be obtained from a single small-signal transistor measurement.

CONCEPT OF NOISE PERFORMANCE

A linear amplifier is a device used to obtain a power-amplified linear representation of a time-varying input signal. Owing to the spectral properties of the input waveform and the noise processes inherent in the device, it is impossible to obtain perfect fidelity from a realizable amplifier. This becomes apparent when these spectral and noise properties are considered. Since information is contained in the input signal, a transformation from the time to the frequency domain reveals that the signal is dispersed over a range of frequencies, and the amplifier must have a bandwidth including these frequencies in order to reproduce this waveform. Inherent in the active and resistive components of the device are noise voltages whose magnitudes are functions of the bandwidth of the amplifier. Statistical distortion, resulting from this noise, prevents a perfect reproduction of the input waveform from appearing at the output. A measure of this distortion is the signal-to-noise (S/N) ratio, which

determines the maximum sensitivity of the amplifier and also describes its noise performance.

DEFINITIONS OF NOISE PERFORMANCE

The output signal-to-noise ratio is a function of (1) the noise generated in the driving source impedance, and (2) the noise generated in the amplifier. North (Ref. 7), recognizing the need for a figure which was a basic measure of the noise generated in the amplifier, introduced the concept of noise factor. Friis (Ref. 8), in a later paper, defines the noise factor F as the ratio of the available signal-to-noise power that is measured at the source to the amplifier to the available signal-to-noise power that is measured at the output. Or, in symbolic form,

$$F = \frac{(S/N)_{as}}{(S/N)_{ao}} \quad (1)$$

It is implicit, from Friis's definition, that conjugate matching is required at both the input and output terminals of an amplifier when noise factor measurements are made. Since stringent implementation of conjugate matching is impossible when wide-band measurements are attempted (due to reactive components existing at the input and output terminals of the amplifier), it becomes necessary to introduce a second definition for the noise factor. This definition removes the restriction of conjugate matching and is written

$$F = \frac{(S/N)_s}{(S/N)_o} \quad (2)$$

Although equations 1 and 2 differ in notation, implementation, and can differ in the noise figures obtained by their use, they are often used

inter-changeably in the literature. The anomaly that exists between Friis's definition and equation 2 can be removed if the frequencies influencing a noise factor measurement are limited by bandpass circuits to an incremental portion of the frequency spectrum. This concept results in a third figure for F called the spot noise factor. In equation form, the spot noise factor is written

$$F = \left. \frac{(S/N)_{as}}{(S/N)_{ao}} \right|_{\Delta f} \quad (3a)*$$

$$= \left. \frac{(S/N)_s}{(S/N)_o} \right|_{\Delta f} \quad (3b)*$$

All the measurements contained in this dissertation are spot noise measurements. Unless otherwise specified, the term "noise factor" whenever used will imply spot noise factor.

With the concept of spot noise factor defined, it now becomes possible to obtain, in equation form, a figure which describes the noise factor of the wide-band amplifier. This becomes

$$\bar{F} = \frac{\int_0^{\infty} F(f)G(f)df}{\int_0^{\infty} G(f)df} \quad (4)$$

where $F(f)$ is the spot noise factor and $G(f)$ is the power gain of the amplifier, and \bar{F} is a fourth figure called the average noise factor. In practical applications, equation 4 is solved by numerical integration.

*A proof which shows the equivalence of equations 3a and 3b is contained in the appendix.

Two other parameters frequently used to describe an amplifier's noise performance are the noise temperature T_a and the equivalent noise resistance R_{eq} . Equations that define these parameters can be derived if all the noise sources contained in the amplifier are grouped into one voltage generator e_{na} , placed in series with the driving source impedance. With this configuration, the noise factor becomes

$$F = \frac{\overline{e_{ns}^2} + \overline{e_{na}^2}}{\overline{e_{ns}^2}} \quad (5)$$

where $\overline{e_{ns}^2}$ represents the mean-square value of noise from the driving source impedance. If a resistive source in thermal equilibrium is assumed, this quantity becomes

$$\overline{e_{ns}^2} = 4kT_s R_s B \quad (6a)$$

Here, k is Boltzmann's constant; T_s is the absolute temperature of the source in degrees Kelvin, and B is the noise bandwidth of the amplifier.

The noise bandwidth is defined by

$$B = \frac{\int_0^\infty |A(f)|^2 df}{|A_0|^2} \quad (6b)$$

where A_0 is the mid-frequency voltage gain of the amplifier.

The amplifier noise temperature is defined by

$$\overline{e_{na}^2} = 4kT_a R_s B \quad (7)$$

and becomes, from equations 5, 6, and 7

$$T_a = (F-1)T_s \quad (8)$$

The equivalent noise resistance of the amplifier is defined by

$$\overline{e_{na}^2} = 4kT_s R_{eq} B \quad (9a)$$

and becomes, from equations 5, 6, and 9a

$$R_{eq} = (F-1)R_s \quad (9b)$$

Although the noise temperature is often used to describe the noise performance of the maser and parametric amplifier, it is seldom used as a noise parameter for amplifiers in which the active device in the input stage is a vacuum tube or a transistor. The equivalent noise resistance is frequently used to specify the noise performance of the vacuum tube amplifier. However, it is found that the noise factor lends itself more readily to the transistor amplifier optimization problem; for this reason, it is on this noise parameter that attention is focused here.

OPTIMUM NOISE PERFORMANCE

The noise factor as defined by equation 2 can also be written in the form

$$(S/N)_o = \frac{(S/N)_s}{F} \quad (10)$$

It is apparent from equation 10 that the problem of optimizing the noise performance of an amplifier, which entails maximizing the signal-to-noise ratio at the output, is in fact twofold. It consists of maximizing the signal-to-noise ratio of the source, and it entails minimizing the noise factor.

To determine when the signal-to-noise ratio of the source and the noise factor can be optimized separately, equation 10 is differentiated. This yields

$$d(S/N)_o = \frac{\partial(S/N)_o}{\partial F} dF + \frac{\partial(S/N)_o}{\partial(S/N)_s} d(S/N)_s \quad (11)$$

It is found, from equation 11, that optimum noise performance requires that

$$dF = d(S/N)_S = 0 \quad (12)$$

However, F and $(S/N)_S$ may each be functions of several controllable and uncontrollable parameters,* e.g.,

$$F = \phi_1(p_1, p_2, \dots, p_n, q_1, \dots, q_m) \quad (13a)$$

$$(S/N)_S = \phi_2(p_{n+1}, \dots, p_r, q_1, \dots, q_m) \quad (13b)$$

Total differentiation of these two equations yields

$$dF = \underbrace{\frac{\partial F}{\partial p_1} dp_1 + \dots + \frac{\partial F}{\partial p_i} dp_i + \frac{\partial F}{\partial q_1} dq_1 + \dots + \frac{\partial F}{\partial q_j} dq_j}_{\text{Controllable Parameters}}$$

$$+ \underbrace{\frac{\partial F}{\partial p_{i+1}} dp_{i+1} + \dots + \frac{\partial F}{\partial p_n} dp_n + \frac{\partial F}{\partial q_{j+1}} dq_{j+1} + \dots + \frac{\partial F}{\partial q_m} dq_m}_{\text{Uncontrollable Parameters}} \quad (14a)$$

$$d(S/N)_S = \underbrace{\frac{\partial(S/N)_S}{\partial p_{n+1}} dp_{n+1} + \dots + \frac{\partial(S/N)_S}{\partial p_k} dp_k + \frac{\partial(S/N)_S}{\partial q_1} dq_1 + \dots + \frac{\partial(S/N)_S}{\partial q_j} dq_j}_{\text{Controllable Parameters}}$$

$$+ \underbrace{\frac{\partial(S/N)_S}{\partial p_{k+1}} dp_{k+1} + \dots + \frac{\partial(S/N)_S}{\partial p_r} dp_r + \frac{\partial(S/N)_S}{\partial q_{j+1}} dq_{j+1} + \dots + \frac{\partial(S/N)_S}{\partial q_m} dq_m}_{\text{Uncontrollable Parameters}} \quad (14b)$$

*A controllable parameter is one over which the designer can exert an influence, e.g., operating point and configuration. Conversely, an uncontrollable parameter is one over which the designer can exert no influence, e.g., frequency and temperature.

It follows from equations 12, 14a, and 14b, since dF must be zero for independent parameter variations, that optimum noise performance requires

$$\frac{\partial F}{\partial p_1} = \dots = \frac{\partial F}{\partial p_1} = \frac{\partial F}{\partial q_1} = \dots = \frac{\partial F}{\partial q_j} = 0 \quad (15a)$$

$$\frac{\partial \left(\frac{S}{N}\right)_S}{\partial p_{n+1}} = \dots = \frac{\partial \left(\frac{S}{N}\right)_S}{\partial p_k} = \frac{\partial \left(\frac{S}{N}\right)_S}{\partial q_1} = \dots = \frac{\partial \left(\frac{S}{N}\right)_S}{\partial q_j} = 0 \quad (15b)$$

Equations 15a and 15b show that if the signal-to-noise ratio of the source and the noise factor are both functions of the same controllable parameters, $q_1 \dots q_j$, the signal-to-noise ratio of the source and the noise factor can be separately optimized only if the optimum values of $q_1 \dots q_j$ will both minimize F and maximize $(S/N)_S$. One frequently encountered, mutually dependent, controllable parameter is the source resistance, R_s . In general, the same value of R_s will not simultaneously minimize F and maximize $(S/N)_S$. However, in this case, it becomes possible to interpose a transformer between the driving source and the input to the amplifier that will satisfy the constraint imposed by equations 15a and 15b.

THE OPTIMIZATION PROBLEM

In this dissertation, the large class of sources which permit a subdivision of the optimization problem is considered. It is assumed that the signal-to-noise ratio of the source has been maximized; optimization now entails minimizing the noise factor. Those controllable and uncontrollable parameters to be considered as influencing the noise performance

are as follows:

1. Operating Voltage, V
2. Operating Current, I
3. Configuration, C
4. Source Resistance, R_s
5. Frequency, f
6. Temperature, T

As an implicit function of these parameters, the noise factor F may be written

$$F = \phi_1(V, I, C, R_s, f, \text{ and } T) \quad (16a)$$

and the noise factor total differential dF is then

$$dF = \underbrace{\frac{\partial F}{\partial V} dV + \frac{\partial F}{\partial I} dI + \frac{\partial F}{\partial C} dC + \frac{\partial F}{\partial R_s} dR_s}_{\text{Controllable Parameters}}$$

$$+ \underbrace{\frac{\partial F}{\partial f} df + \frac{\partial F}{\partial T} dT}_{\text{Uncontrollable Parameters}} \quad (16b)$$

The solution to the amplifier optimization problem entails finding the circuit and operating point parameters that concurrently satisfy

$$\frac{\partial F}{\partial V} = 0 \quad (17a)$$

$$\frac{\partial F}{\partial I} = 0 \quad (17b)$$

$$\frac{\partial F}{\partial C} = 0 \quad (17c)$$

$$\frac{\partial F}{\partial R_s} = 0 \quad (17d)$$

EXPLICIT PARAMETER DEPENDENCE

Each of the four differentials contained in equations 17a, 17b, 17c, and 17d is an implicit function of the controllable and uncontrollable parameters V , I , C , R_s , f , and T . An explicit dependence is required for the general solution of the optimization problem. If it is assumed the statistical properties of the noise sources contained in an amplifier are not functions of the driving source impedance, Z_s , it is possible to formulate the noise factor of the amplifier as an explicit function of this parameter. This dependence is obtained in the following manner.

Effect of Source Impedance on Noise Performance

Part a of fig. 1 shows the amplifier to be analyzed. The equivalent circuit shown in Part b of fig. 1 is obtained by utilizing the results of Peterson's equivalence theorem.*

From Part b of fig. 1, the output open-circuited noise voltage becomes

$$e_{no} = e_{n2} + \frac{z_{21}(e_{ns} - e_{nl})}{Z_s + z_{11}} \quad (18)$$

From equation 18, the mean square noise voltage can be written

$$\overline{e_{no}^2} = \overline{e_{n2}^2} + \frac{|z_{21}|^2}{|z_{11} + Z_s|^2} \left(\overline{e_{ns}^2} + \overline{e_{nl}^2} \right) - 2R_e \left(\overline{e_{nl}^* e_{n2}} z_{21} / Z_s + z_{11} \right) \quad (19)$$

where $\overline{e_{nl}^* e_{n2}}$ is a measure of that cross correlation that exists between the two noise sources.

*The equivalence theorem (Ref. 9) states that the statistical properties of any linear noisy 4-pole can be represented by two noise generators and a noiseless 4-pole with identical transmission parameters.

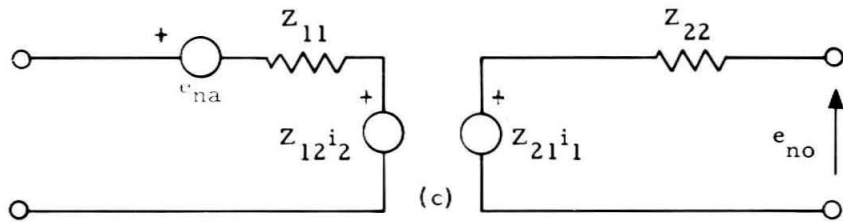
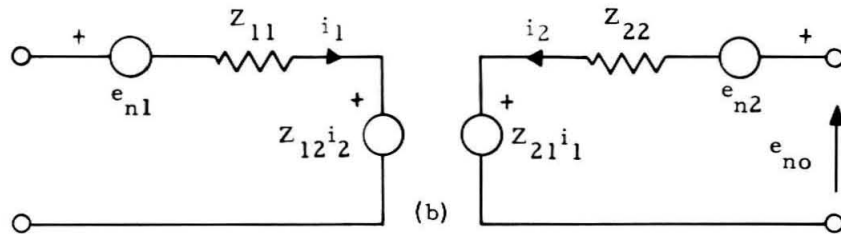
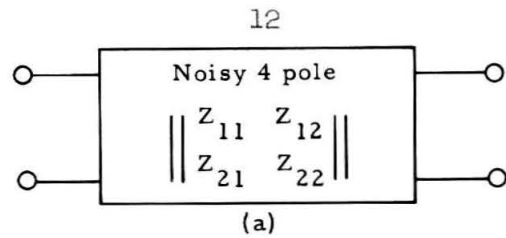


Figure 1. (a) Noisy 4 Pole, (b) Two Generator Equivalent Representation of Noisy 4 Pole, (c) One Generator Equivalent.

If it is assumed the driving source is in thermal equilibrium, the mean square source noise voltage becomes

$$\overline{e_{ns}^2} = 4kT R_e(Z_s) B \quad (20)$$

where $R_e(Z_s)$ signifies the real part of the driving source impedance.

From equations 2 and 20, the noise factor becomes

$$F = 1 + \frac{\overline{e_{nl}^2} + \overline{e_{n2}^2} + (z_{11} + Z_s)/z_{21}}{4kT R_e(Z_s) B} - \frac{\overline{R_e} \left[\overline{e_{nl}^* e_{n2}} (z_{11} + Z_s)/z_{21} \right]}{2kT R_e(Z_s) B} \quad (21)$$

Letting

$$r_{11} + jx_{11} = z_{11}$$

$$R_s + jX_s = Z_s$$

$$r_{21} + jx_{21} = z_{21}$$

$$c_r + jc_x = c = \frac{\overline{e_{n1}^* e_{n2}}}{\left(\overline{e_{n1}^2 e_{n2}^2}\right)^{1/2}}$$

Equation 21 then reads

$$F = 1 + \frac{\overline{e_{n1}^2}}{4kT R_s B} + \frac{\overline{e_{n2}^2} \left[(r_{11} + R_s)^2 + (x_{11} + x_s)^2 \right]}{4kT R_s B (r_{21}^2 + x_{21}^2)} - \frac{\left(\overline{e_{n1}^2 e_{n2}^2}\right)^{1/2}}{2kT R_s B (y_{21}^2 + x_{21}^2)}$$

$$\cdot \left\{ c_r \left[(r_{11} + R_s) r_{21} + (x_{11} + x_s) x_{21} \right] + c_x \left[(r_{11} + R_s) x_{21} - (x_{11} + x_s) r_{21} \right] \right\} \quad (22)$$

With the introduction of four noise factor parameters that are independent of the source impedance, equation 22 can be simplified to read

$$F = K_o + \frac{R_{no}}{R_s} \left(1 + \frac{k_1}{R_{no}} X_s + \frac{G_{nc}}{R_{no}} X_s^2 \right) + G_{nc} R_s \quad (23)$$

where, from equations 22 and 23, the newly defined noise factor parameters are quantified by

$$K_o = 1 + \frac{\overline{e_{n2}^2}}{2kT B} \frac{r_{11}}{r_{21}^2 + x_{21}^2} \left[1 - \left(\frac{\overline{e_{n1}^2}}{\overline{e_{n2}^2}} \right)^{1/2} \frac{c_r r_{21} + c_x x_{21}}{r_{11}} \right] \quad (23a)$$

$$R_{no} = \frac{1}{4kT B} \left\{ \overline{e_{n1}^2} + \overline{e_{n2}^2} \frac{(r_{11}^2 + x_{11}^2)}{(r_{21}^2 + x_{21}^2)} - 2 \frac{\left(\overline{e_{n1}^2 e_{n2}^2}\right)^{1/2}}{r_{21}^2 + x_{21}^2} \left[c_r (r_{11} r_{21} + x_{11} x_{21}) \right. \right. \\ \left. \left. + c_x (r_{11} x_{21} - x_{11} r_{21}) \right] \right\} \quad (23b)$$

$$G_{nc} = \frac{\overline{e_{n2}^2}}{4kT B (r_{21}^2 + x_{21}^2)} \quad (23c)$$

$$k_1 = \frac{1}{2kTB(r_{21}^2 + x_{21}^2)} \left[\frac{e_{n2}^2}{e_{n1}^2} x_{11} - \left(\frac{e_{n1}^2}{e_{n2}^2} \right)^{1/2} (c_r x_{21} - c_x r_{21}) \right] \quad (23d)$$

Equation 23 describes how the noise performance of any four-terminal network (subject to the restrictions previously imposed) can be expected to vary as a function of the resistive and reactive components of the driving source impedance. A quantitative analysis that includes more fully the effect of source reactance on the optimization problem is included in the text of the dissertation. At the present time, only that class of optimization problem in which X_s is zero is considered.

With this restriction, equation 23 simplifies to

$$F = k_o + \frac{R_{no}}{R_s} + G_{nc} R_s \quad (24)$$

It is found, from equation 24, that under any given set of operating conditions a source resistance exists which minimizes the noise factor of an amplifier. This value of source resistance, obtained by differentiating equation 24 with respect to R_s , becomes

$$R_{so} = \left(\frac{R_{no}}{G_{nc}} \right)^{1/2} \quad (25a)$$

Substitution into equation 24 gives for the minimum noise factor

$$F_{min} = k_o + 2(G_{nc} R_{no})^{1/2} \quad (25b)$$

Equation 25b forms a partial solution to the optimization problem in that it satisfies the constraint imposed by equation 17d. However, the magnitude of the three noise factor parameters k_o , R_{no} , and G_{nc} and hence the minimum noise factor are still implicit functions of the operating point, configuration, temperature, and frequency.

Frequency Dependence of Noise-Factor Parameters

The statistical properties of a noisy 4 pole with unilateral or bilateral transmission properties can also be described using the one generator noise model shown in part c of figure 1. However, now the noise voltage e_{na} shown in this figure is a function of the source impedance. Since the spectral properties of this generator have been determined experimentally (Ref. 11, 12, 13) and theoretically (Ref. 14, 15), it is from the one generator noise model that the spectral character of the noise-factor parameters is now obtained.

From an investigation of previous experimental and theoretical results, conducted with vacuum tube and transistor amplifiers, it is found that the mean-square noise voltage $\overline{e_{na}^2}$, as a function of frequency can be written

$$\overline{e_{na}^2}(f) = \overline{e_{na0}^2} \left[1 + \frac{f_1}{f} + \left(\frac{f}{f_2} \right)^2 \right] \quad (26)$$

Here, $\overline{e_{na0}^2}$ is the frequency independent source noise voltage and f_1 and f_2 are two corner frequencies defined by equation 26.

If a resistive source in thermal equilibrium is assumed, the noise factor becomes, from equations 2, 20, and 26

$$F(f) = 1 + \frac{\overline{e_{na0}^2}}{4kTR_s B} \left[1 + \frac{f_1}{f} + \left(\frac{f}{f_2} \right)^2 \right] \quad (27)$$

Experimental observations (contained in later context) reveal the two corner frequencies, f_1 and f_2 , as well as the noise voltage $\overline{e_{na0}^2}$ are functions of the source resistance. To remove the dependence contained in $\overline{e_{na}^2}(f)$ it is assumed that a frequency region exists at which

$$F_o = 1 + \frac{\overline{e_{na0}^2}}{4kTR_s B} \quad (28)$$

It follows, from equation 24, that the noise factor can also be written in the form

$$F_o = K_{oo} + \frac{R_{noo}}{R_s} + G_{nco} R_s \quad (29)$$

where K_{oo} , R_{noo} , and G_{nco} are the frequency-independent noise-factor parameters.

From equations 28 and 29, $\overline{e_{nao}^2}$ as an explicit function of source resistance becomes

$$\overline{e_{nao}^2} = 4kTB \left[K_{oo}^1 R_s + R_{noo} + G_{nco} R_s^2 \right] \quad (30)$$

where $K_{oo}^1 = K_{oo} - 1$.

It follows, from equations 27 and 30, that the noise factor can be written in the form

$$F(f) - 1 = \left(K_{oo}^1 + \frac{R_{noo}}{R_s} + G_{nco} R_s \right) \left[1 + \frac{f_1}{f} + \left(\frac{f}{f_2} \right)^2 \right] \quad (31)$$

However, an implicit source resistance dependence is still contained in the two corner frequencies f_1 and f_2 . This can be removed in the following manner. It is observed, in equation 31, that as the source resistance approaches zero, the noise factor becomes

$$F(f) - 1 = \frac{R_{noo}}{R_s} \left\{ 1 + \frac{f_1(R_s \rightarrow 0)}{f} + \left[\frac{f}{f_2(R_s \rightarrow 0)} \right]^2 \right\} \quad (32a)$$

and as the source resistance approaches an infinite value

$$F(f) - 1 = G_{nco} R_s \left\{ 1 + \frac{f_1(R_s \rightarrow \infty)}{f} + \left[\frac{f}{f_2(R_s \rightarrow \infty)} \right]^2 \right\} \quad (32b)$$

Finally, with the source resistance R_s equal to its optimum value R_{so} , the noise factor becomes, from equations 25a, 25b, and 31

$$F(f) - 1 = \left[k_{\text{oo}} + 2(R_{\text{noo}} G_{\text{nco}})^{1/2} \right] \left\{ 1 + \frac{f_1(R_s = R_{\text{so}})}{f} + \left[\frac{f}{f_2(R_s = R_{\text{so}})} \right]^2 \right\} \quad (32c)$$

It follows, from equations 31, 32a, 32b, and 32c, that six corner frequencies are required to express the source resistance dependence contained in f_1 and f_2 . With the introduction of these corner frequencies, the noise factor as an explicit function of both frequency and source resistance becomes

$$\begin{aligned} F(f) - 1 = & K_{\text{oo}} \left[1 + \frac{f_3}{f} + \left(\frac{f}{f_4} \right)^2 \right] + R_{\text{noo}} \left[1 + \frac{f_5}{f} + \left(\frac{f}{f_6} \right)^2 \right] \\ & + G_{\text{nco}} \left[1 + \frac{f_7}{f} + \left(\frac{f}{f_8} \right)^2 \right] \end{aligned} \quad (33)$$

where the six new corner frequencies are given by the equations

$$f_3 = f_1 \left[R_s = R_{\text{so}} \right] \left\{ 1 + \frac{2(R_{\text{noo}} G_{\text{nco}})^{1/2}}{K_{\text{oo}}} \left[1 - \frac{(f_5 f_7)^{1/2}}{f_1(R_s = R_{\text{so}})} \right] \right\} \quad (33a)$$

$$f_4 = f_1(R_s = R_{\text{so}}) \left\{ 1 + \frac{2(R_{\text{noo}} G_{\text{nco}})^{1/2}}{K_{\text{oo}}} \left[1 - \frac{(f_2(R_s = R_{\text{so}}))^2}{f_6 f_8} \right] \right\}^{-1/2} \quad (33b)$$

$$f_5 = f_1(R_s \rightarrow 0) \quad (33c)$$

$$f_6 = f_2(R_s \rightarrow 0) \quad (33d)$$

$$f_7 = f_1(R_s \rightarrow \infty) \quad (33e)$$

$$f_8 = f_2(R_s \rightarrow \infty) \quad (33f)$$

Equation 33 describes the noise performance of the transistor amplifier as an explicit function of both frequency and source resistance. However, the three noise-factor parameters (K_{oo} , R_{noo} , and G_{nco}) and the six corner frequencies ($f_3 \rightarrow f_8$) contained in this equation are implicit functions of the operating point, configuration, and temperature. To obtain an analytical solution to the optimization problem, this dependence must also be made explicit.

Brief Resume of the Remaining Controllable and Uncontrollable Parameters

The two parameters necessary to specify the operating point of the transistor amplifier are the collector voltage and the emitter current. However, experimental investigations reveal that, with normal biasing,* the magnitude of the collector voltage does not significantly influence the noise performance. Therefore, the only operating-point parameter that needs to be considered in the optimization problem is the emitter current, I_E .

To obtain the noise factor as an explicit function of the emitter current, the physical sources of noise that exist in the transistor structure are investigated. Theoretical studies reveal that, for frequencies where $1/f$ noise can be neglected, the mean-square noise currents found at the input and output of the transistor amplifier can be expressed as functions of the transistor's d.c. and small-signal parameters. As a result, expressions for the noise factor in which the emitter current is explicitly contained can be derived.

It is found that the noise performance of the transistor amplifier, when operated at $1/f$ frequencies, is a function of its surface rather than

*Forward biasing of the collector, as prescribed by Volkers and Pederson (Ref. 10), will be discussed in later context.

of its bulk properties. Because the bulk properties of the transistor determine its small-signal behavior, it is impossible to obtain a theoretical measure of the $1/f$ noise mechanism contained in this device from small-signal measurements. Hence, in this portion of the frequency spectrum, it becomes impossible to obtain the noise factor as an explicit function of the emitter current.*

An explicit configuration dependence is obtained by formulating the noise factor of the amplifier in each of its configurations.

To obtain an expression for the noise factor that is an explicit function of temperature, it is necessary first to formulate the temperature dependence of the d.c. and small-signal parameters contained in the theoretical noise model. The results of an experimental study (discussed later) reveal that, with the introduction of two empirical parameters, it is possible to obtain the desired noise-factor dependence.

The intent has been to show that, with the existing theory, it is possible to obtain an analytical solution to a large class of optimization problems. It was also intended to show that before an analytical solution can be obtained, the noise factor must first be made an explicit function of its controllable and uncontrollable parameters.

EXAMPLE OF AN OPTIMIZATION PROBLEM

It is worth while, at this juncture, to discuss one application of the results contained in the preceding section. The optimization problem considered is one in which the two controllable parameters are the amplifier's emitter current and the source resistance. The solution to the optimization

*Yajimi's collector noise model that contains an explicit emitter current dependence for one noise generator is discussed later.

problem entails finding the value of emitter current and the source resistance for which the differentials

$$\frac{\partial F}{\partial R_s} = 0 \quad (34a)$$

$$\frac{\partial F}{\partial I_E} = 0 \quad (34b)$$

From equation 33, the noise factor can also be written in the form

$$F(f) = K_o(f) + \frac{R_{no}(f)}{R_s} + G_{nc}(f)R_s \quad (35a)$$

Here,

$$K_o(f) = 1 + K_o'(f) \quad (35b)$$

Differentiating equation 35 with respect to the source resistance and equating the resulting differential to zero gives, for the optimum source resistance,

$$R_{so}(f) = \left[\frac{R_{no}(f)}{G_{nc}(f)} \right]^{1/2} \quad (36)$$

Substituting the value of the optimum source resistance given by equation 36 for the source resistance contained in equation 35 yields

$$F_{min}(f) = K_o(f) + 2 \left[R_{no}(f) G_{nc}(f) \right]^{1/2} \quad (37)$$

The minimum noise factor is a function of the emitter current. To complete the solution to the optimization problem, $F_{min}(f)$ is differentiated with respect to the emitter current and the resulting differential is equated to zero. This yields the optimal source resistance, $(R_{so})_o$, and the optimum emitter current that satisfy the constraints imposed by equations 34a and 34b. These two parameters are formulated later.

A fallacious method of optimization, and one commonly used, entails finding the optimum source resistance for one value of emitter current, and then optimizing I_E , assuming that R_{SO} remains constant. Figure 2 shows the results obtained by both the fallacious and the prescribed optimization procedures. The reason for the differences that exist between the two methods is that the optimum source resistance is an implicit function of the emitter current. This dependence is illustrated in figure 2.

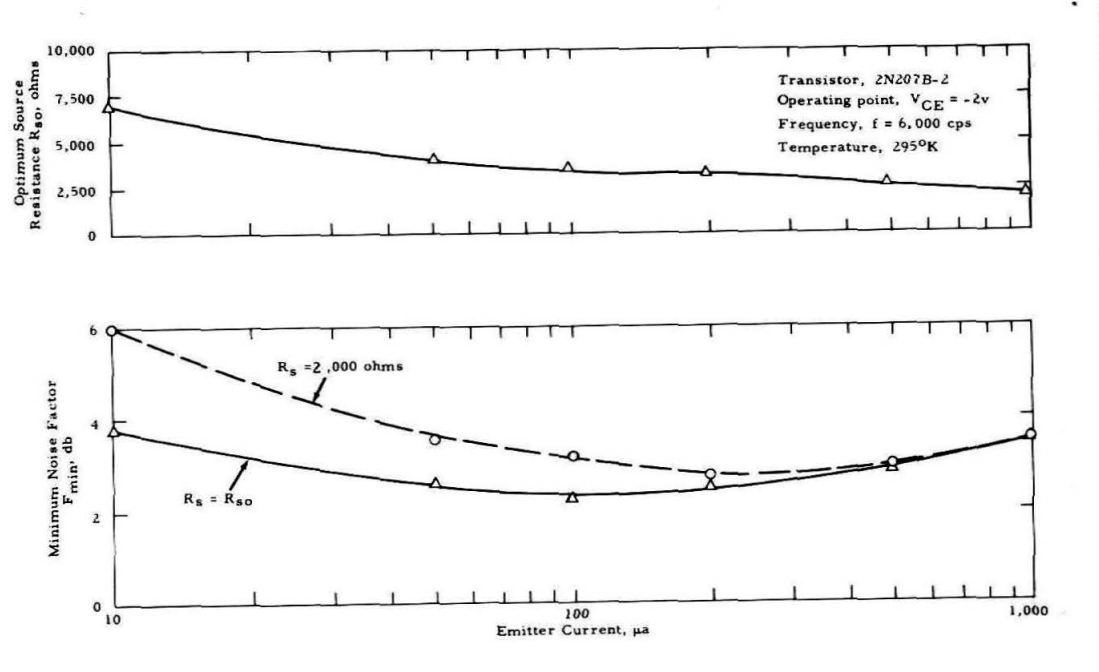


Figure 2. Noise Factor, Minimum Noise Factor and Optimum Source Resistance as a function of emitter current.

Figure 3, which applies to the same optimization problem, illustrates more graphically the emitter-current dependence contained in R_{SO} . This figure shows that, with an emitter current of $10\mu\text{a}$, $R_{SO} = 10,000$ ohms; while with an emitter current of $1,000\mu\text{a}$, $R_{SO} = 2,000$ ohms.

The solution to this optimization problem is again presented in figure 4. Here, the noise factor has been mapped in the emitter-current

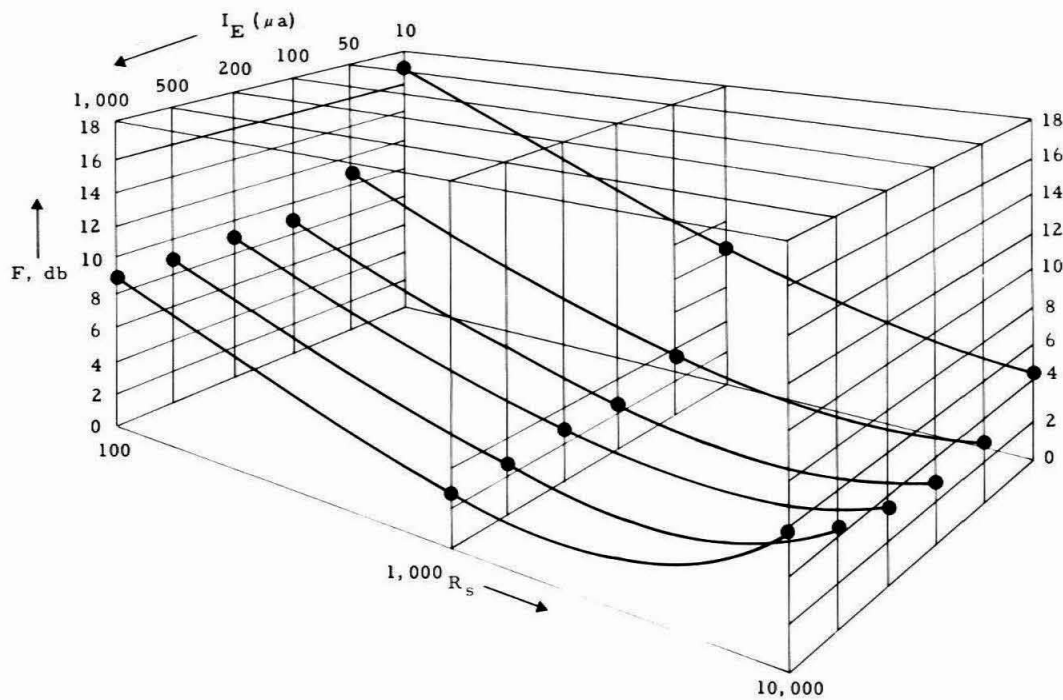


Figure 3. Noise Factor as Joint Function of Source Resistance and Emitter Current.

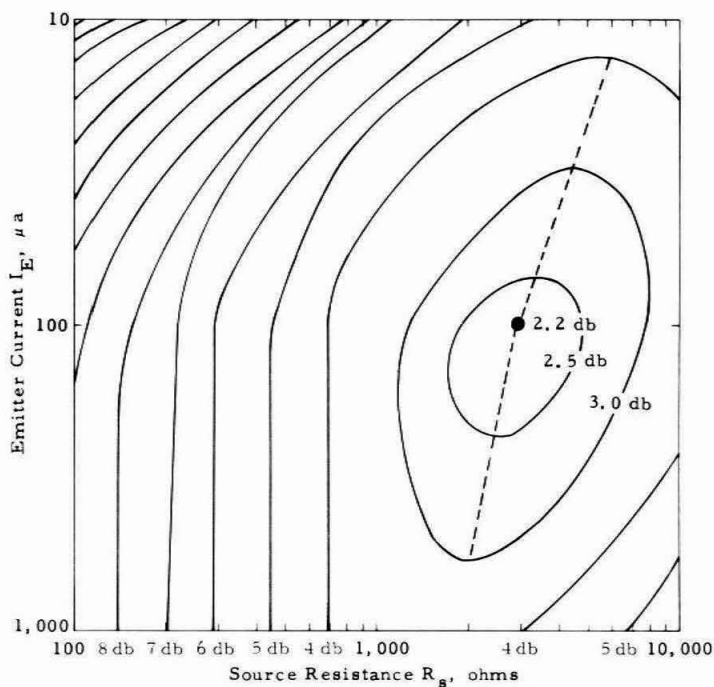


Figure 4. F Plotted in the Source Resistance-Emitter Current Plane.

source resistance plane. The contours depicted are each the locus of points, $F = \text{constant}$. It is easily shown, by writing the total differential of F , that for points on the contours that have zero slope,

$$R_s = R_{so}.$$

The trajectory contained in this figure is F_{\min} as a function of the emitter current. This trajectory again shows the emitter-current dependence contained in R_{so} .

From figures 2 and 4 it is found that there is a unique solution to the optimization problem in which the emitter current and the source resistance are controllable parameters.

THE THREE FREQUENCY REGIONS

It is apparent from equation 33 that there exist for both the transistor and vacuum-tube amplifier three frequency regions of interest. Since these regions are continually referred to in the context, they are defined at this time.

The $1/f$ region is defined to consist of those frequencies for which the noise factor, as given by equation 29, can be written in the form

$$F(f) - 1 = (F_o - 1) \frac{f_1}{f} \quad (38)$$

The mean-frequency noise region is defined to consist of those frequencies for which

$$F(f) = F_o \quad (39)$$

The f^2 region is defined to consist of those frequencies for which

$$F(f) - 1 = (F_o - 1) \left(\frac{f}{f_2} \right)^2 \quad (40)$$

Here,

$$F_o = K_o + \frac{R_{noo}}{R_s} + G_{noo} R_s \quad (41)$$

The frequencies between these regions are defined as transition frequencies. The frequency dependences of the noise factor in the lower and upper transition regions are

$$F(f) - 1 = (F_o - 1) \left(1 + \frac{f_1}{f} \right) \quad (42)$$

$$F(f) - 1 = (F_o - 1) \left[1 + \left(\frac{f}{f_2} \right)^2 \right] \quad (43)$$

The boundaries of each of these regions are functions of the source resistance. This dependence is illustrated in figure 5, which contains curves showing the spectral character of each of the frequency-dependent, noise-factor parameters contained in equation 35. It is found, from figure 5 and equation 35, that as the source resistance approaches an infinite value, the mean-frequency region is limited to the band $f = 30$ kc to $f = 200$ kc, while for small values of source resistance ($R_s \rightarrow 0$), the mean-frequency region extends from $f = 2,000$ cps to $f = 1$ mc.

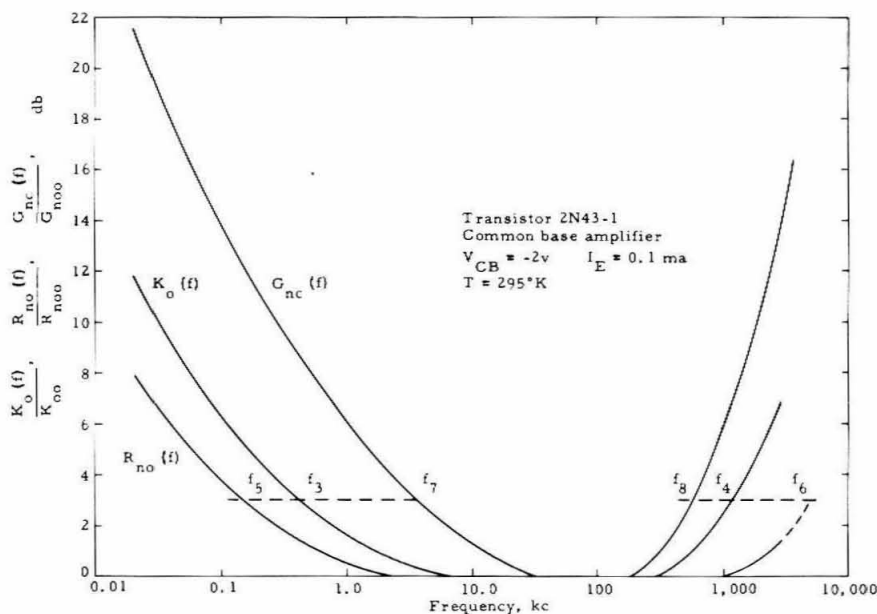


Figure 5. Normalized Noise Factor Parameters as a Function of Frequency.

A BRIEF DESCRIPTION OF THE THESIS

The following is a list of the chapters contained in the main body of the dissertation, along with a brief resume of the contents of each chapter.

MEAN-FREQUENCY REGION

With van der Ziel's noise model and the associated theory, it becomes possible to express the noise-factor parameters K_o^1 , R_{no} , and G_{nc} as explicit functions of the small-signal and d.c. transistor characteristics. As a result, analytical solutions to the optimization problems can be obtained in which the source resistance is an uncontrollable and a controllable parameter. In order to verify the theoretical results, noise measurements were made on a number of transistors, and the results are given in graphical form along with the predicted theoretical results. In general, the agreement is within a decibel.

1/f FREQUENCY REGION

This section begins with a discussion of Fonger's 1/f noise model. With this model and the associated theory as a basis, it is found that the noise-factor parameters have a frequency dependence given by

$$K_o^1(f) = K_{oo}^1 \frac{f_3}{f} \quad (44a)$$

$$R_{no}(f) = R_{noo} \frac{f_5}{f} \quad (44b)$$

$$G_{nc}(f) = G_{nco} \frac{f_7}{f} \quad (44c)$$

Utilizing equations 44a, 44b, and 44c and Peterson's equivalence theorem, it is found that in the lower transition region the frequency dependence of the noise factor parameters becomes

$$K_o^{-1}(f) = K_{oo}^{-1} \left(1 + \frac{f_3}{f} \right) \quad (44a)$$

$$R_{no}(f) = R_{noo} \left(1 + \frac{f_5}{f} \right) \quad (44e)$$

$$G_{nc}(f) = G_{nco} \left(1 + \frac{f_7}{f} \right) \quad (44f)$$

Equations 44a, 44e, and 44f form the basis of a simplified experimental solution to the optimization problem in which the source resistance and the emitter current are controllable parameters. Experimental corroboration is given of the derived theoretical results.

Also included in this study is an analytical solution to the optimization problem in which the emitter current is the only controllable parameter.

HIGH-FREQUENCY REGION

To obtain a solution to the high-frequency optimization problem in which the source resistance is the only controllable parameter, it is assumed that

$$\alpha(f) = \frac{\alpha_o}{1 + j f/f_c} \quad (45a)$$

$$y_e(f) = y_{eo} \left(1 + j f/f_c \right) \quad (45b)$$

Here, $\alpha(f)$, the common-base current gain, and $y_e(f)$, the emitter-junction admittance, are two parameters contained in van der Ziel's noise model.

The solution shows that, with the proper selection of the source resistance, it is possible to obtain reasonably low noise factors up to the α cutoff frequency, f_c . Experimental measurements corroborate the theoretical results. Also contained in this section is a theoretical study of the effect of source reactance on the high-frequency optimization problem.

TRANSFORMER COUPLING

The theoretical results obtained in section 1 reveal that a restriction is imposed on the value of the source resistance if the optimum noise performance is to be obtained. If R_s is not the correct value to satisfy the constraint imposed by theory, it becomes necessary to interpose a transformer between the driving source and the amplifier that will reconcile these differences. However, now there is a restriction on N , the turns ratio of the transformer. In this section, using simplifying assumptions as to the noise added by the transformer, the value for N is derived.

TEMPERATURE

This section contains an experimental and analytical study of the effect of temperature on the noise performance of the transistor amplifier. The temperatures considered range from 77 to 320°K .

EMITTER DEGENERATION, BIAS STABILIZATION

In this section the effects of these two stabilizing elements on the noise factor parameters are determined. It is assumed in making the derivations that only thermal noise is generated in these elements.

With simplifying assumptions as to the relative magnitude of these resistive components, it is possible to formulate in a convenient form the degradation produced by their presence in the circuit.

LOAD RESISTANCE AND MULTISTAGING

This section contains an analytical study of the effect of the load resistance of the first stage on the noise performance of the multistage amplifier. An expression for the noise factor of the multistage system is then derived.

MEASURING METHODS

An analytical description of the methods used in obtaining transistor noise factor measurements is presented. Also included is a method of determining whether noise in the measuring system is negligible.

1. MEAN-FREQUENCY REGION

The mean-frequency region, as related to transistor-noise generation, has been defined as that portion of the frequency spectrum where the statistical processes responsible for the noise generated in the transistor produce a power spectral density that is independent of frequency. Therefore, in the region to be considered, $1/f$ noise can be neglected. The noise processes remaining are

1. Equilibrium or Johnson noise generated by the random motion of the thermally excited, charged carriers
2. Non-equilibrium noise generated by the random diffusion and generation-recombination of the charged minority carriers in the active base region

Unlike $1/f$ noise which is a surface phenomenon, thermal, generation-recombination, and diffusion noise are characteristic of the transistor's bulk properties. Therefore, it is possible to formulate the statistical properties of the noise generated by these processes in terms of the small signal and D.C. transistor parameters.

Employing the theories of Guggenbuehl and van der Ziel that pertain to the mean-frequency region, it is possible to formulate an analytical solution to the problem that entails optimizing the noise performance of the transistor amplifier when both the source resistance and the emitter current are controllable parameters. It is also possible to formulate, in the mean-frequency region, an analytical solution to the optimization problem when the emitter current is the only controllable parameter.

MEAN-FREQUENCY NOISE MODEL

The mean-frequency model proposed by van der Ziel and Guggenbuehl consists of two current generators that describe the shot-noise fluctuations produced by a forward- and reverse-biased diode. Modifications are placed on the magnitude of these two noise sources to account for the zero-current thermal noise. Correlation between the two generators exists through the forward transconductance of the intrinsic transistor. A third noise source is placed in the base leg of the transistor to account for the thermal noise generated in the extrinsic base resistance $r_{b \parallel b}$. Part a of figure 6 depicts the equivalent "T" representation of the mean-frequency noise model. In this model, with the assumptions that

1. There is one-dimensional current flow in the active base region
2. Drift current is negligible in the active base region
3. Surface recombination is negligible

Van der Ziel found that the mean-square fluctuation contained in the input and output current could be described by

$$\overline{i_{nl}^2} = 4kT R_e B - 2eI_E B \quad (1-1a)$$

$$\overline{i_{n2}^2} = 4kT R_c B + 2eI_C B \quad (1-1b)$$

$$\overline{i_{nl}^* i_{n2}} = 2kT y_{eci} B = 2k\alpha y_e B \quad (1-1c)$$

$$\overline{e_{nb}^2} = 4kT r_{b \parallel b} B \quad (1-1d)$$

Part b of figure 6 depicts a simplified equivalent representation of the mean-frequency noise model. In this figure,

$$e_{ne} = i_{nl}/y_e \quad (1-2)$$

$$i_{nc} = i_{n2} - \alpha i_{nl} \quad (1-3)$$

In the simplified model, if it is assumed that

$$\mu v_{cb} = 0 \quad (1-4)$$

$$y_e = \frac{eI_E}{kT} \quad (1-5)$$

and

$$I_C = \alpha_0 I_E + I_{CO} \quad (1-6)$$

it follows, from equations 1-1a to 1-6, that the generators will have mean-square values given by

$$\overline{e_{ne}^2} = 2kTr_e B \quad (1-7a)$$

$$\overline{i_{nc}^2} = 2eI_E \alpha_0 (1-\alpha_0) B + 2eI_{CO} B \quad (1-7b)$$

$$\overline{e_{nb}^2} = 4kTr_{bb} B \quad (1-7c)$$

where r_e is the small-signal, emitter-junction resistance ($r_e = 1/y_e$).

The advantage of the simplified model is that the correlation that formerly existed between the two current noise sources (contained in the original model) is now zero, i.e., $\overline{e_{ne}^* i_{nc}} = 0$.

It is evident, from equations 1-7a to 1-7d, that the noise performance of the transistor amplifier can be expressed in terms of measurable d.c. and small-signal parameters. These parameters are

r_{bb} = the extrinsic base resistance

I_{CO} = the collector cutoff current

I_E = the emitter current

α_0 = the mean-frequency, common-base current gain

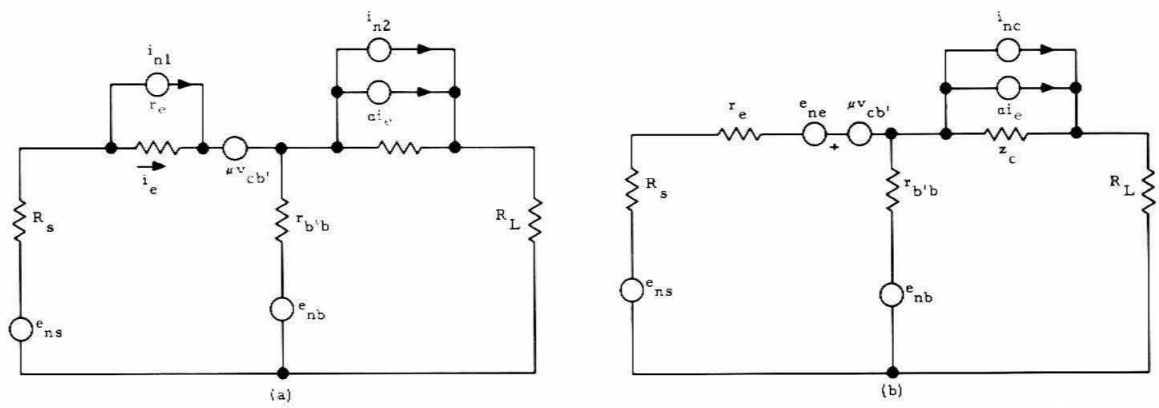


Figure 6. Representation of Transistor Mean-Frequency Noise Model: (a) Current Source i_{nl} in Parallel with r_e , (b) Voltage Source e_{ne} in Series with r_e .

COMMON-BASE AND COMMON-EMITTER AMPLIFIERS

It follows, from figure 1-2 and equations 1-7a to 1-7d, that the noise factor of the common-base amplifier is

$$F = 1 + \frac{r_e}{2R_s} + \frac{r_{b'b}}{R_s} + \frac{\left(\frac{i^2}{i_{nc}} |z_c|^2 + \frac{e^2}{e_{nb}} \right) (R_s + r_e + r_{b'b})^2}{4kT R_s B \alpha_o^2 |z_c + r_{b'b}/\alpha_o|^2} \quad (1-8)$$

For the common-emitter amplifier, the noise factor becomes

$$F = 1 + \frac{r_e}{2R_s} + \frac{r_{b'b}}{R_s} + \frac{\left(\frac{i^2}{i_{nc}} |z_c|^2 + \frac{e^2}{e_{ne}} \right) (R_s + r_e + r_{b'b})^2}{4kT R_s B \alpha_o^2 |z_c - \frac{r_e}{\alpha_o}|^2} \quad (1-9)$$

where $z_c = 1/y_c$.

At mean frequencies, under normal biasing conditions, the collector impedance, z_c , is usually greater than 100,000 ohms. Therefore, it is safe to assume that

$$z_c \gg r_{b'b}/\alpha_o \quad (1-10)$$

$$|z_c|^2 \gg \frac{2r_{b'b}r_e}{\alpha_o(1-\alpha_o)} \quad (1-11)$$

$$|z_c|^2 \gg \frac{2r_e^2}{\alpha_o(1-\alpha_o)} \quad (1-12)$$

From equations 1-8 to 1-12, the noise factor of the common-base and of the common-emitter transistor stage can now be written

$$F = 1 + \frac{r_e/2 + r_{b'b}}{R_s} + \frac{1}{2\beta r_e R_s} (1 + F) (R_s + r_e + r_{b'b})^2 \quad (1-13)$$

Here, β is the common-emitter current gain,

$$\beta = \frac{\alpha_o}{1 - \alpha_o}$$

and Γ is the collector cutoff-current noise parameter,

$$\Gamma = \frac{\beta I_{CO}}{\alpha_o^2 I_E}$$

It is seen from the foregoing equation that Γ is a function of the emitter current. Typical values of this parameter (shown in Tables 1-1, 1-2, and 1-3) vary from 6 with $I_E = 10\mu\text{a}$ to 0.3 with $I_E = 1\text{ma}$.

In order to facilitate the analysis of the noise-optimization problem, in which both the source resistance and the emitter current are the controllable parameters, it is again possible to express the noise factor in terms of the three noise factor parameters (equation 24), i.e.,

$$F = K_o + \frac{R_{no}}{R_s} + G_{nc} R_s \quad (1-14)$$

It follows, from equations 1-13 and 1-14, that for the common-base and common-emitter amplifier

$$K_o = 1 + \frac{1}{\beta r_e} (1 + \Gamma) (r_e + r_{b\parallel b}) \quad (1-15a)$$

$$R_{no} = r_e/2 + r_{b\parallel b} + \frac{1}{2\beta r_e} (1 + \Gamma) (r_e + r_{b\parallel b})^2 \quad (1-15b)$$

$$G_{nc} = \frac{1}{2\beta r_e} (1 + \Gamma) \quad (1-15c)$$

Substituting the values for the noise factor parameters given by equations 1-15a, 1-15b, and 1-15c into equations 25a and 25b, the optimum source resistance and the minimum noise factor become

$$R_{so} = \left[\left(r_e + r_{b'b} \right)^2 + \frac{2\beta r_e}{1 + \beta} \left(r_e + r_{b'b} \right) \right]^{1/2} \quad (1-16)$$

$$F_{min} = 1 + \frac{1}{\beta r_e} (1 + \beta) (r_e + r_{b'b}) + 2 \left[r_e/2 + r_{b'b} + \frac{1 + \beta}{2\beta r_e} \left(r_e + r_{b'b} \right)^2 \right] \left(\frac{1 + \beta}{2\beta r_e} \right)^{1/2} \quad (1-17)$$

The minimum noise factor, F_{min} , is an implicit function of the emitter current.* Therefore, the solution to the optimization problem in which both the source resistance and the emitter current are controllable parameters entails differentiating F_{min} with respect to the emitter current and equating the resulting differential to zero. If it is assumed

$$\frac{\partial r_{b'b}}{\partial I_E} = 0 \quad (1-18)$$

$$\frac{\partial \beta}{\partial I_E} \ll \frac{\beta}{I_E} \quad (1-19)$$

and

$$\left(\frac{\beta}{1 + \frac{\beta I_{CO}}{\alpha_0^2 I_E}} \right)^{1/2} \ll 1 \quad (1-20)$$

the result of this differentiation yields for the optimum emitter current

$$I_{E0} = \left(\frac{kT\beta I_{CO}}{2e r_{b'b}} \right)^{1/2} \quad (1-21)$$

If the restriction imposed by equation 1-20 is removed, the optimum emitter current lies between limits that differ by a factor of the $\sqrt{2}$.

*This dependence can be made explicit with the equation $I_E = \frac{kT}{er_e}$.

These limits are

$$\left(\frac{kTB I_{CO}}{2er_{b'b}} \right)^{1/2} < I_{E0} < \left(\frac{kTB I_{CO}}{er_{b'b}} \right)^{1/2} \quad (1-22)$$

From equations 1-16 and 1-21, the optimal source resistance $(R_{so})_o$

becomes

$$(R_{so})_o = \frac{r_{b'b}}{r} \left[(2 + r)^2 + 4\beta \right]^{1/2} \quad (1-23)$$

If it is assumed that

$$\beta \gg \left(1 + \frac{\beta I_{CO}}{2\alpha_o^2 I_E} \right)^2$$

equation 1-23 simplifies to

$$(R_{so})_o = \frac{2r_{b'b}}{r} \beta^{1/2} \quad (1-24)$$

Equations 1-21 and 1-24 apply to the common-base and common-emitter amplifier operated in the mean-frequency region. These two equations show that it is possible to solve the noise optimization problem in which both the source resistance and the emitter current are controllable parameters without making noise measurements on the amplifier.

COMMON-COLLECTOR AMPLIFIER

The noise factor of the common-collector amplifier, derivable from equations 1-7a to 1-7d, becomes

$$F = 1 + \frac{r_{b'b}}{R_s} + \frac{r_e/2 |R_s + r_{b'b} + z_c|^2}{R_s |z_c|^2} + \frac{\overline{i^2} (R_s + r_{b'b})^2}{4kT R_s} \\ + \frac{\left[r_e + (1 - \alpha_o)(R_s + r_{b'b}) \right]^2}{R_s R_L} \quad (1-25)$$

With typical values for load resistance ($R_L = 10,000$ ohms), emitter junction resistance ($r_e = 26$ ohms), collector impedance ($z_c = 1000,000$ ohms), and small-signal current gain ($\beta = 60$), it can safely be assumed that

$$R_L \gg 2r_e \quad (1-26)$$

$$z_c \gg \beta^{1/2} r_e \quad (1-27)$$

$$z_c \gg r_{b'b} \quad (1-28)$$

$$|z_c|^2 \gg \frac{2\beta r_e^2}{(1 + \Gamma)} \quad (1-29)$$

With these assumptions equation 1-25 can be simplified to read

$$F = 1 + \frac{r_{b'b} + r_e/2}{R_s} + \frac{\alpha_0^2}{2\beta r_e R_s} (1 + \Gamma)(r_e + r_{b'b})^2 \quad (1-30)$$

An analysis similar to that carried out for the common-base amplifier yields as the optimizing parameters for the common-collector stage

$$(R_{so})_o = \frac{2r_{b'b}}{\alpha_0} \beta^{1/2} \quad (1-31)$$

$$I_{EO} = \frac{1}{\alpha_0} \left(\frac{kTB I_{CO}}{2\pi r_{b'b}} \right)^{1/2} \quad (1-32)$$

EXPERIMENTAL MEASUREMENTS

In order to establish the validity of the assumptions made in deriving the equations contained in this section, and in order to establish the validity of the equations themselves, mean-frequency noise measurements were made on a large group of alloy, micro-alloy, and diffused base transistors. For each transistor tested, with the operating point fixed, noise-factor measurements were made with several discrete values of source resistance. The resulting noise-factor versus source-resistance curve was

drawn to obtain experimental values for the optimizing parameters R_{so} and F_{min} . This procedure was repeated with the emitter current as the independent variable. For each transistor tested, a curve was plotted to depict F_{min} and R_{so} as a function of the emitter current. A partial compilation of the experimental results is contained in the three parts of figure 7.

In order to obtain theoretical curves showing F_{min} and R_{so} as a function of the emitter current, measurements were made of I_{C0} , β , and r_{bb} . From these measurements and equations 1-16 and 1-17, the theoretical curves shown in figure 7 were drawn. The theoretical results are also given in Tables 1-1, 1-2, and 1-3.

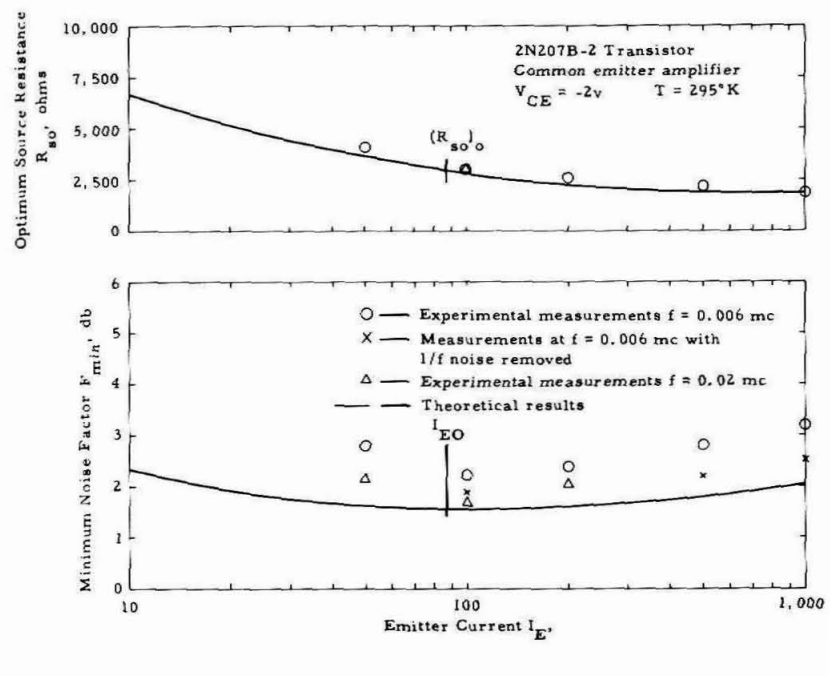
A comparison of the theoretical and experimental results reveals that for frequencies above a few kilocycles, the theoretical model forms a valid basis for obtaining the optimization parameters of the amplifier.

For the 2N207-B transistor (characteristics shown in part a of figure 7) the theoretical optimum emitter current was found to be 87 μ a; experimentally, the value 100 μ a was obtained. For the 2N43 transistor (part b of figure 7) the theoretical value obtained was 450 μ a, and the experimental value 200 μ a. For the 2N544 transistor (part c of figure 7), the theoretical value is 350 μ a; the experimental value is 200 μ a.

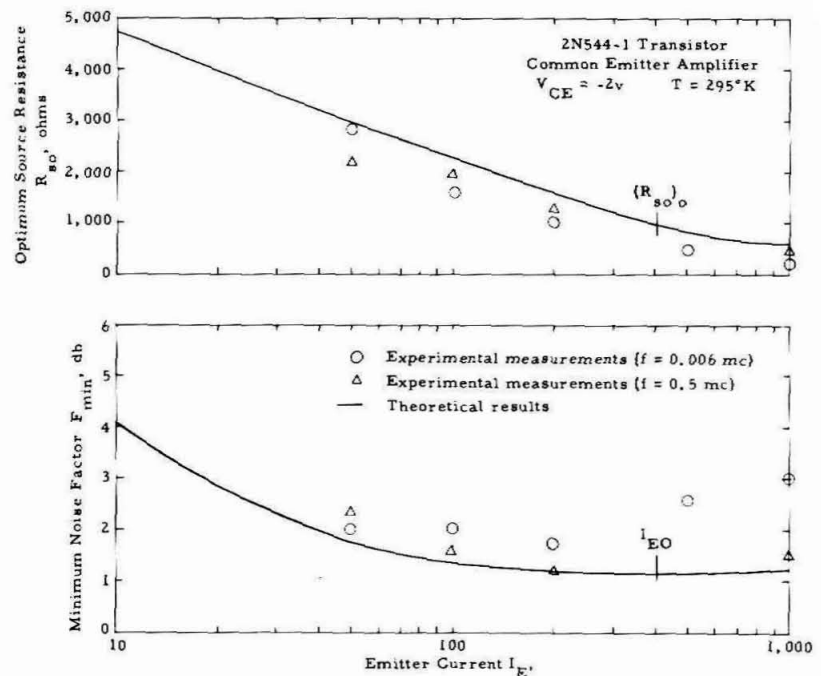
SOURCE RESISTANCE AS AN UNCONTROLLABLE PARAMETER

Equations 1-21 and 1-24 quantify the emitter current and the source resistance that give the optimum noise performance for a given transistor. Because the optimal source resistance can be modified by the use of a transformer at the input of the amplifier, a wide latitude exists for the source resistance that will satisfy the constraint imposed by equation 1-24.

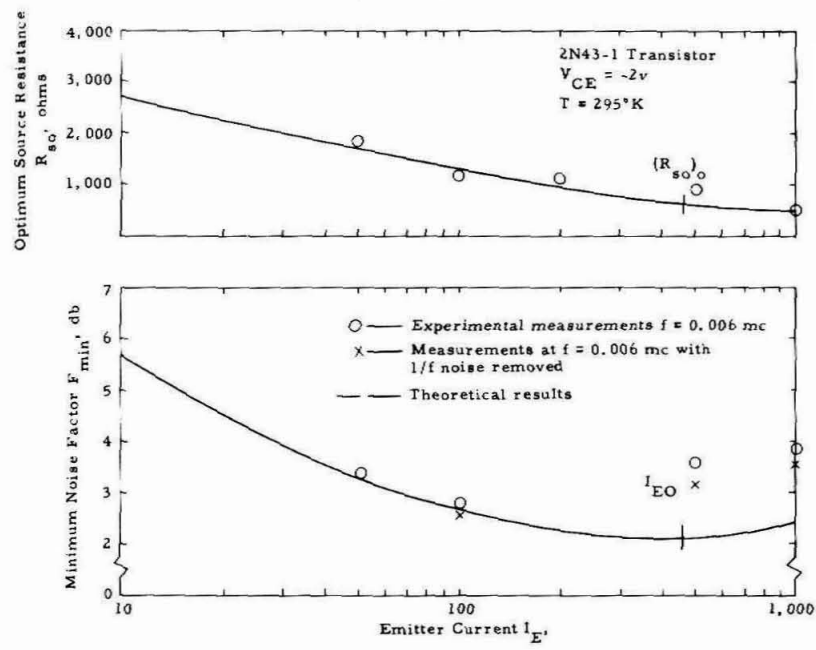
However, in many cases, it is found that other considerations prohibit the use of transformer coupling. If the source resistance is fixed, the



(a)



(c)



(b)

Figure 7. Minimum Noise Factor and Optimum Source Resistance as Function of Emitter Current : (a) Low-Noise Alloy-Junction Transistor, (b) Low-Frequency Alloy-Junction Transistor, (c) High-Frequency Diffused-Base Transistor

Table 1-1. Theoretical Measure of the Noise Parameters as a Function of Emitter Current for the 2N207-B Transistor.

| Transistor 2N207B No.4 | I_E , Microamperes | | | | | |
|------------------------------|----------------------|-------|-------|-------|-------|-------|
| | 10 | 50 | 100 | 200 | 500 | 1,000 |
| K_o | 1.14 | 1.06 | 1.08 | 1.10 | 1.09 | 1.11 |
| R_{no} , ohms | 2,160 | 700 | 550 | 445 | 380 | 350 |
| G_{nc} , μ mhos | 44 | 52 | 66 | 88 | 130 | 150 |
| Γ | 6.0 | 2.8 | 1.8 | 1.3 | 0.6 | 0.34 |
| F_{min} , db | 2.3 | 1.6 | 1.6 | 1.7 | 1.8 | 2.0 |
| R_{so} , ohms | 6,950 | 3,600 | 2,900 | 2,300 | 1,920 | 1,520 |

Table 1-2. Theoretical Measure of the Noise Parameters as a Function of Emitter Current for the 2N43 Transistor.

| Transistor 2N43 No.1 | I_E , Microamperes | | | | | |
|----------------------------|----------------------|-------|-------|-------|-----|-------|
| | 10 | 50 | 100 | 200 | 500 | 1,000 |
| K_o | 1.6 | 1.4 | 1.2 | 1.2 | 1.2 | 1.2 |
| R_{no} , ohms | 2,800 | 650 | 370 | 260 | 230 | 180 |
| G_{nc} , μ mhos | 380 | 240 | 250 | 300 | 380 | 570 |
| Γ | 5.2 | 3.1 | 2.3 | 1.4 | 0.8 | 0.6 |
| F_{min} , db | 5.7 | 3.2 | 2.7 | 2.3 | 2.1 | 2.5 |
| R_{so} , ohms | 2,700 | 1,650 | 1,200 | 1,150 | 780 | 400 |

Table 1-3. Theoretical Measure of the Noise Parameters as a Function of Emitter Current for the 2N544 Transistor.

| Transistor 2N544 | I _E , Microamperes | | | | | |
|------------------------------|-------------------------------|-------|-------|-------|------|-------|
| | 10 | 50 | 100 | 200 | 500 | 1,000 |
| K _o | 1.50 | 1.10 | 1.06 | 1.05 | 1.05 | 1.05 |
| R _{no} , ohms | 2,600 | 600 | 410 | 280 | 130 | 90 |
| G _{nc} , μ mhos | 120 | 62 | 75 | 96 | 150 | 240 |
| Γ | 2.1 | 2.1 | 1.3 | 0.8 | 0.4 | 0.3 |
| F _{min} , db | 1.8 | 1.6 | 1.7 | 1.2 | 1.2 | 1.2 |
| R _{so} , ohms | 4,600 | 3,100 | 2,400 | 1,600 | 890 | 600 |

dictated source resistance will, in general, not satisfy equation 1-24.

Optimization, in this case, entails finding the emitter current that minimizes the noise factor of the amplifier. It can be found by differentiating the noise factor with respect to the emitter current and equating the resulting differential to zero. For the common-base and common-emitter amplifier, if it is assumed that

$$\beta \gg 2\Gamma + 1 \quad (1-33)$$

the optimum emitter current is given by

$$I_{EO} = \frac{kT}{e} \frac{\beta^{1/2}}{(R_s + r_{bb})} \quad (1-34)$$

For the common-collector amplifier

$$I_{EO} = \frac{kT}{e} \frac{\beta^{1/2}}{\alpha_o (R_s + r_{bb})} \quad (1-35)$$

In order to corroborate equation 1-34, noise measurements were made on several transistors. A partial compilation of the results is shown in

figure 8 as well as the theoretical results obtained with equation 1-34.

The correspondence shows that, for frequencies above a few kilocycles, equation 1-34 forms a valid basis for the solution of the optimization problem in which the emitter current is the only controllable parameter.

EQUIVALENT NOISE RESISTANCE

The equivalent noise resistance can be used to illustrate the degradation in the noise performance caused by each of the noise generators contained in the mean-frequency model (part b of figure 6). This parameter defined by

$$R_{eq} = (F - 1)R_s$$

becomes for the common-base and common-emitter transistor amplifier

$$R_{eq} = r_e/2 + r_{b\parallel b} + \frac{(1 + \Gamma)}{2\beta r_e} (R_s + r_{b\parallel b} + r_e)^2 \quad (1-36)$$

where

$r_e/2$ = the degradation caused by e_{ne}

$r_{b\parallel b}$ = the degradation caused by e_{nb}

$\frac{1 + \Gamma}{2\beta r_e} (R_s + r_{b\parallel b} + r_e)^2$ = the degradation caused by i_{nc}

Figure 9 illustrates the relative magnitude of each term of equation 1-36 as a function of the source resistance and the experimentally obtained curve showing the equivalent noise resistance as a function of the source resistance.

COLLECTOR VOLTAGE AND ITS EFFECT ON MEAN-FREQUENCY NOISE PERFORMANCE

An inspection of the equations that dictate the noise performance of the transistor amplifier in the mean-frequency region reveals that, theoretically, the collector voltage is a noise parameter in a transistor stage only because of its influence on β and z_c at low reverse biases,

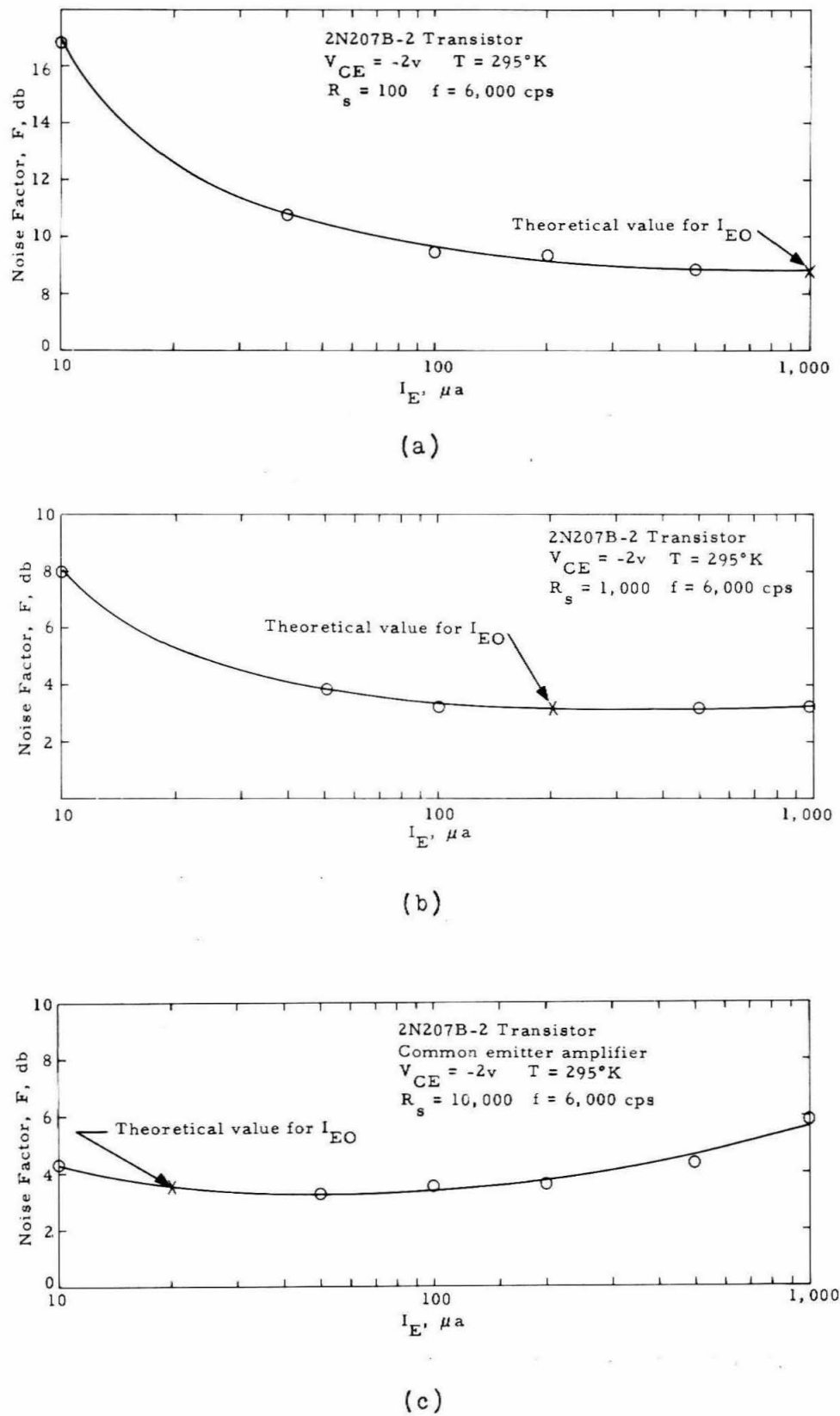


Figure 8. Noise Factor As Function of Emitter Current with:
 (a) $R_s = 100$ ohms, (b) $R_s = 1,000$ ohms, (c) $R_s = 10,000$ ohms.

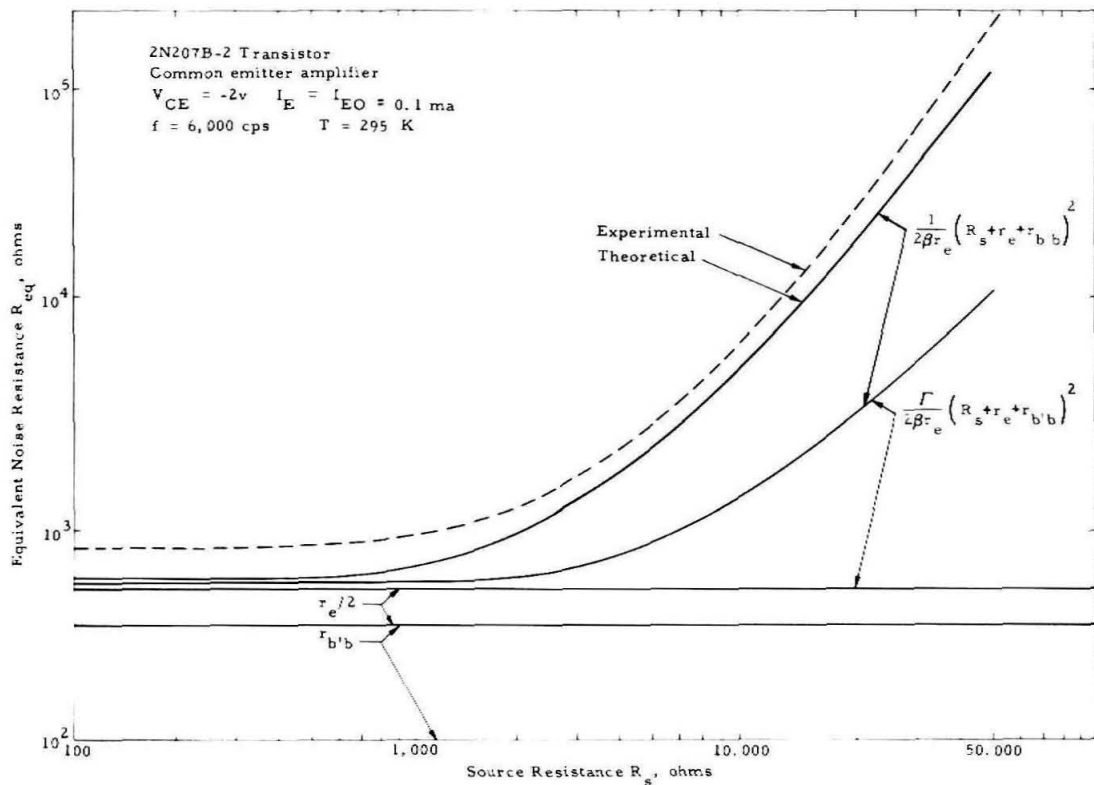


Figure 9. Equivalent Noise Resistance as a Function of Source Resistance.

and its influence on I_{CO} at high reverse biases. In order to obtain an experimental verification of the theory, noise studies were made on several transistors with the collector voltage as the only independent parameter. The results of these measurements revealed that although the noise level observed at the output of the transistor stage decreased sharply as zero biasing was approached, the decrease in the power gain offset any advantage produced by the lower noise level. At the other extreme, as the collector breakdown voltage was approached, a perceptible increase in the noise level was observed. However, with collector voltages within the range 0.25 v to 10 v reverse bias, little change was observed in either the noise level or the noise factor.

CONCLUSIONS

This section has been concerned with the formulation of an analytical solution to two distinct optimization problems. The first problem considered was one in which both the source resistance and the emitter current were controllable parameters. The analytical solution entailed finding theoretical values for R_s and I_E which concurrently satisfied

$$\frac{\partial F}{\partial R_s} = 0 \quad (1-37)$$

and

$$\frac{\partial F}{\partial I_E} = 0 \quad (1-38)$$

With van der Ziel's mean-frequency noise model as a basis, it was found that the optimizing parameters $(R_{so})_0$ and I_{E0} , which satisfied equations 1-37 and 1-38, could be expressed in terms of the d.c. and small-signal transistor parameters. The parameters involved were β , the common-emitter current gain, r_{bb} , the extrinsic base resistance, and I_{C0} , the collector cutoff current.

An interesting aspect of the theoretical study was the dominant role played by the collector cutoff current in determining the noise performance of the amplifier in the mean-frequency region. This is in sharp contrast with Yajimi's 1/f collector noise model (see p.73), which proposes that the collector cutoff current could be neglected, as a noise source, at 1/f frequencies. As a result of the validity of Yajimi's theory, it is found that with large values of source resistance, i.e., $R_s \gg R_{so}$, optimum noise performance entails operating the transistor with a starved emitter. Referring to Tables 1-1, 1-2, and 1-3 (by comparing values of the noise factor parameter G_{nc}) this is found to be no longer true at mean frequencies.

For the 2N43 transistor of Table 1-2, the minimum value of G_{nc} is obtained with an emitter current of approximately 80 μ a. For the 2N544 transistor, the minimum value of G_{nc} is obtained with an emitter current of approximately 60 μ a.

The second optimization problem considered was one in which the emitter current was the only controllable parameter. Optimizing the noise performance of the amplifier now entailed finding that value of emitter current which satisfied

$$\frac{\partial F}{\partial I_E} = 0 \quad (1-39)$$

With van der Ziel's mean-frequency noise model as a basis, it is possible to express the noise factor as an explicit function of the emitter current. Therefore, the solution to this optimization problem could be obtained by directly performing the mathematical process dictated by equation 1-32. The analytical solution shows that the optimum emitter current is now a function of the source resistance, the extrinsic base resistance, and the common-emitter current gain.

An interesting aspect of this theoretical study concerns the magnitude of the optimum source resistance R_{so} . Montgomery (Ref. 16), in an experimental study conducted in 1952, found that this parameter could be accurately approximated by $r_e + r_{b1b}$, the input impedance of the common-base and common-emitter transistor amplifier (output open-circuited).

It is easily shown that this is the value obtained for this parameter if the two input noise sources, e_{ne} and e_{nb} (part b of figure 6) are assumed to be zero.

Since the major portion of the noise that Montgomery observed was 1/f noise generated in the collector-base region of the transistor, this was

a valid assumption at that time. However, with the transistors now available, the two input noise sources are both instrumental in determining the magnitude of the optimum source resistance. To illustrate, the following example is offered. (The d.c. and small-signal parameters given are typical of those found in transistors used in the present-day, low-noise, transistor amplifier.)

$$\begin{aligned}I_{CO} &= 2 \mu\text{a} \\I_E &= 0.1 \text{ mA} \\r_{b'b} &= 200 \text{ ohms} \\\beta &= 40 \\r_e &= 260 \text{ ohms}\end{aligned}$$

Substituting these values into equation 1-17,

$$R_{SO} = \underline{1950} \text{ ohms}$$

whereas

$$r_e + r_{b'b} = \underline{460} \text{ ohms}$$

Nielsen (Ref. 17), in a study conducted in 1957, observed that in the common-emitter transistor amplifier, the ratio of the optimum source resistance, R_{SO} , to the power matching resistance, R_{SP} , did not exceed the factor $\sqrt{2}$.* Although this ratio is closest to 1 for the transistor in this configuration, there is no apparent limit to R_{SO}/R_{SP} . In the example cited,

$$\begin{aligned}R_{SP} &= r_{b'b} + r_e/1 - \alpha_0 \\R_{SP} &= 10,900 \text{ ohms}\end{aligned}$$

whereas

$$R_{SO} = 1950 \text{ ohms}$$

*This observation was concluded from the results of his experimental study. No theoretical justification for this conclusion is given.

and the ratio

$$\frac{R_{SO}}{R_{SP}} = \frac{1}{5.6}$$

Equation 1-16 shows that three parameters must first be measured before the optimum source resistance can be determined. They are

r_{bb} , the extrinsic base resistance

α_o , the common base current gain

I_{CO} , the collector cutoff current

2. $1/f$ FREQUENCY REGION

The design of low-level, audio-frequency, transistorized amplifiers is made critical by the existence of "excess" transistor noise which has spectral properties similar to the flicker noise in vacuum tubes. Although several theories have been proposed to explain the mechanism responsible for excess ($1/f$) noise in semiconductors (Ref. 18 - 23), no one theory has yet gained universal acceptance. This is due, mainly, to the failure of any single theory to account for the extreme range of frequencies (Ref. 24 - 26) over which this noise has been found to exist. However, experimental investigations conducted with surface-treated crystal filaments substantiate the theories of McWhorter (Ref. 26) and North (Ref. 27) which propose that excess noise is a surface phenomenon caused by fluctuations in the surface potential of the semiconductor. These fluctuations are induced by the trapping and untrapping of majority carriers in the slow surface states.

Because $1/f$ noise is a surface phenomenon, it is impossible to obtain a measure of the $1/f$ mechanism existing in the transistor from the transistor's d.c. and small-signal parameters. For this reason, experimental noise measurements must be made to find operating parameters that will optimize the transistor's noise performance in the frequency region where $1/f$ noise predominates. Moreover, the complete optimization process, which gives the unique set of controllable parameters that optimize the transistor's noise performance, requires a separate experimental study for each change in any one of the controllable or uncontrollable parameters.

This section considers first the optimization problem in which the two controllable parameters are the transistor's operating point and the source resistance. Brief mention is then made of experimental findings

that indicate that the collector voltage, one of the two parameters necessary to specify the operating point of the transistor amplifier, is inconsequential in its effects on the noise performance of the amplifier. If the insignificant effects produced by changes in the collector voltage are neglected, obtaining the optimum noise performance entails finding, by experimental noise measurements, the unique value of source resistance and emitter current which concurrently satisfy

$$\frac{\partial F}{\partial R_s} = 0 \quad (2-1a)$$

$$\frac{\partial F}{\partial I_E} = 0 \quad (2-1b)$$

The statistical processes responsible for the noise behavior of the transistor at $1/f$ frequencies are independent of the generation-recombination, diffusion, and thermal noise that dictate the noise performance of the device at mean frequencies. Thus, the optimal source resistance (R_{so})_o and the optimum emitter current I_{E0} , which satisfy equations 2-1a and 2-1b, are implicit functions of frequency. It is therefore necessary, in order to obtain a solution to the optimization problem that is applicable to the $1/f$ and transition-frequency region, to calculate the optimizing parameters at each of several selected frequencies. However, the existing theory can be used to obtain a simplified optimization procedure.

The simplified method, which will be shown to be adequate for quantifying the spectral behavior of the optimizing parameters, is illustrated in figure 10. Block I in figure 10 shows the optimization procedure that must be employed if no assumptions are made regarding the noise

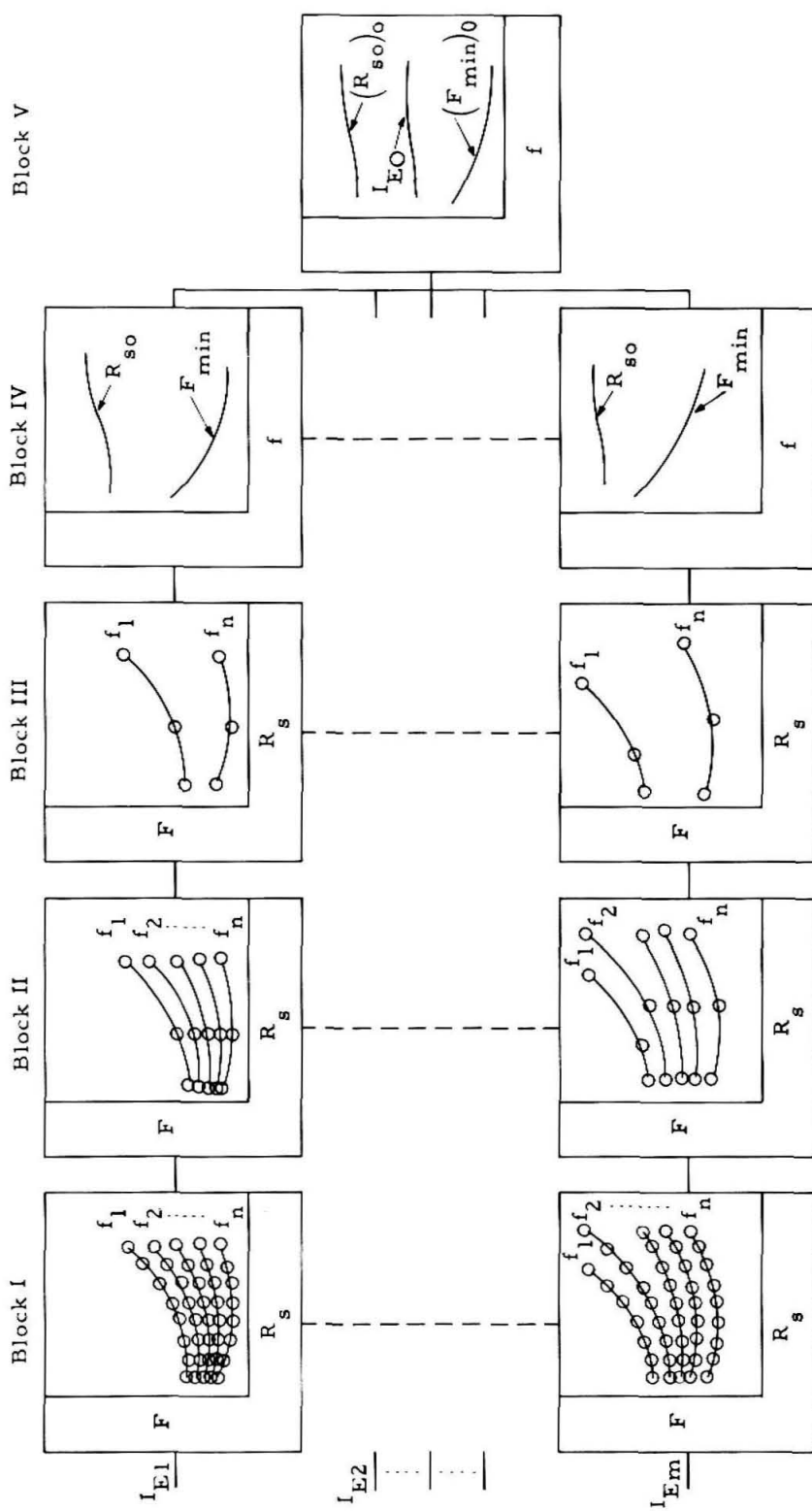


Figure 10. Diagrammatic Representation of Simplified and Conventional Optimization Procedure.

properties of the transistor. At each of several frequencies in the $1/f$ and transition-frequency region, a diverse set of source resistances must be used to determine the spectral behavior of the optimizing parameters $F_{\min}(f)$ and $R_{so}(f)$. However, by assuming that the noise sources contained in the device are not functions of the input termination, the number of source resistances necessary to quantify $R_{so}(f_1)$ and $F_{\min}(f_1)$, at an arbitrary frequency f_1 , is reduced to three. This is shown in Block II. Moreover, by assuming the validity of Fonger's phenomenological spectral function $\phi(f)$, measurements at only two frequencies are necessary to determine the spectral behavior of $R_{so}(f)$ and $F_{\min}(f)$. This is shown in Blocks III and IV.

Since $R_{so}(f)$ and $F_{\min}(f)$ are implicit functions of the emitter current, the procedure is repeated with emitter current as the independent variable to obtain the curves shown in Block V. The optimizing parameters contained in Block V are obtained from Block IV by taking, at each of several frequencies, that value of emitter current and that value of source resistance which gives the lowest noise factor at each of the selected frequencies. Block V also contains the minimal noise factor $(F_{\min})_o$.

A small portion of this section is devoted to the optimization problem in which the source resistance is an uncontrollable parameter. The problem is further limited by discussing only that class of source resistance (i.e., $R_s \gg R_{so}$) that lends itself to a simplified empirical analysis using Yajimi's collector noise model.

$1/f$ AND TRANSITION-FREQUENCY NOISE MODELS

Fonger's $1/f$ noise model, which represents North's theory applied to the junction transistor, is shown in part a of figure 11. Although the

terminology used to describe the noise sources contained in this figure differs from that used by Fonger, the implicit dependence of these sources on his phenomenological spectral function $\phi(f)$ is unchanged by the change in notation. Part b of figure 11 shows an equivalent "T" representation of Fonger's original model. A simplified equivalent "T" representation of Fonger's original noise model is shown in part c of figure 11. Here, the word "simplified" pertains to the complexity of the noise model and not to the statistical properties of the model. The value given for each of the noise sources contained in this figure is the value required in order to retain statistical equivalence at both the input and output terminals of the amplifier.

The $1/f$ noise model is limited by its implicit spectral function $\phi(f)$ to frequencies where the noise behavior of the transistor stage is determined solely by $1/f$ noise. Therefore a new, or supplementary, noise model must be used in the transition region where both $1/f$ and "white" noise are instrumental in determining the transistor's noise performance. If the validity of Peterson's equivalence theorem is assumed, the model shown in part a of figure 12 will suffice to describe the noise behavior observed in the transition region.

Combining the two voltage and the two current noise sources (part b of figure 12), the transition noise model becomes outwardly identical to the $1/f$ noise model (part c of figure 11). The differences that exist between these two models are implicit in the spectral dependence of the noise sources contained in each model.

The noise factor F for the transistor stage in each of its three configurations becomes (from equation 2 applied to part b of figure 12) for

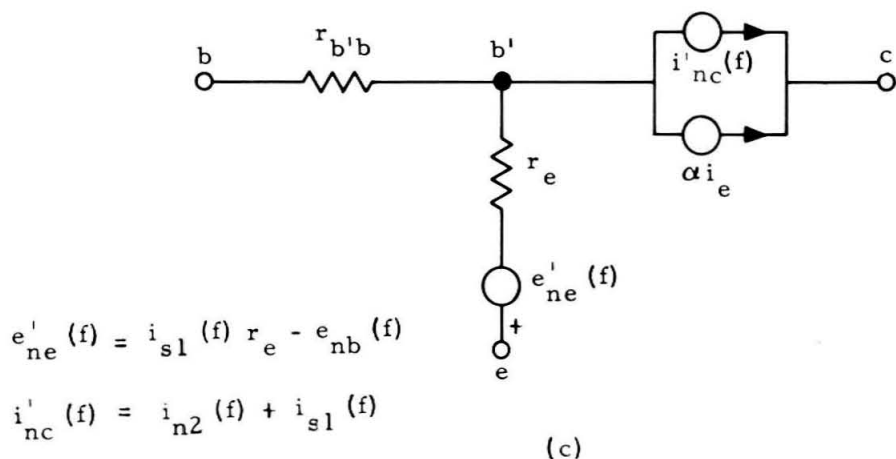
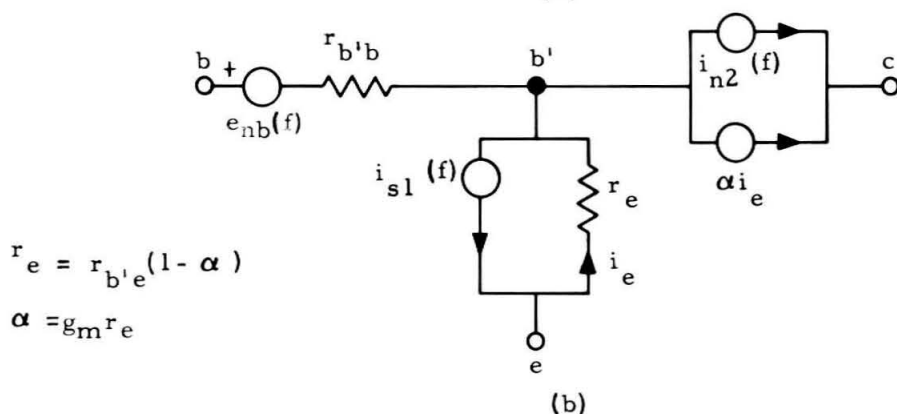
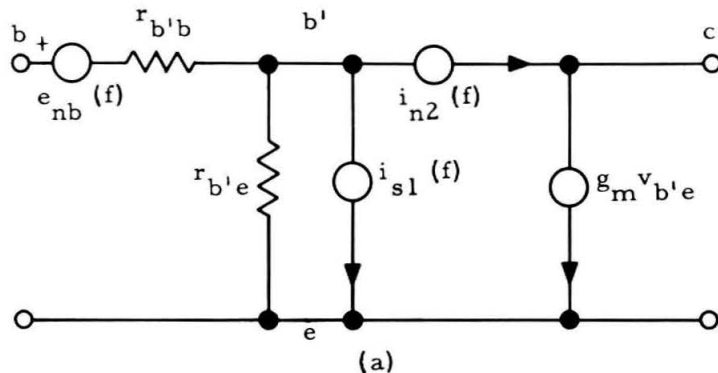
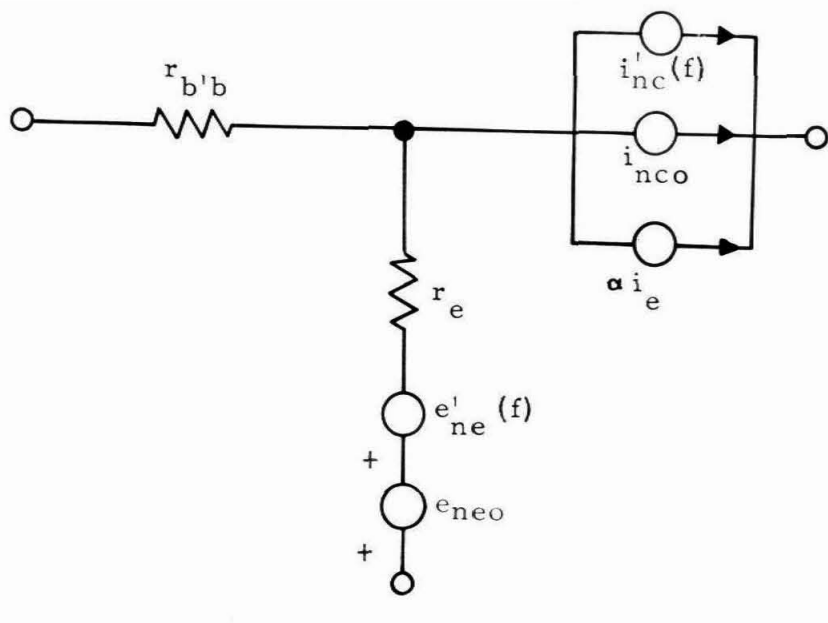
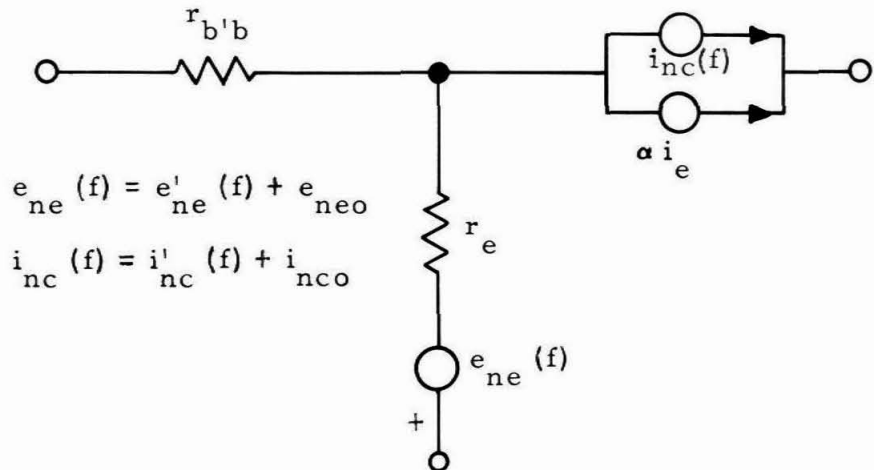


Figure 11. (a) Fonger's Transistor 1/f Noise Model, (b) Equivalent "T" Representation of 1/f Model, (c) Simplified 1/f Model.



(a)



(b)

Figure 12. (a) Transistor Transition-Frequency Noise Model, (b) Simplified Transition-Frequency Model.

the common-base and the common-emitter stage

$$F(f) = 1 + \frac{R_{ne}(f)}{R_s} + \frac{g_{nc}(f)}{R_s} (R_s + r_e + r_{b'b})^2 - \frac{2R\{c(f)\}}{R_s} \left[g_{nc}(f)R_{ne}(f) \right]^{1/2} (R_s + r_e + r_{b'b}) \quad (2-2a)$$

and for the common-collector stage

$$F(f) = 1 + \frac{R_{ne}(f)}{R_s} + \frac{1}{R_s R_L} \left[r_e + (1-\alpha) R_s + r_{b'b} \right]^2 \quad (2-2b)$$

$$+ \frac{\alpha^2 \left[g_{nc}(f) \right]}{R_s} (R_s + r_{b'b})^2 - \frac{2\alpha R\{c(f)\}}{R_s} \left[g_{nc}(f)R_{ne}(f) \right]^{1/2} (R_s + r_{b'b})$$

For typical values of R_L , α , R_s , and r_e , equation 2-2b can be simplified to read

$$F(f) = 1 + \frac{R_{ne}(f)}{R_s} + \frac{\alpha^2 g_{nc}(f)}{R_s} (R_s + r_{b'b})^2 - \frac{2\alpha R\{c(f)\}}{R_s} \cdot \left[g_{nc}(f)R_{ne}(f) \right]^{1/2} (R_s + r_{b'b}) \quad (2-2c)$$

Here, $R_{ne}(f)$ is the emitter thermal noise resistance, defined by

$$\overline{e_{ne}^2(f)} = 4kT R_{ne}(f) B \quad (2-3a)$$

g_{nc} is the collector thermal noise conductance, defined by

$$\overline{i_{nc}^2} = \alpha^2 (4kT g_{nc} B) \quad (2-3b)$$

and $R\{c(f)\}$ is the real part of the normalized correlation coefficient $c(f)$, where

$$c(f) = \frac{\overline{e_{ne}^*(f) i_{nc}(f)}}{\left[\overline{e_{ne}^2(f)} \overline{i_{nc}^2(f)} \right]^{1/2}} \quad (2-3c)$$

In the formulation of equations 2-2a, 2-2b, and 2-3, it has been assumed that only thermal noise was generated in the source and in the load resistances, i.e.,

$$\overline{e_{ns}^2} = 4kT R_s B$$

$$\overline{e_{nL}^2} = 4kT R_L B$$

If it is assumed that the noise generators contained in the transition frequency noise model are not functions of the source resistance, the terms $R_{ne}(f)$, $g_{nc}(f)$, and $c(f)$ contained in equations 2-2a, 2-2b, and 2-2c will also be independent of R_s . With this assumption, the noise factor can be written in terms of three noise-factor parameters, $K_o(f)$, $R_{no}(f)$, and $G_{nc}(f)$ which are not functions of the input termination.

$$F(f) = K_o(f) + \frac{R_{no}(f)}{R_s} + G_{nc}(f)R_s \quad (2-4)$$

From equations 2-2a and 2-4, the noise-factor parameters of the common-base and common-emitter amplifier become

$$K_o(f) = 1 + 2g_{nc}(f)(r_e + r_{b1b}) - 2R\{c(f)\} \left[g_{nc}(f)R_{ne}(f) \right]^{1/2} \quad (2-5a)$$

$$R_{no}(f) = R_{ne}(f) + g_{nc}(f)(r_e + r_{b1b})^2 - 2R\{c(f)\} \left[g_{nc}(f)R_{ne}(f) \right]^{1/2} (r_e + r_{b1b}) \quad (2-5b)$$

$$G_{nc}(f) = g_{nc}(f) \quad (2-5c)$$

In order to obtain the frequency dependence of the noise parameters contained in equations 2-5a, 2-5b, and 2-5c, it is assumed that the noise sources shown in the low-frequency noise model (part c of figure 11) exhibit a $1/f$ spectral dependence, i.e.,

$$\overline{e_{ne}^2(f)} = \overline{e_{neo}^2} \frac{f_i}{f} \quad (2-6a)$$

$$\overline{i_{nc}^2(f)} = \overline{i_{nco}^2} \frac{f_j}{f} \quad (2-6b)$$

Here, f_i and f_j are two empirical noise parameters. Also, since the $1/f$ and the mean-frequency noise processes are mutually independent, it can safely be assumed that no correlation exists between the $1/f$ and the mean-frequency noise sources, i.e., that all cross-correlation terms except

$\overline{e_{ne}^*(f)i_{nc}^*(f)}$ and $\overline{e_{neo}^*i_{nco}^*}$ are zero (see part a of figure 12).

It follows, from figure 12b, equations 2-3a, 2-3b, 2-6a, and 2-6b and the assumption pertaining to the correlation, that the noise parameters $R_{ne}(f)$ and $g_{nc}(f)$ will have a frequency dependence given by

$$R_{ne}(f) = R_{neo} \left(1 + \frac{f_i}{f} \right) \quad (2-7a)$$

$$g_{nc}(f) = g_{nco} \left(1 + \frac{f_j}{f} \right) \quad (2-7b)$$

where R_{neo} is the mean-frequency emitter noise resistance

$$\overline{e_{neo}^2} = 4kTR_{neo}B \quad (2-7c)$$

and g_{nco} is the mean-frequency collector noise conductance

$$\overline{i_{nco}^2} = \alpha^2 4kTg_{nco}B \quad (2-7d)$$

It is found, from equations 2-2a, 2-4, 2-7a, and 2-7b, that the noise factor of the transistor amplifier can now be written as an explicit function of frequency. This dependence becomes

$$F(f) - 1 = K_{oo}^! \left(1 + \frac{f_3}{f} \right) + R_{noo} \left(1 + \frac{f_5}{f} \right) + G_{nco} \left(1 + \frac{f_7}{f} \right) \quad (2-8)$$

Here, $K_{oo}^! = K_{oo} - 1$, and K_{oo} , R_{noo} , and G_{nco} are the mean-frequency, noise-factor parameters. For the common-base and the common-emitter transistor amplifier:

$$K_{oo}^! = 2g_{nco}(r_{b'b} + r_e) - 2R(c_o)(R_{neo}g_{nco})^{1/2} \quad (2-8a)$$

$$f_3 = \frac{1}{K_{oo}^!} \left\{ f_j(2g_{nco})(r_{b'b} + r_e) - f_k \left[2R(c_o) \right] \left[R_{neo}g_{nco} \right]^{1/2} \right\} \quad (2-8b)$$

$$R_{noo} = R_{neo} + g_{nco}(r_{b'b} + r_e)^2 - \left[2R(c_o) \right] (R_{neo}g_{nco})^{1/2} (r_e + r_{b'b}) \quad (2-8c)$$

$$f_5 = \frac{1}{R_{noo}} \left\{ f_i(R_{neo}) + f_j(g_{nco})(r_{b'b} + r_e)^2 - f_k \left[2R(c_o) \right] \right. \\ \left. \cdot (R_{neo}g_{nco})^{1/2} (r_e + r_{b'b}) \right\} \quad (2-8d)$$

$$G_{nco} = g_{nco} \quad (2-8e)$$

$$f_7 = f_j \quad (2-8f)$$

Here, c_o is the normalized mean-frequency correlation coefficient

$$c_o = \frac{e_{neo}^* i_{nco}}{\left[\frac{e_{neo}^2}{2} \frac{i_{nco}^2}{2} \right]^{1/2}} \quad (2-8g)$$

$$f_k = \left[f_i f_j \right]^{1/2} \frac{R \{ c(1/f) \}}{R(c_o)} \quad (2-8h)$$

and $c(1/f)$ is the normalized $1/f$ frequency correlation coefficient.

SIMPLIFIED OPTIMIZATION PROCEDURE

Equation 2-8 forms the basis of the simplified optimization procedure, showing that it is possible, with six measurements, to quantify the behavior of the frequency-dependent, noise-factor parameters $K_o(f)$, $R_{no}(f)$, and $G_{nc}(f)$ from low audio frequencies to the upper limit of the mean-frequency region.

It should be noted that once these six parameters have been determined, it becomes possible, using equation 2-8, to quantify the noise performance of the transistor amplifier when any value of source resistance is used. Therefore, assuming the validity of the simplified optimization procedure, these six measurements provide all the information that is obtained from the conventional optimization procedure shown in figure 10.

The measurements made to quantify the three mean-frequency noise-factor parameters K_{oo}^1 , R_{noo} , and G_{nco} and the three corner frequencies f_3 , f_5 , and f_7 , contained in equation 2-8, are not arbitrary. Therefore, it is worth while to discuss the method used to determine these six parameters. Again, writing the noise factor in terms of the frequency-dependent, noise-factor parameters,

$$F(f) = K_o(f) + \frac{R_{no}(f)}{R_s} + G_{nc}(f)R_s$$

Differentiating this equation with respect to R_s and equating the resulting differential to zero, there is obtained for the optimum source resistance,

$$R_{so}(f) = \left[\frac{R_{no}(f)}{G_{nc}(f)} \right]^{1/2} \quad (2-9)$$

Substituting $R_{so}(f)$ for R_s in equation 2-9, there is obtained for the minimum noise factor

$$F_{min}(f) = K_o(f) + 2 \left[R_{no}(f) G_{nc}(f) \right]^{1/2} \quad (2-10)$$

It is found, from equations 2-9 and 2-10, that the noise factor can also be written in the form

$$F(f) = K_o(f) + \frac{R_{no}(f)}{R_s} \left[1 + \left(\frac{R_s}{R_{so}(f)} \right)^2 \right] \quad (2-11)$$

Therefore, for values of $R_s \ll R_{so}$, the noise factor can be approximated by

$$F(f) = K_o(f) + \frac{R_{no}(f)}{R_s} \quad (2-12a)$$

By a similar algebraic substitution, it is easily shown that for values of $R_s \gg R_{so}$, the approximation for F becomes

$$F(f) = K_o(f) + G_{nc}(f) R_s \quad (2-12b)$$

As the first step in quantifying the six parameters contained in equation 2-8, noise measurements are made at a frequency, f_1 , located in the $1/f$ region. At this frequency, three measurements, employing source resistances R_{s1} , R_{s2} , and R_{s3} , yield $F_1(f_1)$, $F_2(f_1)$, and $F_3(f_1)$. The values for R_{s1} , R_{s2} , and R_{s3} were selected so that the approximations given by equations 2-12a and 2-12b could be used, i.e.,

$$F_1(f_1) = K_o(f_1) + \frac{R_{no}(F_1)}{R_{s1}} \quad (2-13a)$$

$$F_2(f_1) = K_o(f_1) + \frac{R_{no}(f_1)}{R_{s2}} + G_{nc}(f_1) R_{s2} \quad (2-13b)$$

$$F_3(f_1) = K_o(f_1) + G_{nc}(f_1) R_{s3} \quad (2-13c)$$

Assuming that $R_{s1} \ll R_{s2} \ll R_{s3}$, it follows from equations 2-13a, 2-13b, and 2-13c, that

$$K_o(f_1) = F_2(f_1) - F_1(f_1) \frac{R_{s1}}{R_{s2}} - F_3(f_1) \frac{R_{s2}}{R_{s3}} \quad (2-14a)$$

$$R_{no}(f_1) = R_{s1} \left[F_1(f_1) - F_2(f_1) + F_3(f_1) \frac{R_{s2}}{R_{s3}} \right] \quad (2-14b)$$

$$G_{nc}(f_1) = \frac{1}{R_{s3}} \left[F_3(f_1) - F_2(f_1) + F_1(f_1) \frac{R_{s1}}{R_{s2}} \right] \quad (2-14c)$$

To obtain $K_o(f_2)$, $R_{no}(f_2)$, and $G_{nc}(f_2)$, the procedure is repeated at a frequency f_2 , located in the transition-frequency region.

From equation 2-8 and the results of the six measurements,

$$K_{oo} = \frac{f_2 K_o(f_2) - f_1 K_o(f_1)}{f_2 - f_1} \quad (2-15a)$$

$$R_{noo} = \frac{f_2 R_{no}(f_2) - f_1 R_{no}(f_1)}{f_2 - f_1} \quad (2-15b)$$

$$G_{nco} = \frac{f_2 G_{nc}(f_2) - f_1 G_{nc}(f_1)}{f_2 - f_1} \quad (2-15c)$$

$$f_3 = \frac{f_1 f_2 [K_o(f_1) - K_o(f_2)]}{f_2 [K_o(f_2) - 1] - f_1 [K_o(f_1) - 1]} \quad (2-15d)$$

$$f_5 = \frac{f_1 f_2 [R_{no}(f_1) - R_{no}(f_2)]}{f_2 [R_{no}(f_2)] - f_1 [R_{no}(f_1)]} \quad (2-15e)$$

$$f_7 = \frac{f_1 f_2 [G_{nc}(f_1) - G_{nc}(f_2)]}{f_2 [G_{nc}(f_2)] - f_1 [G_{nc}(f_1)]} \quad (2-15f)$$

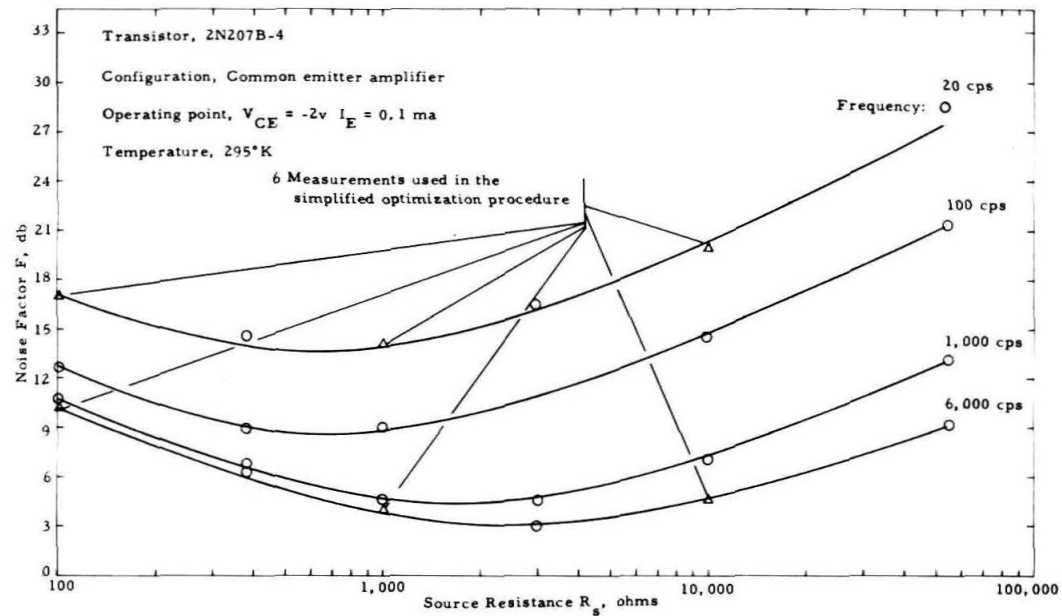
EXPERIMENTAL CONFIRMATION OF SIMPLIFIED METHOD

In order to establish the validity of the simplified optimization procedure, spot-noise measurements were made on a number of commercially available transistors at two selected frequencies, f_1 and f_2 , employing, at each frequency, three source resistances. The noise factors obtained from these six measurements were used to quantify the six unknown parameters contained in equation 2-8. Once these parameters had been determined, it was possible, utilizing equation 2-8, to plot curves showing the theoretical spectral behavior of the two optimizing parameters $R_{so}(f)$ and $F_{min}(f)$.

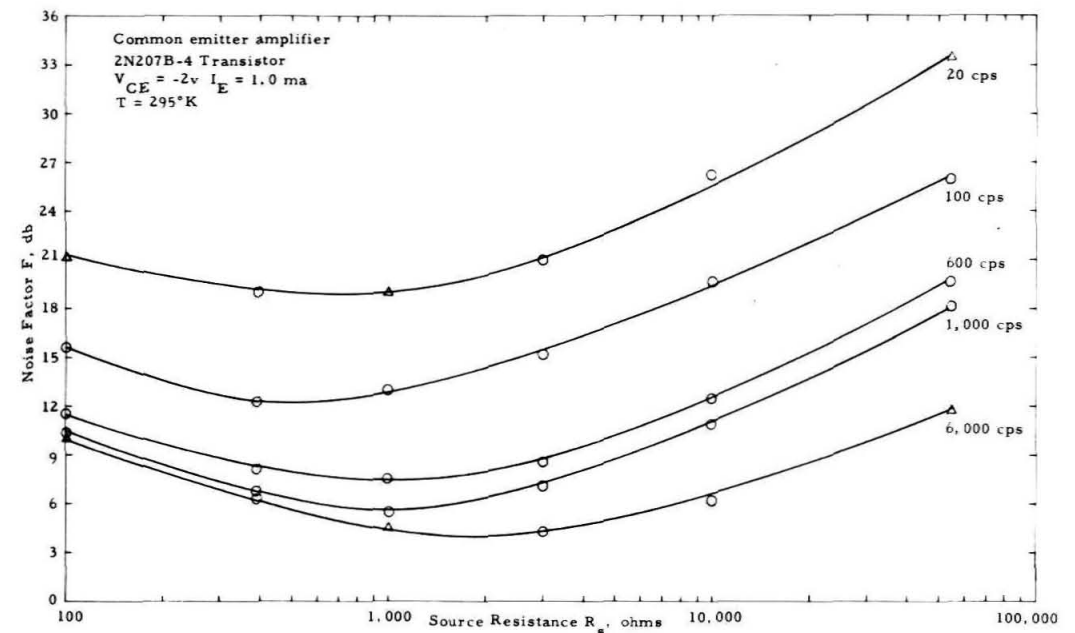
After the curves had been drawn, experimental noise measurements were made at several frequencies in the range from 6 to 20,000 cps. At each of the selected frequencies, a diverse group of source resistances was used to determine the optimizing parameters F_{min} and R_{so} . The optimizing parameters obtained from this group of measurements were then plotted as functions of frequency.

Figures 13 to 22 show the results obtained for $F_{min}(f)$ and $R_{so}(f)$ when both the simplified and the conventional optimization procedures were used. When the results of the two methods are compared, a convergence is found, in most instances, to within a fraction of a decibel in the minimum noise factor and a correspondence to within 20% in the optimum source resistance. This corroboration substantiates not only the simplified method but also the model on which the simplified procedure is based.

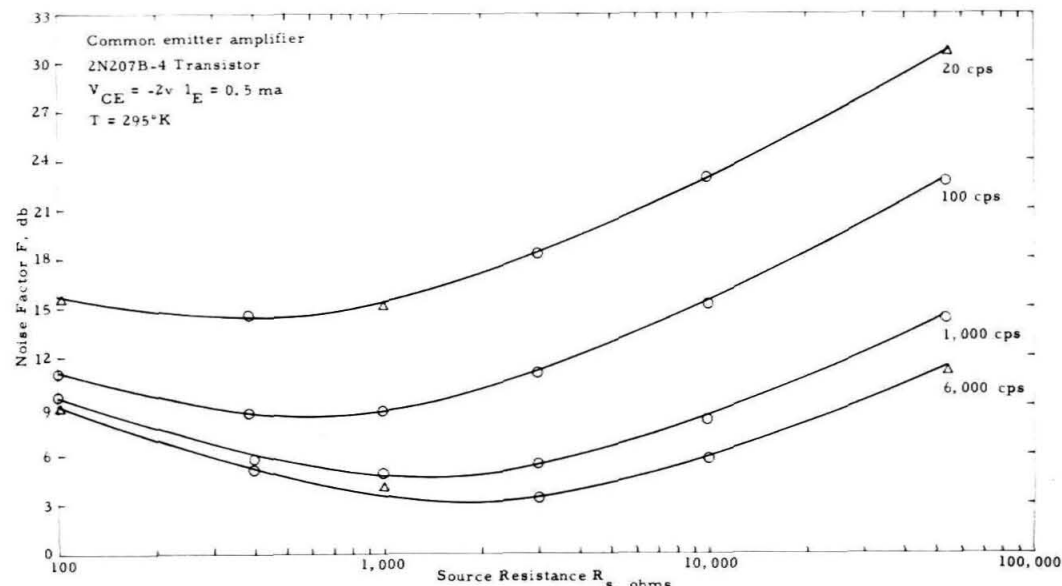
Once the validity of the simplified method has been established, it is possible to use this method to solve the optimization problem in which the source resistance and the emitter current are both controllable parameters. A partial compilation of the experimental results, which shows the



(a)

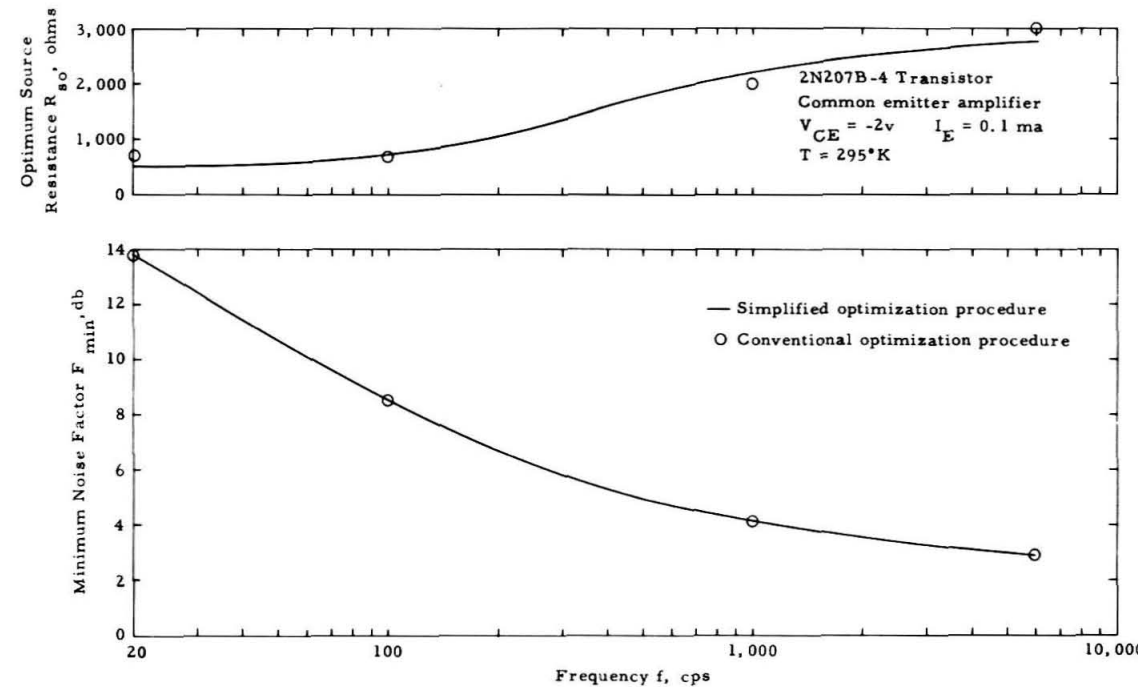


(c)

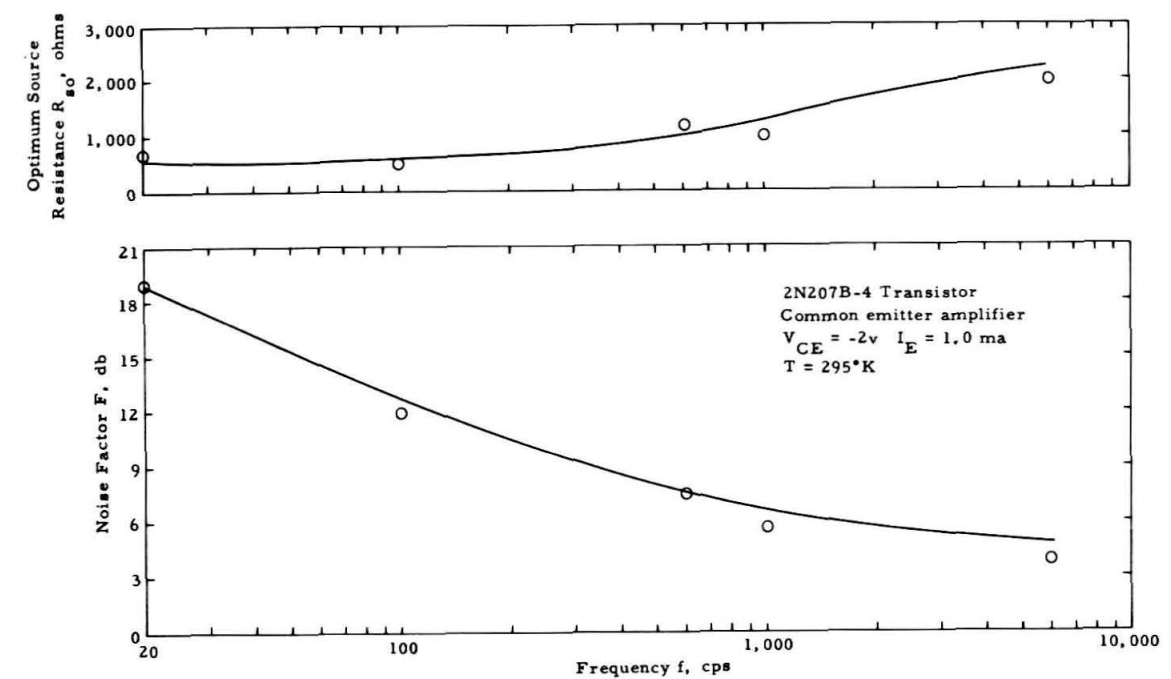


(b)

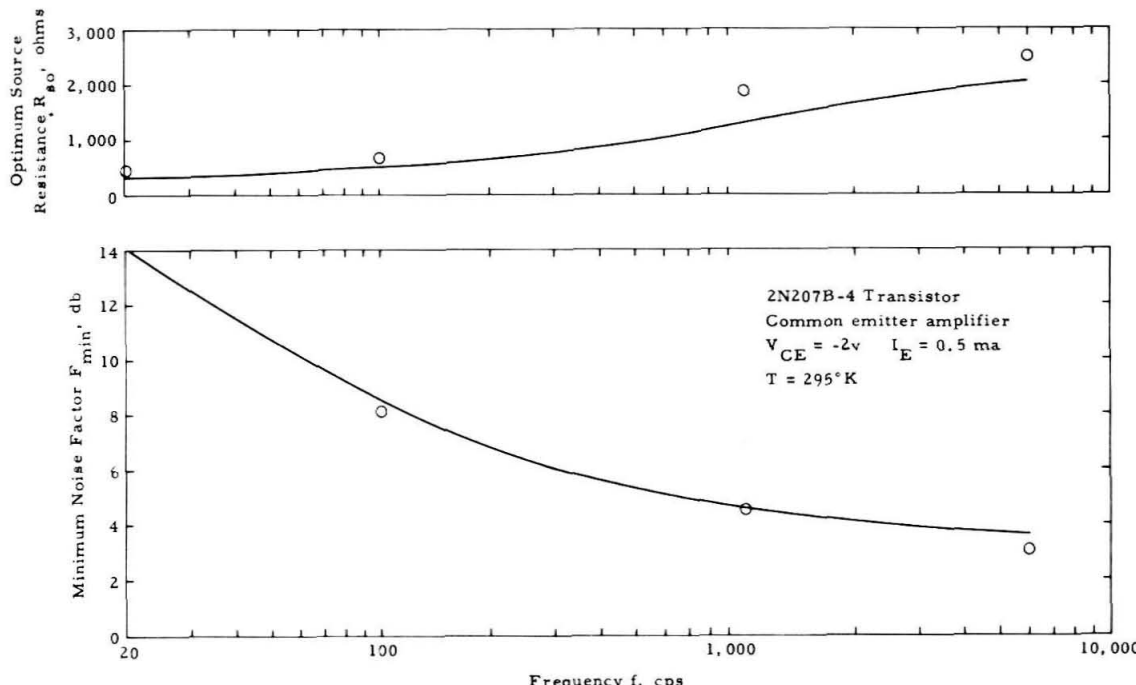
Figure 13. Noise Factor as a Function of Source Resistance for Several Frequencies in the $1/f$ and Lower Transition Region: (a) $I_E = 0.1$ ma., (b) $I_E = 0.5$ ma., (c) $I_E = 1.0$ ma.



(a)



(c)



(b)

Figure 14. Minimum Noise Factor and Optimum Source Resistance as a Function of Frequency: (a) $I_E = 0.1\text{ ma}$, (b) $I_E = 0.5\text{ ma}$, (c) $I_E = 1.0\text{ ma}$.

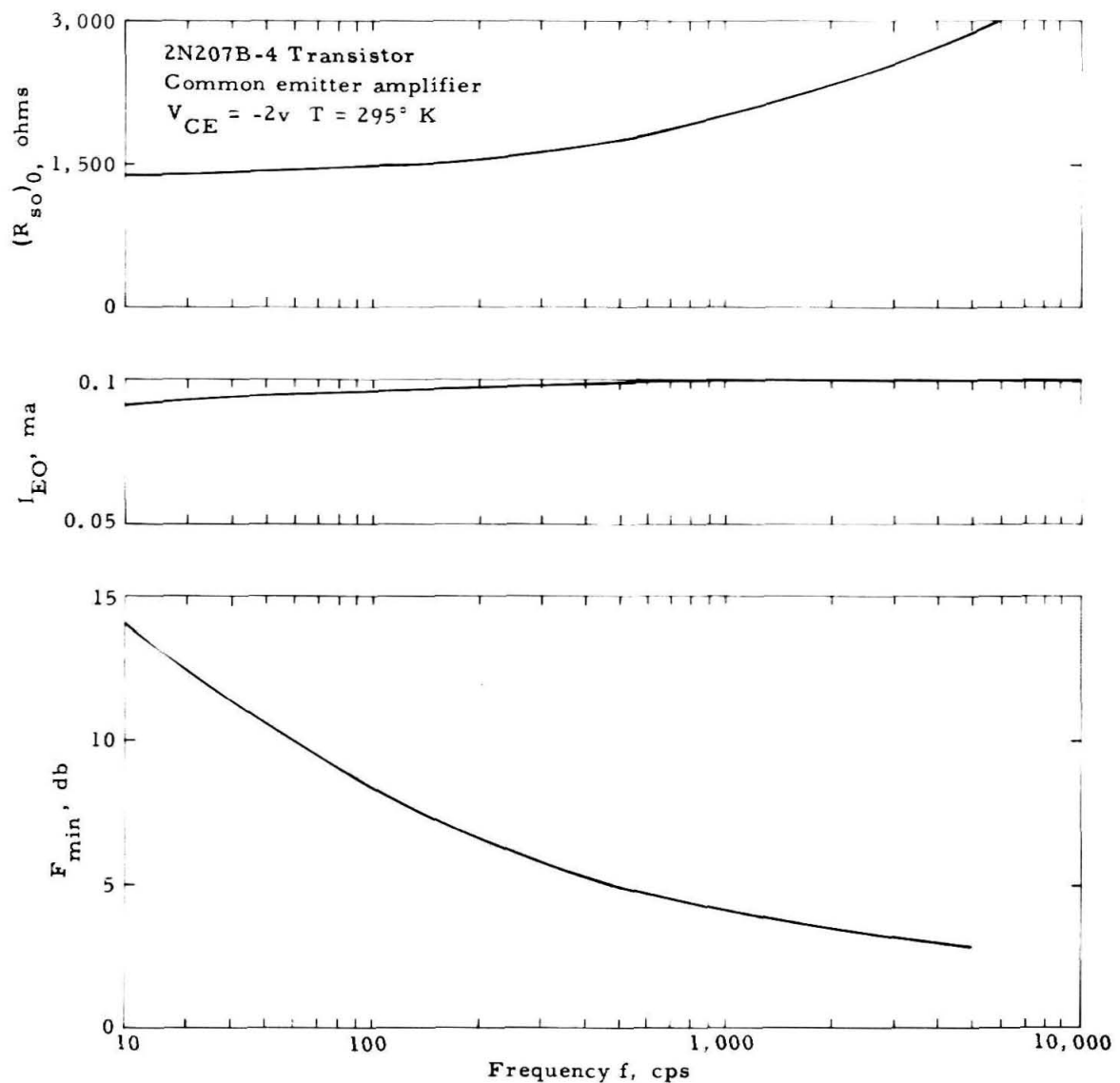
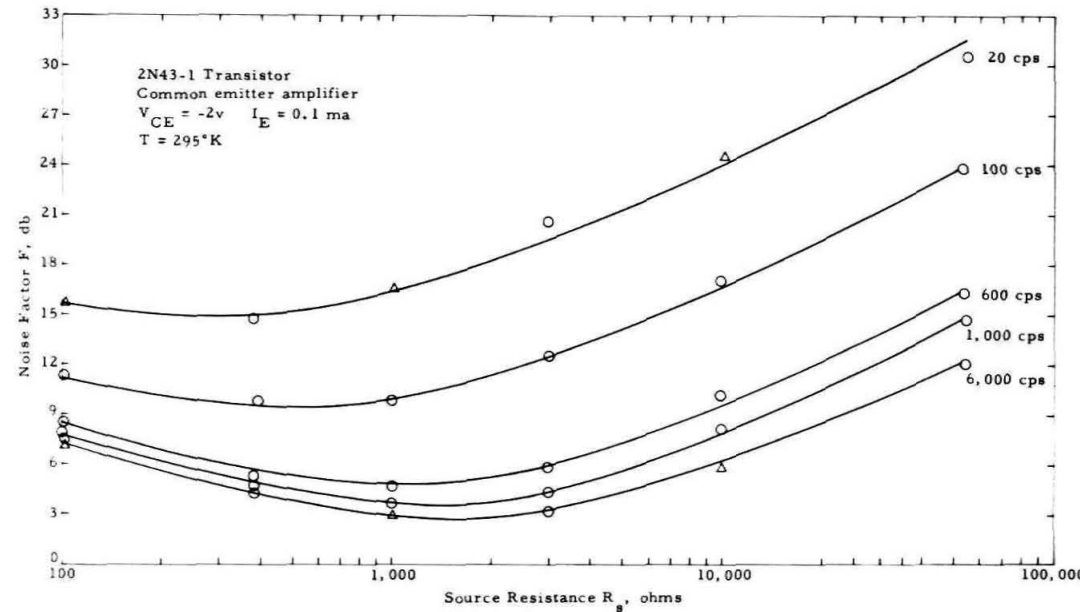
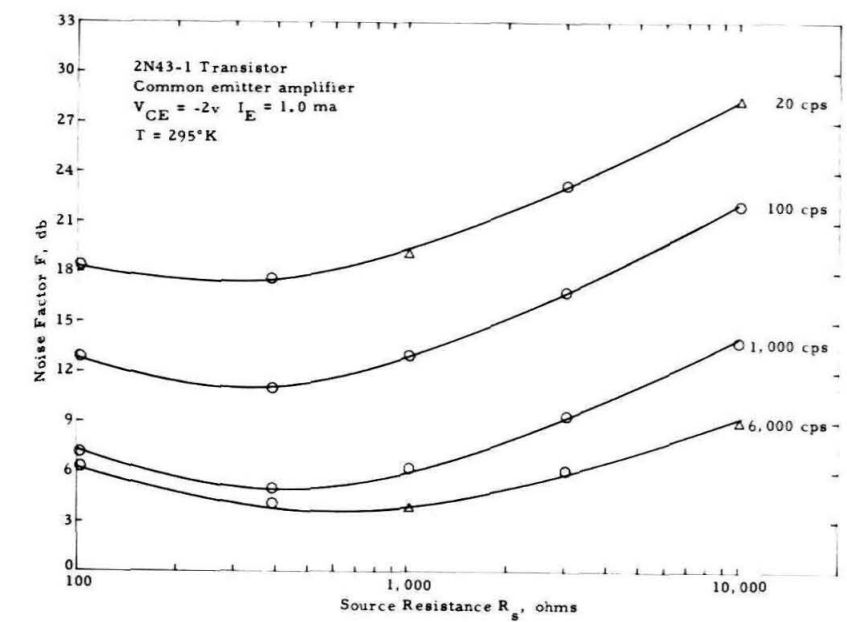


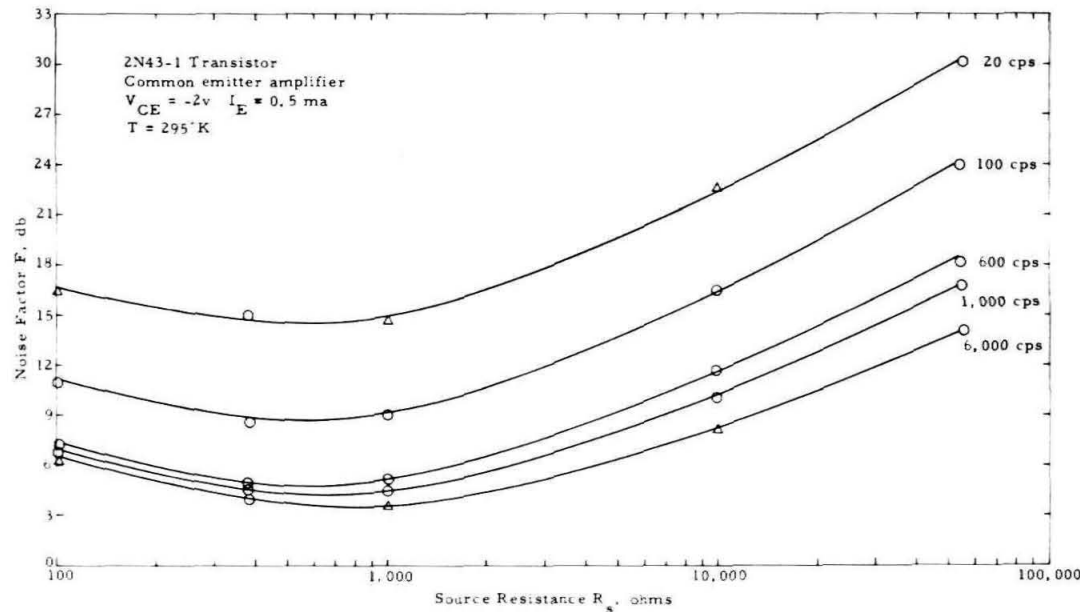
Figure 15. Minimal Noise Factor, Optimum Emitter Current, and Optimal Source Resistance as a Function of Frequency



(a)

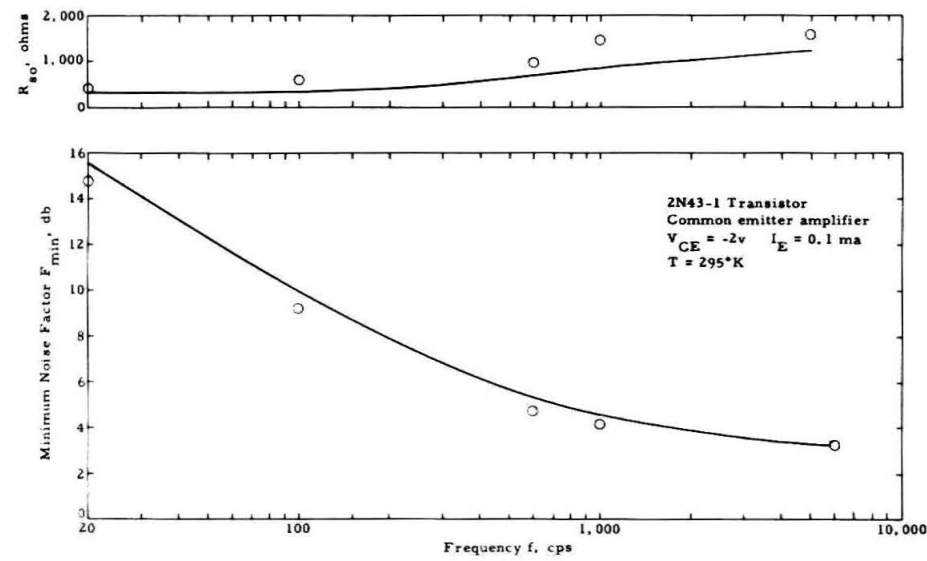


(c)

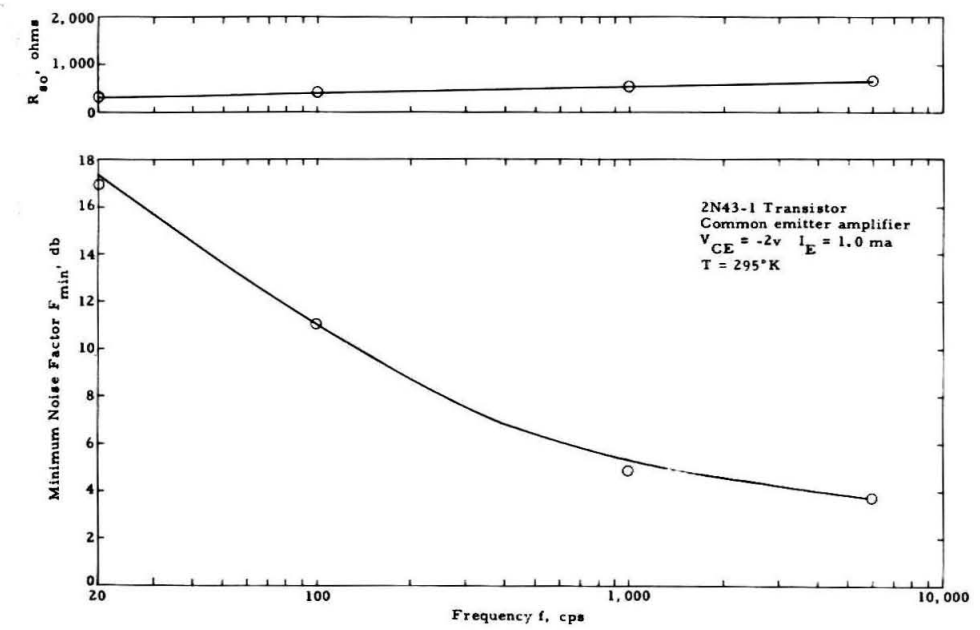


(b)

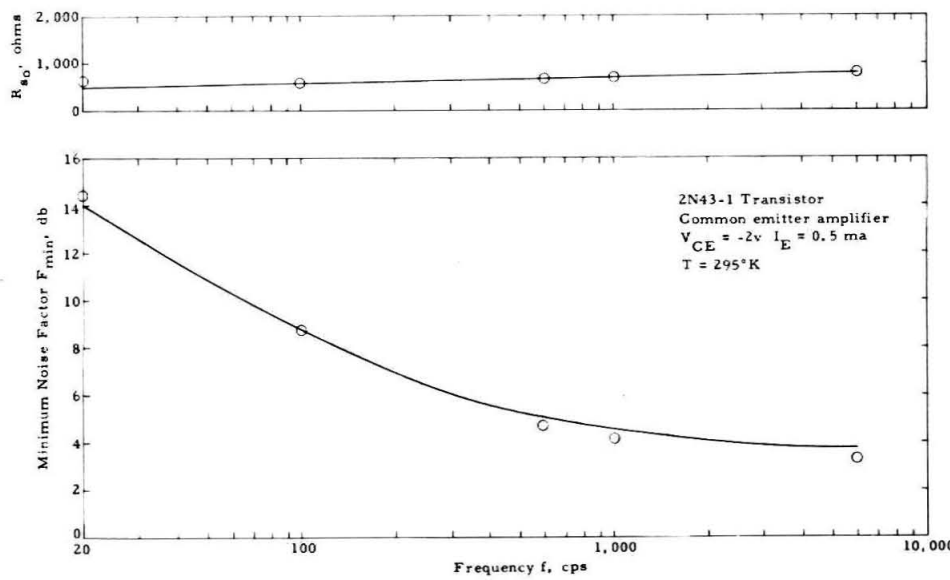
Figure 16. F vs. R_s : (a) $I_E = 0.1$ ma, (b) $I_E = 0.5$ ma, (c) $I_E = 1.0$ ma.



(a)



(c)



(b)

Figure 17. F_{min}' and R_{so}' vs. f : (a) $I_E = 0.1$ ma,
(b) $I_E = 0.5$ ma, (c) $I_E = 1.0$ ma.

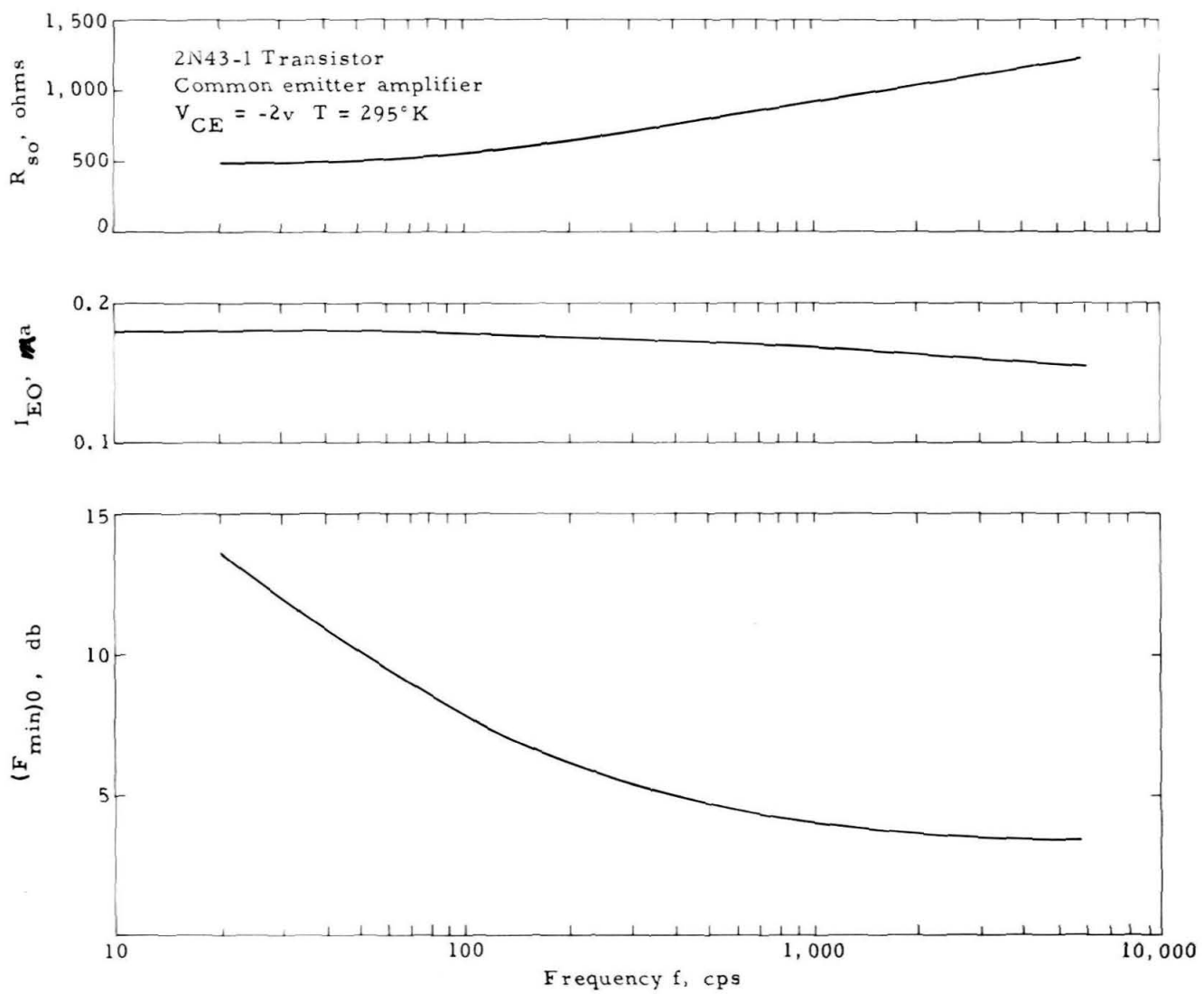
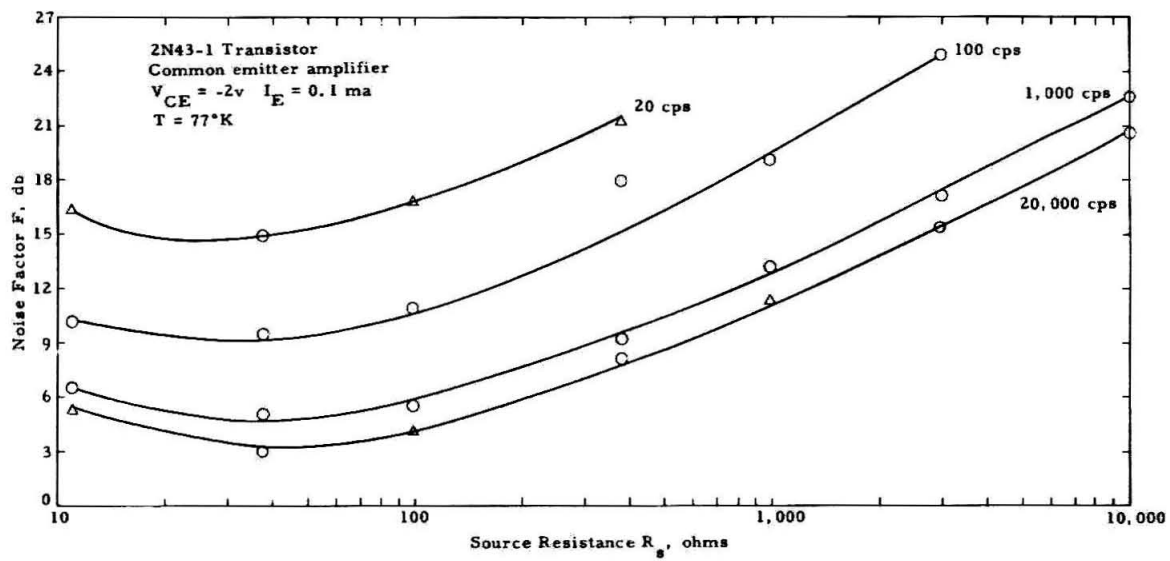
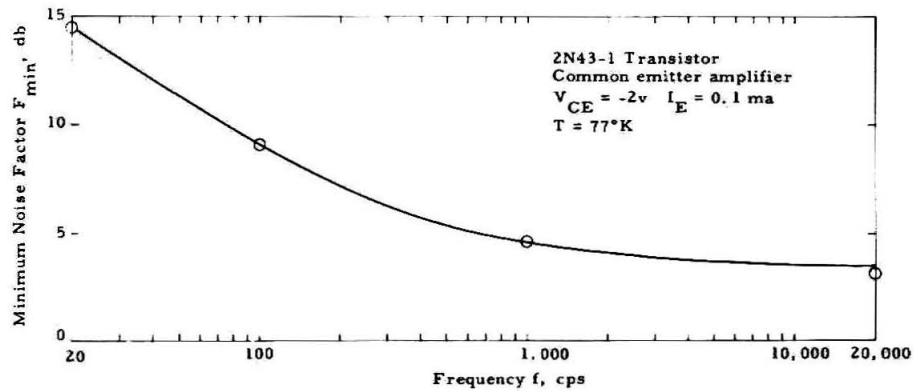
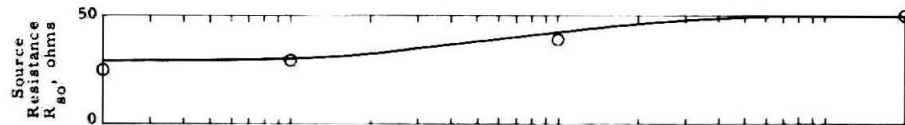


Figure 18. $(F_{min})_o$, I_{E0} , and $(R_{so})_o$ vs. f .

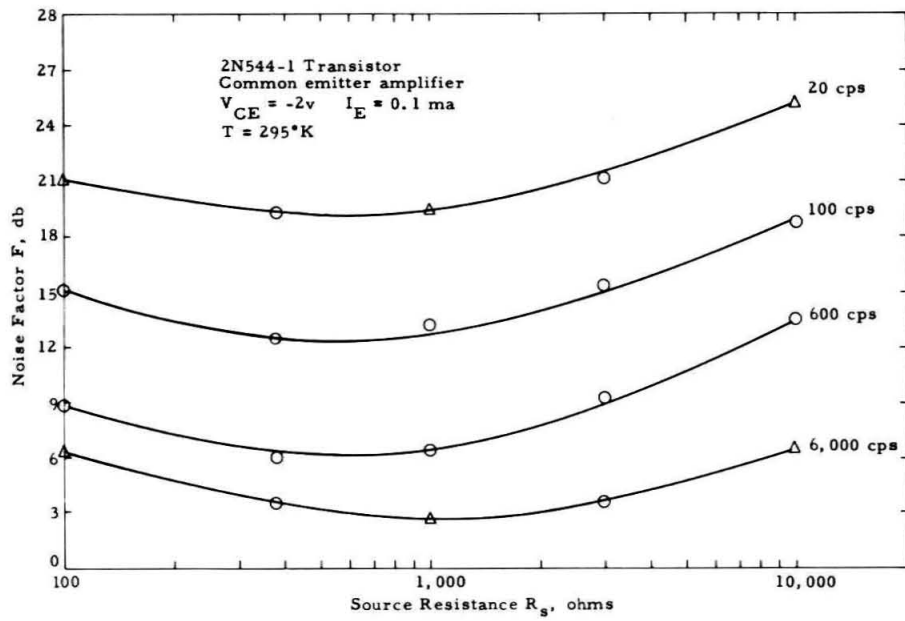


(a)

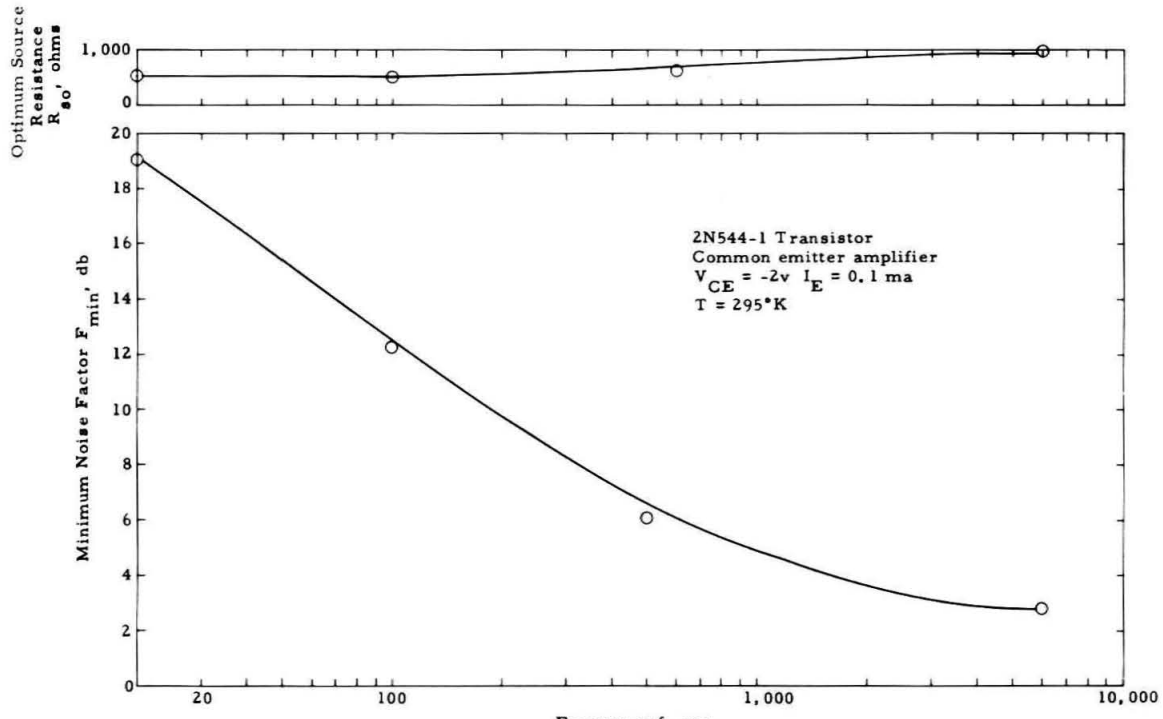


(b)

Figure 19. (a) F vs. R_s , $T = 77^{\circ}\text{K}$, (b) F_{min} vs. f , $T = 77^{\circ}\text{K}$.

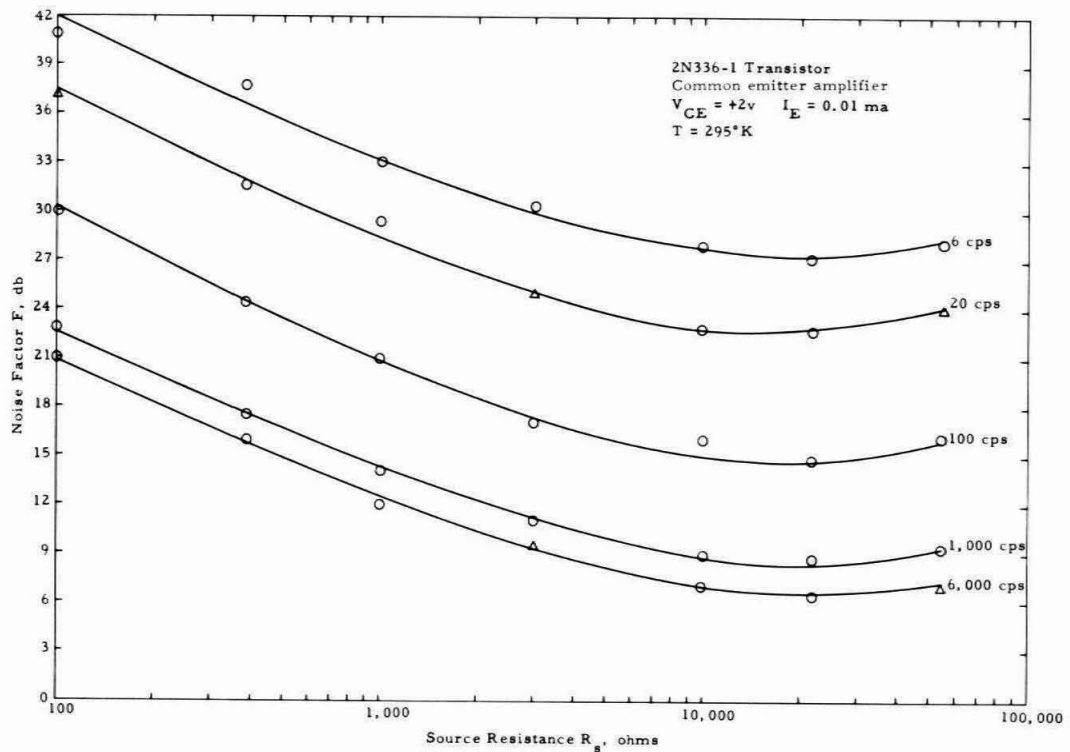


(a)

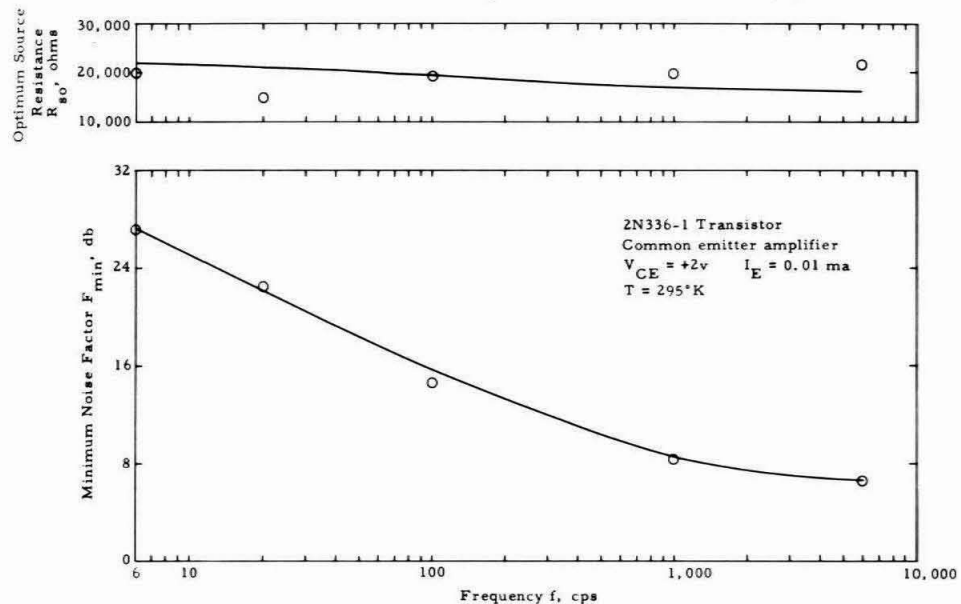


(b)

Figure 20. Noise Factor of Germanium Diffused-Base Transistor as a Function of Source Resistance, (b) Minimum Noise Factor and Optimum Source Resistance as a Function of Frequency.

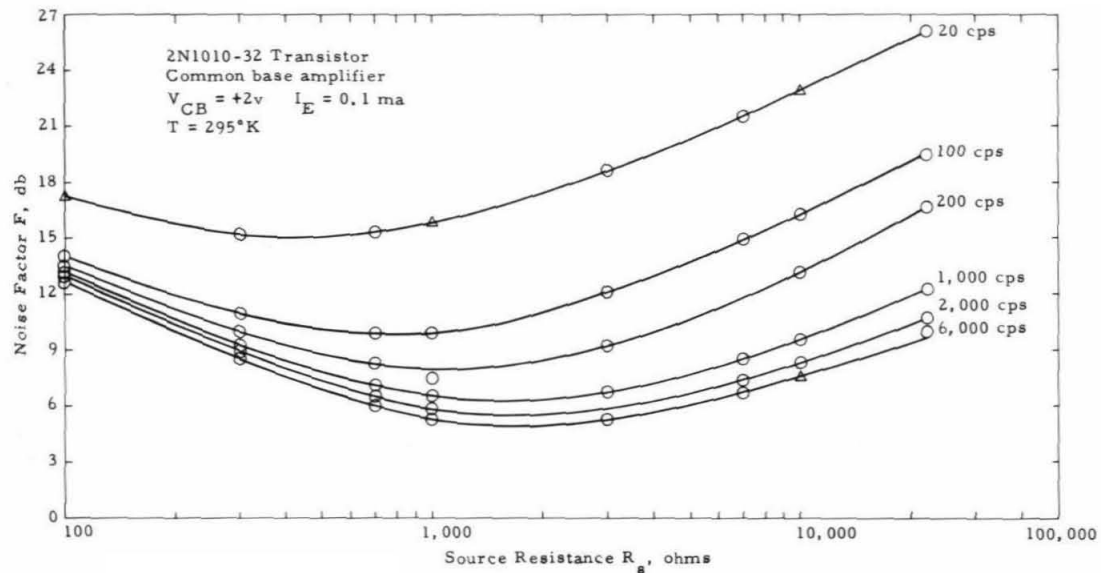


(a)

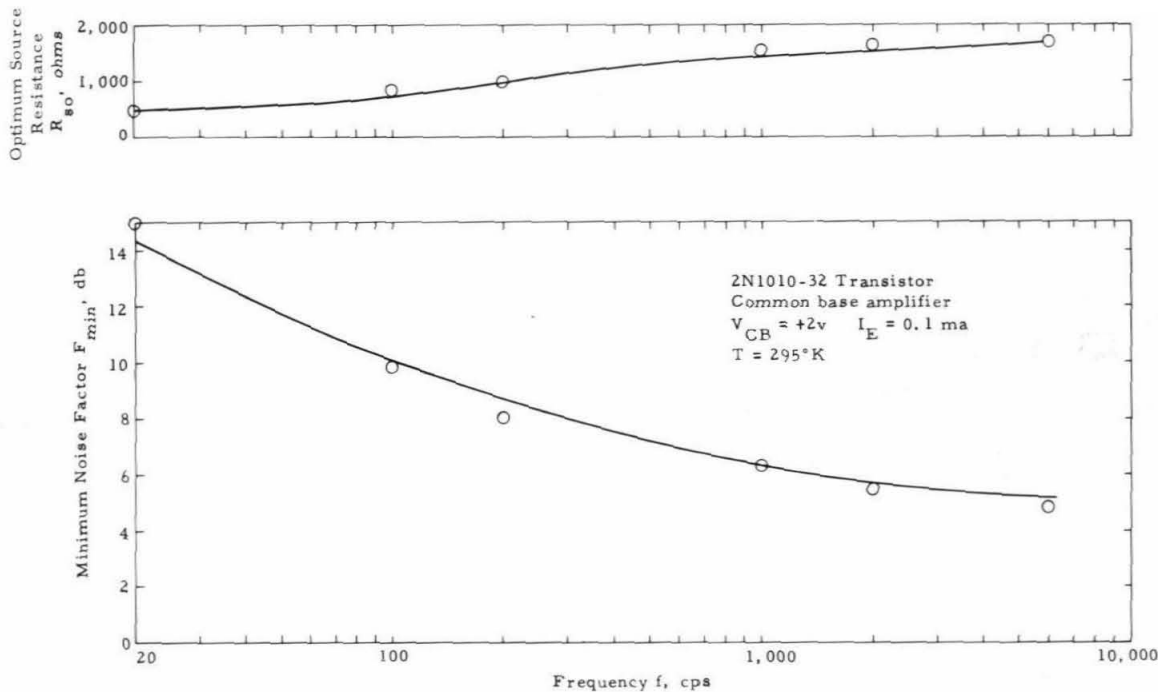


(b)

Figure 21. (a) Noise Factor of a Silicon npn Alloy-Junction Transistor as a Function of Source Resistance, (b) F_{min} and R_{so} vs. f .



(a)



(b)

Figure 22. (a) Noise Factor of Low-Noise, Germanium npn Transistor as a Function of Source Resistance, (b) F_{min} and R_{so} vs. f .

solution to this optimization problem for two of the transistors tested, is given in figures 15 and 18.

It should be noted that the selection of emitter currents used to quantify the optimization parameters $(R_{so})_0$ and I_{E0} is arbitrary. However, a discriminative set, based on van der Ziel's mean-frequency theory, proves useful in reducing the total number of measurements required to obtain $(R_{so})_0$ and I_{E0} . Although it is not applicable in the $1/f$ region, van der Ziel's theory provides an analytical expression for the optimum emitter current in the mean-frequency region. Since the noise behavior of the transistor in the lower transition region is determined partially by white noise sources existing in the unit, the value for I_{E0} obtained from van der Ziel's theory provides a starting point for determining the optimization parameters at $1/f$ and transition frequencies.

For those units tested, it was found that I_{E0} did not vary more than a factor of two as the operating frequency was shifted from $1/f$ to mean frequencies.

SOURCE RESISTANCE AS AN UNCONTROLLABLE PARAMETER

The optimization problem is greatly simplified if the source resistance is an uncontrollable parameter. Optimization now entails finding that value of emitter current which satisfies the equation

$$\frac{\partial F}{\partial I_E} = 0 \quad (2-16)$$

To further simplify the problem, Yajimi's model for the collector noise source is now employed. Yajimi proposes that, at $1/f$ frequencies,

the collector noise generator (figure 11c) can be described by

$$\overline{i_{nc}^2} = \frac{f_y}{f} \alpha(1-\alpha)2eI_E B \quad (2-17)$$

In the foregoing equation f_y is an experimentally determined parameter that is independent of emitter current and source resistance, α is the common-base current gain, and e signifies the electronic charge.

For values of source resistance much greater than the optimum source resistance it follows, from equation 2-4, that the noise factor can be approximated by

$$F(f) = K_o(f) + g_{nc}(f)R_s$$

With this assumption as to the relative magnitude of R_s , the noise factor of the common base and common emitter amplifier becomes

$$F(f) = 1 + 2g_{nc}(f)r_e + r_{b'b} - 2R\{c(f)\} \left[g_{nc}(f)R_{ne}(f) \right]^{1/2} + g_{nc}(f)R_s \quad (2-18)$$

Retaining only the dominant term in equation 2-18, the noise factor becomes

$$F(f) = g_{nc}(f)R_s \quad (2-19)$$

It is found, from Yajimi's collector noise model and equation 2-19, that for values of source resistance much greater than the optimum source resistance, the noise factor can be written

$$F(f) = \frac{f_y}{f} \frac{1-\alpha}{\alpha} \frac{eI_E}{2kT} R_s \quad (2-20)$$

From equation 2-20 it is found optimization entails operating the transistor with an emitter current that minimizes

$$\frac{1-\alpha}{\alpha} I_E \quad (2-21)$$

In typical low-noise transistors this minimum occurs with an emitter current of a few microamperes. Therefore, if noise performance is the prime consideration, and if large values of source resistance are used, it is necessary to operate the transistor with a starved emitter.

To determine the validity of Yajimi's model, noise measurements were made on a number of transistors. In these measurements the emitter current was the only independent variable. The source resistance used (22,000 ohms) was large enough to insure the validity of the assumptions that preceded equation 2-20.

Figure 23 shows the curve obtained from one set of measurements. Also presented in figure 23 is the curve obtained when equation 2-20 is used.

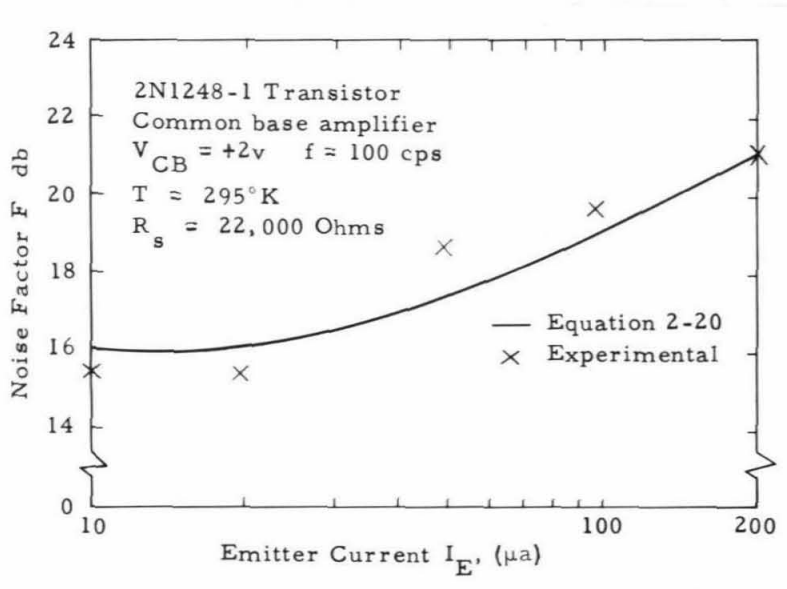


Figure 23. Noise Factor of a Low-Noise, Silicon npn Transistor as a Function of I_E . f calculated at $I_E = 200$ microamperes.

THE COLLECTOR VOLTAGE AS AN OPTIMIZATION PARAMETER

The collector voltage was first considered as a transistor optimization parameter by Volkers and Pedersen. They discovered that the noise performance obtainable from early versions of the junction transistor could be vastly improved if the collector was slightly biased in the forward direction. Their success with the hushed amplifier was due to the fact that a large portion of the $1/f$ noise generated in these early units was caused by defect channeling across the normally back biased collector-base junction. This noise is a function of the collector base leakage current, which is in turn a function of the collector-base voltage.

Defect noise was an important factor in determining the noise performance of the transistor amplifier when Volkers and Pedersen made their experimental investigations; however, present-day technology has reduced this type of noise to a point where it can now be neglected. This was corroborated by an experimental study conducted with a number of commercially available transistors. The results revealed that, for all units tested, the minimum noise factor remained constant (to within a decibel) as the collector voltage was varied from a few tenths of a volt to approximately one half the breakdown voltage. Petritz (reference 28) attributes the increase found to exist at higher collector voltages to temporary microscopic breakdowns in the base depletion layer.

CONCLUSIONS

It is apparent, from the results shown in figures 15 and 18, that a transition region exists for both the source resistance and the emitter current which will minimize the effects of internally generated transistor noise. This transition occurs as the operating region of the transistor is shifted from $1/f$ to mean frequencies. Therefore unless cognizance is taken

of the existing theory, finding parameters that will optimize the noise performance of the audio-frequency transistor amplifier requires spot noise measurements at several frequencies in the $1/f$ and transition-frequency regions. The optimization procedure can be simplified if it is assumed that the noise sources contained in the model are not functions of the input termination. It can be further simplified if the noise sources are assumed to have a $1/f$ spectral density. The experimental study described here has corroborated both of these assumptions. Although the optimization procedure has been directed toward finding the optimization parameters, the results obtained from this simplified procedure completely specify the noise performance of the amplifier under any set of operating conditions.

An interesting aspect of the experimental study concerns the frequency dependence of the optimization parameter, R_{SO} . As the frequency was increased from the $1/f$ region, it was found, without exception, the optimum source resistance also increased. This can be explained by examining the two noise sources contained in the transition-frequency noise model. If it is assumed that the emitter noise source contained in this model can be neglected, the optimum source resistance becomes $r_e + r_{b'b}$. On the other hand, if it is assumed that the collector noise source can be neglected, the optimum source resistance becomes infinite. From this cursory analysis and the results of the experimental study, it is apparent that the collector noise plays a more dominant role in determining the noise performance of the transistor amplifier at $1/f$ frequencies than it does at mean frequencies.

It is also found that if the emitter noise source can be neglected at $1/f$ frequencies (which is an apparently valid assumption in the light of the results of the experimental study), and if the validity of Yajimi's

model is assumed, then an analytical solution to the optimization problem when both the source resistance and the emitter current are controllable parameters can be obtained. This solution becomes, for the common-base and common-emitter amplifier operated at $1/f$ frequencies

$$I_{E0} = \frac{kT}{er_{b'b}} \quad (2-22)$$

$$(R_{so})_o = 2r_{b'b} \quad (2-23)$$

For the 2N207B transistor, whose optimization curves are presented in figure 15, there is obtained for the optimization parameters (at 20cps)

$$I_{E0} = 0.08 \text{ ma}$$

$$(R_{so})_o = 1,200 \text{ ohms}$$

From equations 2-22 and 2-23, the optimization parameters become

$$I_{E0} = 0.065 \text{ ma}$$

$$(R_{so})_o = 800 \text{ ohms}$$

The experimental and theoretical results for the 2N43 transistor (figure 18) are

$$I_{E0} = 0.18 \text{ ma} \quad \text{measured}$$

$$(R_{so})_o = 500 \text{ ohms}$$

$$I_{E0} = 0.14 \text{ ma} \quad \text{calculated}$$

$$(R_{so})_o = 380 \text{ ohms}$$

HIGH FREQUENCY REGION

The problems involved in the design of low-level transistor amplifiers, which operate in the audio-frequency portion of the spectrum, are made critical by the existence of surface noise that exhibits a $1/f$ frequency dependence. This design problem is again made critical at very high frequencies by the existence, in both vacuum tubes and transistors, of mean-square noise currents which now exhibit an f^2 frequency dependence.

Although additional theory was required to explain the f^2 (or induced grid) noise exhibited by the vacuum tube amplifier, no additional theory is required for the transistor circuit. Here, the f^2 noise is caused by the implicit frequency dependence contained in α and y_e , two parameters used by van der Ziel to quantify the noise generators contained in his mean-frequency model.

In this section it is assumed that the frequency dependence of α , the common-base current gain, can be expressed as

$$\alpha = \frac{\alpha_0}{1 + jf/f_c} \quad (3-1)$$

where α_0 is the low frequency value of the common-base current gain, $j = \sqrt{-1}$, and f_c is the alpha-cutoff frequency.

It is further assumed that the a.c. emitter junction admittance

$$y_e = y_{eo} (1 + jf/f_c) \quad (3-2)$$

With these assumptions and van der Ziel's noise model, the frequency dependence of the three noise factor parameters, $K_o(f)$, $R_{no}(f)$ and $G_{nc}(f)$ can be formulated.

From these results, the optimization problem in which the controllable parameters are the source resistance and the source reactance is solved.* The solution obtained shows that operating the transistor amplifier with a source reactance equal to its optimum value does little to improve the noise performance of the amplifier. The solution further shows that by optimizing the source resistance it becomes possible to obtain reasonably low noise factors up to the alpha cutoff frequency f_c . An experimental investigation is made to verify the derived results.

VAN DER ZIEL'S NOISE MODEL

Part a of figure 24 depicts van der Ziel's noise model connected in the common-base configuration. Here

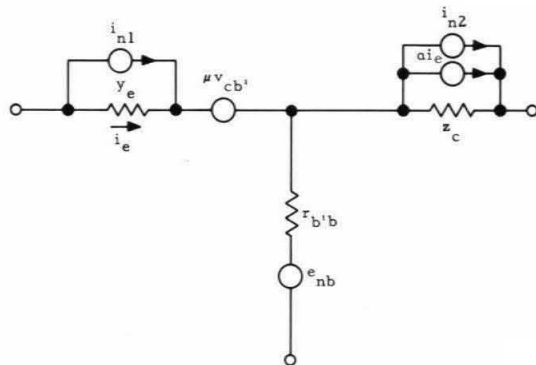


Figure 24a. Transistor High-Frequency Noise Model.

*The emitter current is not considered as a controllable parameter because it was found impossible to formulate the alpha cutoff frequency as an explicit function of I_E .

$$\overline{i_{nl}^2} = 4kTR(y_e)B - 2eI_E B \quad (3-3a)$$

$$\overline{i_{n2}^2} = 2eI_C B + 4kTR(y_c)B \quad (3-3b)$$

$$\overline{i_{nl}^* i_{n2}} = -2kTy_{ec} B = 2kTay_e B \quad (3-3c)$$

$$\overline{e_{nb}^2} = 4kTr_{b'b} B \quad (3-3d)$$

A simplified representation of the noise model shown in figure 24a is illustrated in figure 24b. Equivalence is retained in the two models if

$$\mu v_{cb} = 0 \quad (3-4)$$

$$e_{ne} = i_{nl}/y_e \quad (3-5)$$

$$i_{nc} = i_{n2} - \alpha i_{nl} \quad (3-6)$$

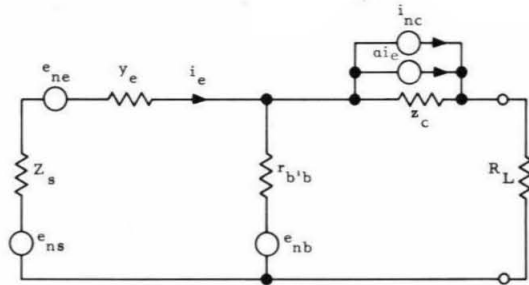


Figure 24b. Equivalent Representation of High-Frequency Noise Model Connected as Common-Base Amplifier.

Referring to figure 24b, if it is assumed that

$$r_e = \frac{kT}{eI_E} = \frac{1}{y_{eo}} \quad (3-7)$$

and

$$I_C = \alpha I_E + I_{C0} \quad (3-8)$$

it follows, from equations 3-1 through 3-8, that the generators contained in this model will have mean-square values given by

$$\overline{e_{ne}^2} = \frac{2kT r_e B}{1 + f^2/f_c^2} \quad (3-9a)$$

$$\overline{i_{nc}^2} = \frac{2eI_E \alpha_o (1 - \alpha_o + f^2/f_c^2) B}{1 + f^2/f_c^2} + 2eI_{C0} B \quad (3-9b)$$

The cross-correlation term becomes

$$\overline{e_{ne}^* i_{nc}} = j \frac{2kT \alpha_o f/f_c}{1 + f^2/f_c^2} \quad (3-9c)$$

where $j = \sqrt{-1}$.

From figure 24b and equations 3-9a, 3-9b, and 3-9c, it is now possible to formulate the noise factor and the noise factor parameters for the transistor amplifier in each of its three configurations.

COMMON BASE AND COMMON EMITTER AMPLIFIER

If it is assumed*

$$\overline{e_{nb}^2} \ll \overline{i_{nc}^2} |z_c|^2 \quad (3-10a)$$

$$\overline{e_{ne}^2} \ll \overline{i_{nc}^2} |z_c|^2 \quad (3-10b)$$

and

$$r_{bb} \ll z_c / \alpha^* \quad (3-10c)$$

*These assumptions are valid (under normal biasing conditions) at low frequencies. However, owing to the capacitive component of z_c , they are increasingly less valid at higher frequencies. They are retained as assumptions because of the simplicity they add to the noise factor formulation.

the noise factor obtained for the common-base transistor stage is identical to that obtained when the stage is connected in the common-emitter configuration. This becomes

$$F = 1 + \frac{\overline{e_{ne}^2}}{\overline{e_{ns}^2}} + \frac{\overline{e_{nb}^2}}{\overline{e_{ns}^2}} + \frac{\overline{i_{nc}^2} |Z_s + z_e + r_b' b|^2}{|\alpha|^2 \overline{e_{ns}^2}} + 2R \left\{ \frac{\overline{e_{ne}^* i_{nc}}}{\alpha^*} (Z_s + z_e + r_b' b) \right\} \quad (3-11)$$

If the source resistance (R_s) and the source reactance (X_s) are the only two controllable parameters, minimizing the noise factor of the transistor stage entails driving the stage from an impedance for which

$$\frac{\partial F}{\partial R_s} = 0 \quad (3-12a)$$

$$\frac{\partial F}{\partial X_s} = 0 \quad (3-12b)$$

Performing the differentiation prescribed by equation 3-12b on equation 3-11, there is obtained for the optimum source reactance

$$X_{so} = -x_e + \frac{|\alpha|^2}{i_{nc}^2} I_m \left\{ \frac{\overline{e_{ne}^* i_{nc}}}{\alpha^*} \right\} \quad (3-13)$$

From equations 3-1, 3-2, 3-9b, 3-9c, and 3-13, this becomes

$$X_{so} = \frac{r_e f/f_c}{1+f^2/f_c^2} + \frac{2kT\alpha_o^2 f/f_c}{\left(1+f^2/f_c^2\right) \left[2eI_E\alpha_o \left(1-\alpha_o + f^2/f_c^2\right) + 2eI_{C0} \left(1+f^2/f_c^2\right) \right]} \quad (3-14)$$

or

$$X_{so} = \frac{r_e f/f_c}{1+f^2/f_c^2} \left(1 + \frac{\beta_o}{1 + \Gamma + f^2/f_c^2 \left[\Gamma + \beta_o/\alpha_o \right]} \right) \quad (3-15)$$

where β_o is the low frequency, common-emitter current gain and Γ is the collector cutoff current noise parameter,

$$\Gamma = \frac{\beta_o I_{C0}}{\alpha_o^2 I_E}$$

For typical values of Γ (see tables 2-1, 2-2, and 2-3), it can safely be assumed that $\beta_o \gg \Gamma$. With this assumption, equation 3-15 reduces to

$$X_{so} = \frac{r_e f/f_c}{1 + f^2/f_c^2} \left[1 + \frac{\beta_o}{1 + \Gamma + \beta_o/\alpha_o (f^2/f_c^2)} \right] \quad (3-16)$$

Figure 25 illustrates the frequency dependence of the optimum source reactance formulated in equation 3-16.

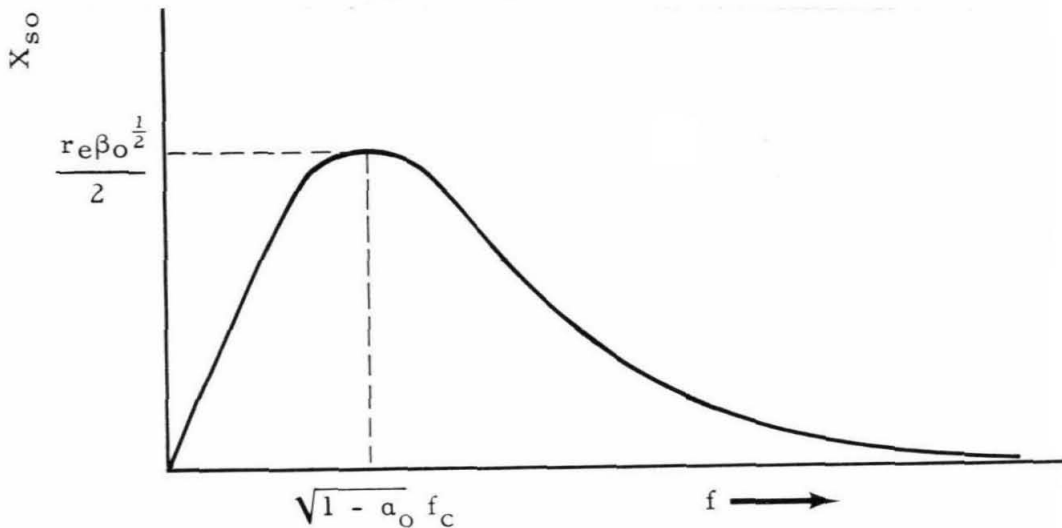


Figure 25. Optimum Source Reactance as a Function of Frequency.

In order to determine whether any appreciable improvement in the noise performance of a transistor amplifier can be made by optimizing the source reactance, this parameter is matched at that frequency at which X_{so} is a maximum. This value for the optimum source reactance and the frequency at which it occurs are then substituted for X_s and f in the noise factor equation (3-11). By this procedure, the noise factor parameters with re-

active matching can be determined.

This procedure is repeated, assuming the source is real, i.e., $X_s = 0$. Any noticeable improvement in the noise performance of the amplifier can then be ascertained by a comparison of the respective noise-factor parameters.

The frequency at which X_{so} is a maximum can be found by differentiating equation 3-16 with respect to frequency and equating the resulting differential to zero. With the assumptions

$$\beta_o \gg 1$$

$$\Gamma \ll 1$$

this differentiation yields, for the frequency at which the source reactance is a maximum,

$$f|_{X_{so_{max}}} = \sqrt{1-\alpha_o} f_c \quad (3-17)$$

From equations 3-16 and 3-17, the maximum optimum source reactance becomes

$$X_{so_{max}} = \frac{r_e \sqrt{1-\alpha_o}}{1 + (1-\alpha_o)} \left(1 + \frac{\beta_o}{1 + \Gamma + \alpha_o} \right) \sim \frac{r_e \beta_o}{2}^{1/2} \quad (3-18)$$

Substituting $\sqrt{1-\alpha_o} f_c$ for f and $\frac{r_e \beta_o}{2}^{1/2}$ for X_{so} in equation 3-11

gives for the noise-factor parameters

$$(K_o)_{X_s=X_{so}} = 1 + \frac{2}{\beta_o r_e} (1 + \Gamma/2) (r_{b'b} + r_e) \quad (3-19a)$$

$$(R_{no})_{X_s=X_{so}} = \frac{r_e}{4} + r_{b'b} + \frac{1}{\beta r_e} (1 + \Gamma/2) \left[(r_{b'b} + r_e)^2 \right] + \frac{r_e}{8} \quad (3-19b)$$

$$(G_{nc})_{X_s=X_{so}} = \frac{1}{\beta_o r_e} (1 + \Gamma/2) \quad (3-19c)$$

From equation 3-11, with $X_S = 0$ and $f = \sqrt{1-\alpha_o} f_c$, the noise-factor parameters become

$$(K_o)_{X_S=0} = \alpha_o + \frac{2}{\beta_o r_e} \left[(1 + \Gamma/2)(r_{b\parallel b} + r_e) \right] \quad (3-19d)$$

$$(R_{no})_{X_S=0} = \frac{r_e \alpha_o}{2} + r_{b\parallel b} \alpha_o + \frac{1 + \Gamma}{2\beta_o r_e} (r_e + r_{b\parallel b})^2 \quad (3-19e)$$

$$(G_{nc})_{X_S=0} = \frac{1}{\beta_o r_e} (1 + \Gamma/2) \quad (3-19f)$$

A comparison of the two preceding sets of equations reveals that optimizing the source reactance does not significantly alter the noise performance of the amplifier. Since this is the case, it will be assumed that the driving source is real.

With $X_S = 0$, the frequency-dependent noise-factor parameters for the common-base and common-emitter stage become

$$K_o(f) = 1 + \frac{1}{\beta_o r_e} \left[(1 + \Gamma)(r_e + r_{b\parallel b}) + \frac{f^2}{f_c^2} (1 + \beta_o + \Gamma) r_{b\parallel b} \right] \quad (3-20a)$$

$$R_{no}(f) = r_e/2 + r_{b\parallel b} + \frac{(1 + \Gamma)}{2\beta_o r_e} (r_e + r_{b\parallel b})^2 + \frac{f^2}{f_c^2} \left(\frac{1}{\alpha_o} + \frac{\Gamma}{\beta_o} \right) \frac{r_{b\parallel b}}{2r_e} \quad (3-20b)$$

$$G_{nc}(f) = \frac{(1 + \Gamma)}{2\beta_o r_e} + \frac{f^2}{f_c^2} \left(\frac{\beta_o + 1 + \Gamma}{\beta_o} \right) \frac{1}{2r_e} \quad (3-20c)$$

Here,

$$\beta_o = \frac{\alpha_o}{1 - \alpha_o} \quad (3-20d)$$

$$\Gamma = \frac{\beta_o I_{CO}}{\alpha_o^2 I_E} \quad (3-20e)$$

Inspection of equations 3-20a, 3-20b, and 3-20c reveals that these three equations can also be written in the form

$$K_o^1(f) = K_{oo}^1 \left(1 + f^2/f_4^2 \right) \quad (3-21a)$$

$$R_{no}(f) = R_{noo} \left(1 + f^2/f_6^2 \right) \quad (3-21b)$$

$$G_{nc}(f) = G_{nco} \left(1 + f^2/f_8^2 \right) \quad (3-21c)$$

Here, $K_o^1(f) = K_o^1(f) - 1$. K_{oo}^1 , R_{noo} , and G_{nco} are the mean-frequency noise-factor parameters.

With the added assumptions

$$\beta_o \gg 1 \quad (3-22)$$

$$r \ll 1 \quad (3-23)$$

the corner frequencies (f_4 , f_6 , and f_8) become, for the common-base and common-emitter amplifier

$$f_4 = \left(\frac{r_e}{r_{b'b}} \right)^{1/2} f_c \quad (3-24a)$$

$$f_6 = \frac{r_e}{r_{b'b}} \left(1 + \frac{2r_{b'b}}{r_e} \right)^{1/2} f_c \quad (3-24b)$$

$$f_8 = \left(\frac{1}{1 + \beta_o} \right)^{1/2} f_c \quad (3-24c)$$

Equations 3-24a, 3-24b, and 3-24c reveal that, for typical values of r_e , $r_{b'b}$, and β_o , a great latitude exists in the magnitude of the corner frequencies. The effects of this divergence on the noise performance of the amplifier can be ascertained by examining the optimizing parameters R_{so} and F_{min} .

It follows, from equations 1-11, 3-21a, 3-21b, and 3-21c, that for the common-base and common-emitter transistor amplifier

$$F_{\min}(f) - 1 = K_{\text{oo}}(1 + f^2/f_4^2) + 2(R_{\text{nno}}G_{\text{nco}})^{1/2} \cdot \left[1 + f^2 \left(\frac{1}{f_6^2} + \frac{1}{f_8^2} + \frac{f^4}{f_6^2 f_8^2} \right) \right]^{1/2} \quad (3-25)$$

Since, for typical values of r_e , $r_{b'b}$, and β_o , it can safely be assumed that

$$f_8 \ll f_4 \quad (3-26)$$

$$f_8 \ll f_6 \quad (3-27)$$

the minimum noise factor, for frequencies less than the corner frequency f_4 , can be written as

$$F_{\min}(f) = K_{\text{oo}} + 2(R_{\text{nno}}G_{\text{nco}})^{1/2} \left(1 + \frac{f^2}{f_8^2} \right)^{1/2} \quad (3-28)$$

Expanding equation 3-28 in a Taylor series, it is found that for frequencies where

$$f_4 > f > f_8$$

the minimum noise factor can be approximated by

$$F_{\min}(f) = F_{\min \circ} (1 + f/f_k) \quad (3-29)$$

Here, $F_{\min \circ}$ is the mean-frequency value of the minimum noise factor and f_k is a corner frequency given by

$$f_k = \frac{2(R_{\text{nno}}G_{\text{nco}})^{1/2}}{K_{\text{oo}}} f_8 \quad (3-30)$$

The interesting aspect of equation 3-30 is that, although each of the noise-factor parameters has a double zero at its corner frequency, the minimum noise factor has a single zero at the corner frequency f_k ; therefore the minimum noise factor increases at a rate of 3 db/octave in the frequency

region analyzed. Thus, it should be possible to obtain reasonably low noise factors up to the frequency f_4 . To determine the values of source resistance that must be used to obtain this performance, the second optimizing parameter, R_{so} , is now examined.

It follows, from equations 1-10, 3-21b, and 3-21c, that for the common-base and common-emitter amplifier

$$R_{so}(f) = R_{soo} \left(\frac{1 + f^2/f_6^2}{1 + f^2/f_8^2} \right)^{1/2} \quad (3-31)$$

For frequencies where

$$f_6 > f > f_8$$

the optimum source resistance can be approximated by

$$R_{so}(f) = R_{soo} f_8/f \quad (3-32)$$

For frequencies greater than the corner frequency f_6 , the optimum source resistance approaches an asymptotic value given by

$$R_{soo} \frac{f_8}{f_6} \quad (3-33)$$

In typical applications $f_8 \ll f_6$; therefore, extremely low values of source resistance must be used to obtain reasonably low noise factors when the transistor is operated in the f^2 frequency region.

COMMON-COLLECTOR TRANSISTOR AMPLIFIER

If it is assumed (part b of figure 24) that

$$\beta_o r_e^2 \ll |z_c|^2 \quad (3-34)$$

$$\frac{2}{y_e} \ll R_L \quad (3-35)$$

$$r_{b'b} \ll \frac{2z_c}{1 + z_c/z_c^*} \quad (3-36)$$

$$K_o(f) = 1 + \frac{\alpha_o^2 r_{b'b}}{\beta_o r_e} \left(\frac{1 + \beta_o f^2/f_c^2}{1 + f^2/f_c^2} + \Gamma \right) \quad (3-37a)$$

$$R_{no}(f) = r_{b'b} + \frac{r_e}{2(1 + f^2/f_c^2)} + \frac{\alpha_o^2 r_{b'b}^2}{2\beta_o r_e} \left(\frac{1 + \beta_o f^2/f_c^2}{1 + f^2/f_c^2} + \Gamma \right) \quad (3-37b)$$

$$G_{nc}(f) = \frac{\alpha_o^2}{2\beta_o r_e} \left(\frac{1 + \beta_o f^2/f_c^2}{1 + f^2/f_c^2} + \Gamma \right) \quad (3-37c)$$

Inspection of equations 3-37a, 3-37b, and 3-37c reveals that they can be written in the following form

$$K_o'(f) = K_{oo}' \left(\frac{1 + f^2/f_4^2}{1 + f^2/f_c^2} \right) \quad (3-38a)$$

$$R_{no}(f) = R_{noo} \left(\frac{1 + f^2/f_9^2}{1 + f^2/f_c^2} \right) \quad (3-38b)$$

$$G_{nc}(f) = G_{nco} \left(\frac{1 + f^2/f_8^2}{1 + f^2/f_c^2} \right) \quad (3-38c)$$

Here, it is assumed

$$\beta_o \gg 1 \quad (3-39)$$

$$\Gamma \ll 1 \quad (3-40)$$

Also, in the foregoing equations,

$$f_9 = \left(\frac{2 + r_e/r_{b'b}}{2 + r_{b'b}/r_e} \right)^{1/2} f_c \quad (3-41)$$

For the common-collector stage, the optimizing parameter F_{min} has a spectral form given by

$$F_{\min}(f) - 1 = \frac{1}{1 + f^2/f_c^2} K_{\text{oo}}^1 (1 + f^2/f_4^2) + 2(R_{\text{noo}} G_{\text{nco}})^{1/2} \cdot (1 + f^2/f_8^2 + f^2/f_7^2 + f^4/f_8^2 f_9^2)^{1/2} \quad (3-42)$$

It is observed, from equation 3-42, that for frequencies where $f < f_c$ the high-frequency behavior of the common-collector stage is nearly identical to that derived for the common-base amplifier. The small difference that exists is due to a difference in the corner frequency associated with the input short circuit noise resistance, $R_{\text{no}}(f)$.

For the common-base and common-emitter amplifier, the optimizing parameter F_{\min} increases with a f^2 frequency dependence for frequencies above f_c . However, for the common-collector amplifier, $F_{\min}(f)$ approaches an asymptotic value given by

$$F_{\min}(f \rightarrow \infty) = K_{\text{oo}} \left(\frac{f_c^2}{f_4^2} \right) + 2(R_{\text{noo}} G_{\text{nco}})^{1/2} \frac{f_c^2}{f_3 f_7} \quad (3-43)$$

EXPERIMENTAL TECHNIQUE

To obtain an experimental verification of the formulation contained in this section, noise-factor measurements were made on a variety of commercially available transistors. The test equipment used for these measurements is depicted in diagrammatic form in figure 26. The tank circuit shown at the input of the test stage was used to neutralize the input stray capacity. The capacitor C_1 was tuned to minimize the output noise power when the diode current I_{D1} was set to zero. A second tank circuit was used to neutralize the effects of stray capacity at the output of the test stage and the input of the cathode follower. The capacitor C_2 was tuned to maximize the noise power observed at the RMS indicator.

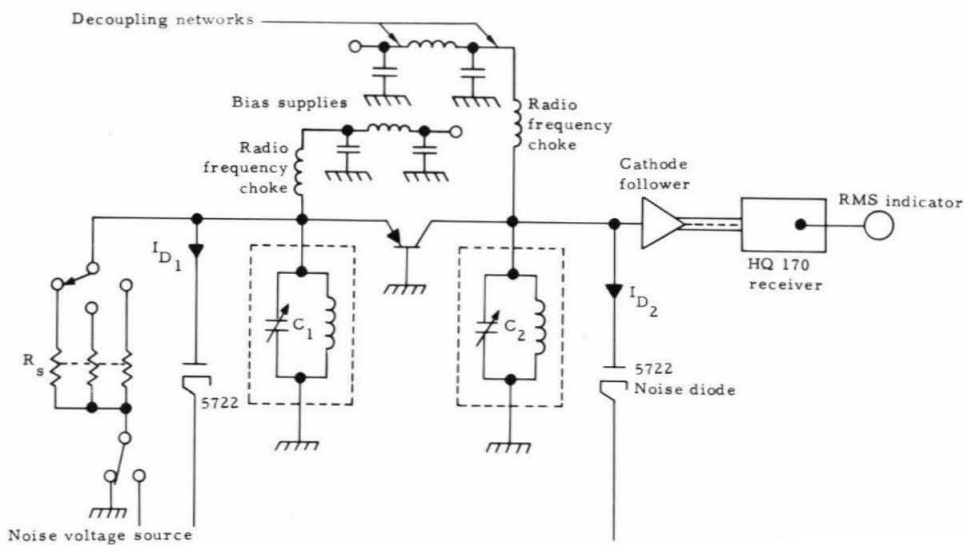
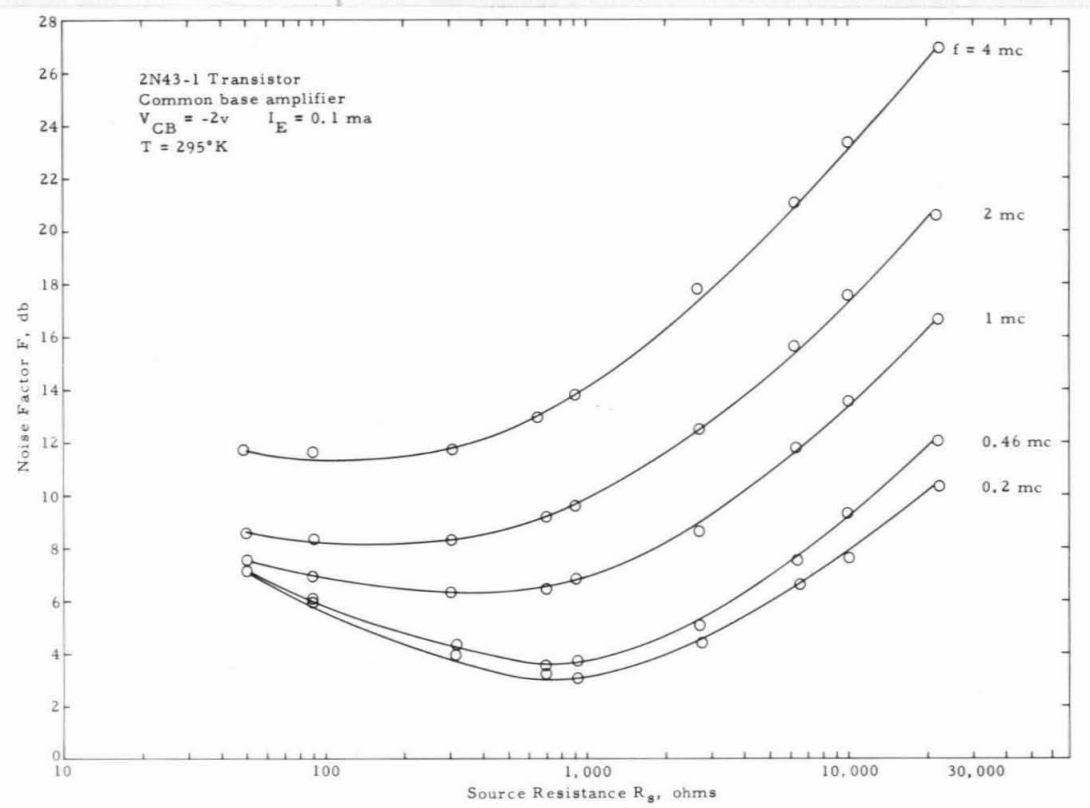


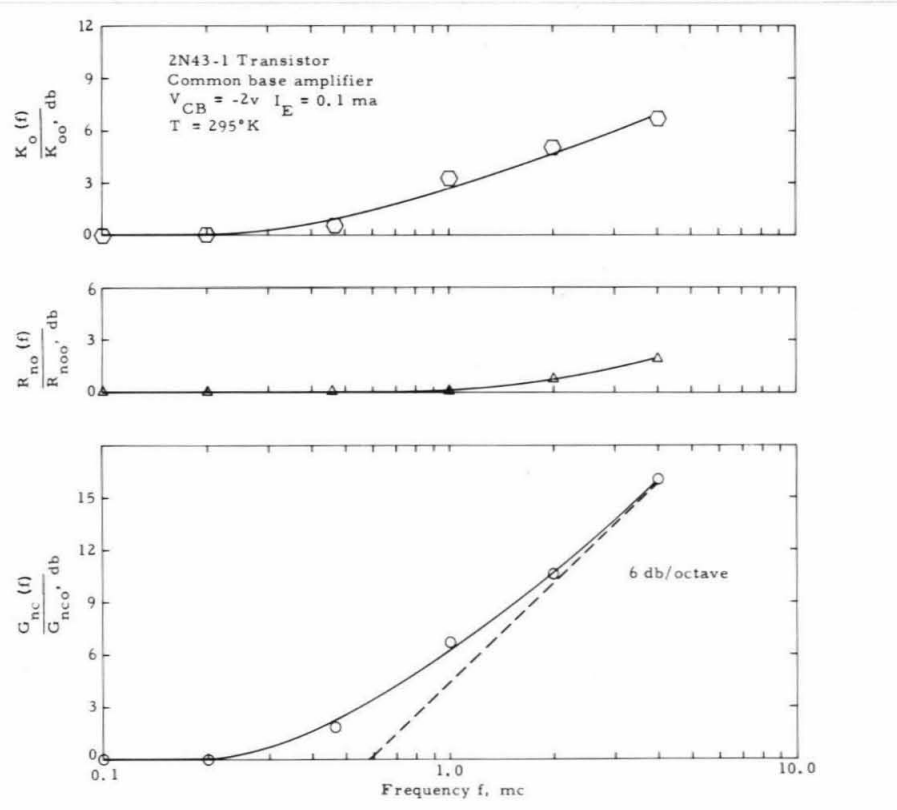
Figure 26. Test Apparatus used for High Frequency Noise Measurements.

A cathode follower was used as an impedance transformer. Its input impedance was sufficiently high that it did not load the collector circuit of the test stage and its output impedance was adjusted to match the input impedance of the receiver. The linearity of the receiver was established over several decades of input power by a plot of output noise power versus noise diode current, I_{D2} .

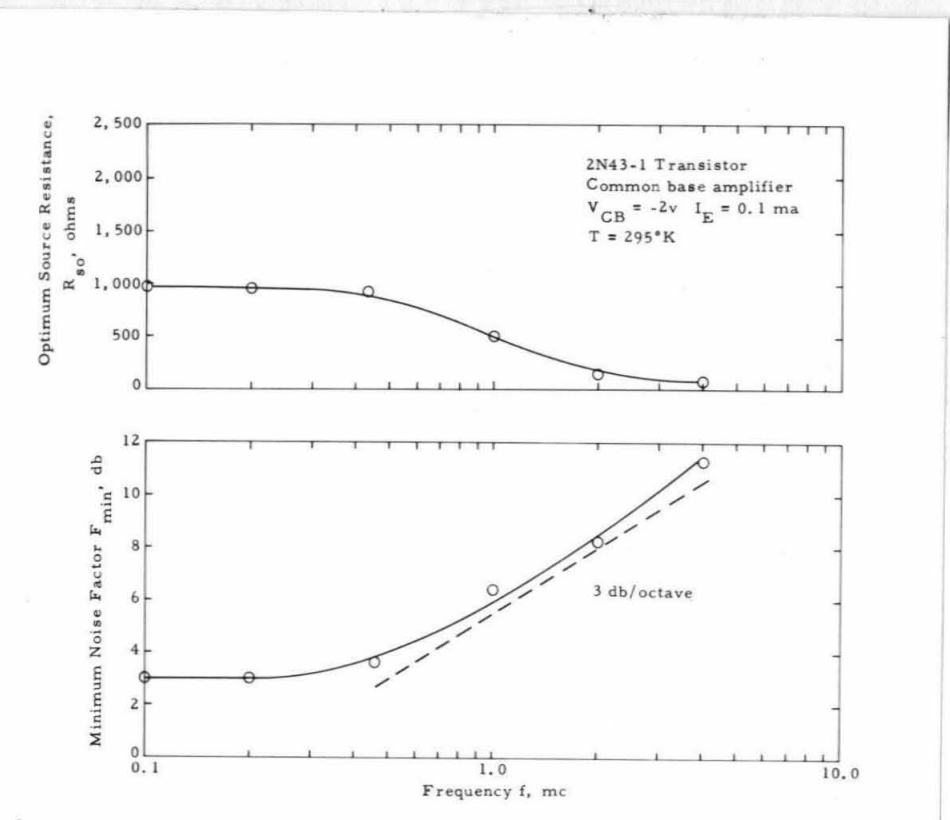
A partial compilation of the experimental results is contained in figures 27 to 29. These results clearly show the 6-db/octave increase in the collector noise factor parameters, G_{nc} , and the 3-db/octave increase in the minimum noise factor, F_{min} , both of which are predicted by the theory. The wide latitude that exists in the noise-factor parameter corner frequencies is illustrated in part b of figures 27, 28, and 29. The transition in the magnitude of the optimum source resistance, which results from this latitude, is shown in part c of figures 27, 28, and 29.



(a)

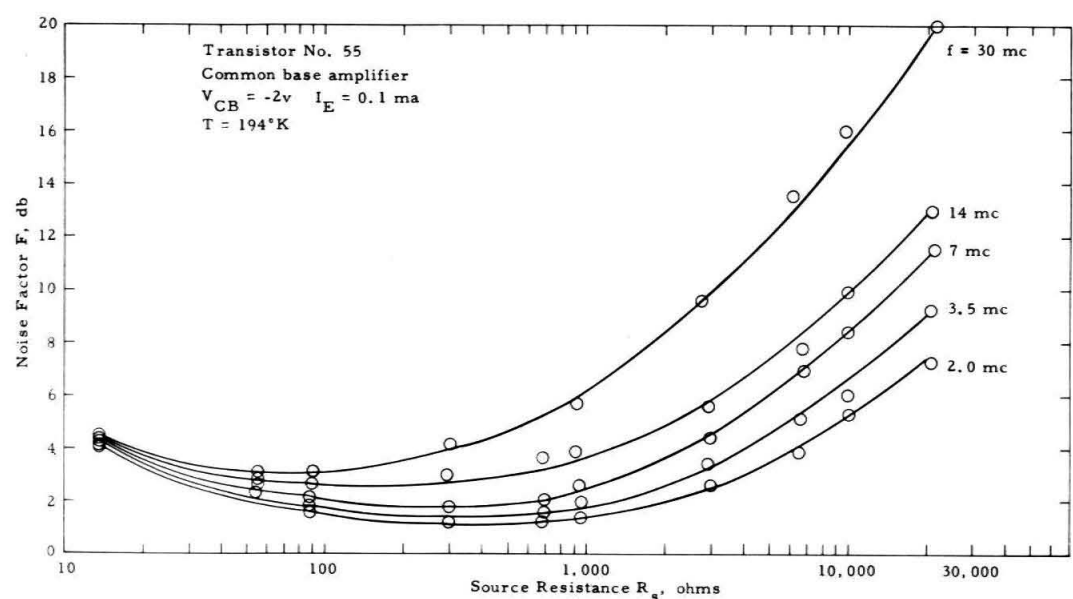


(b)

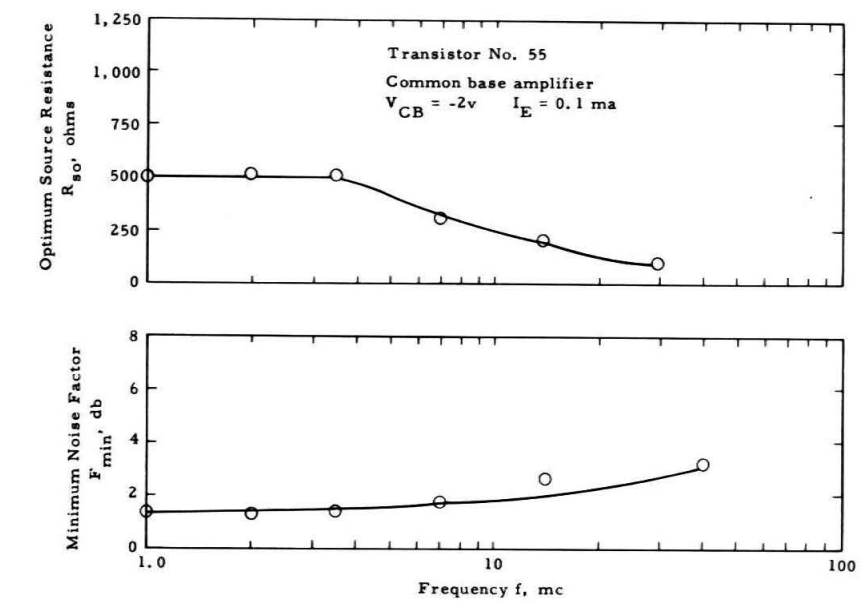


(c)

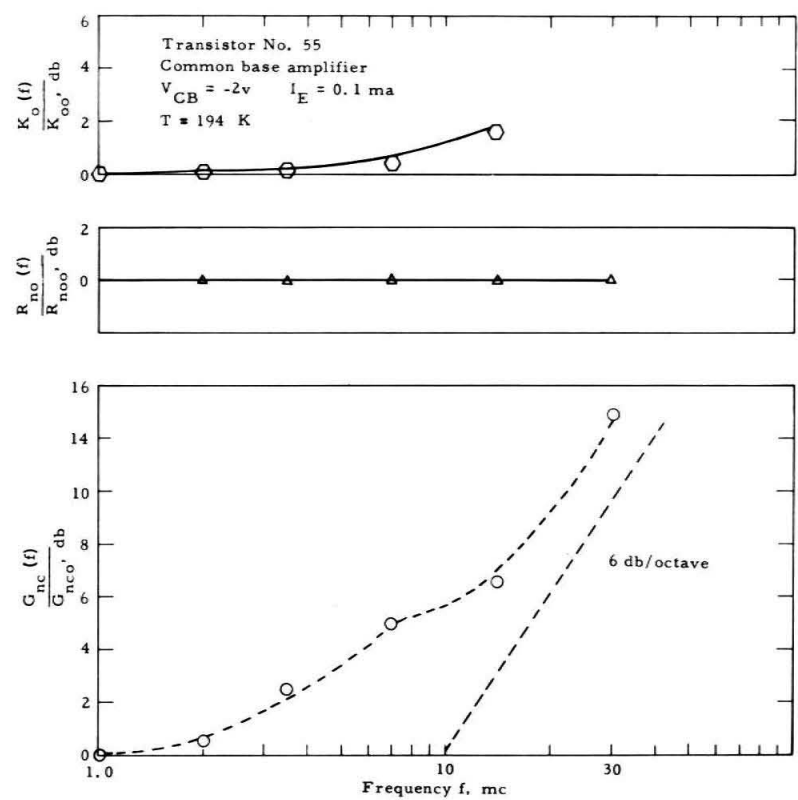
Figure 27. (a) Noise Factor As Function of Source Resistance for Several Frequencies in Upper-Transition and f^2 region, (b) Noise Factor Parameters as a Function of Frequency, (c) Minimum Noise Factor and Optimum Source Resistance as a Function of Frequency.



(a)

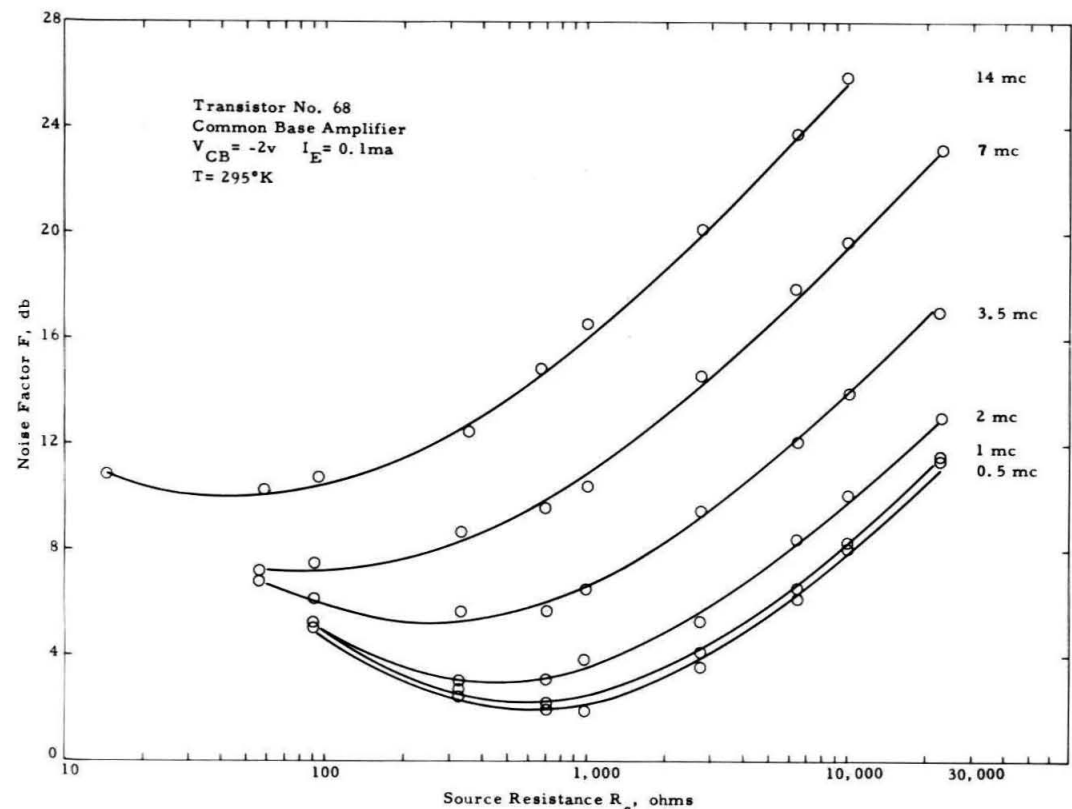


(c)

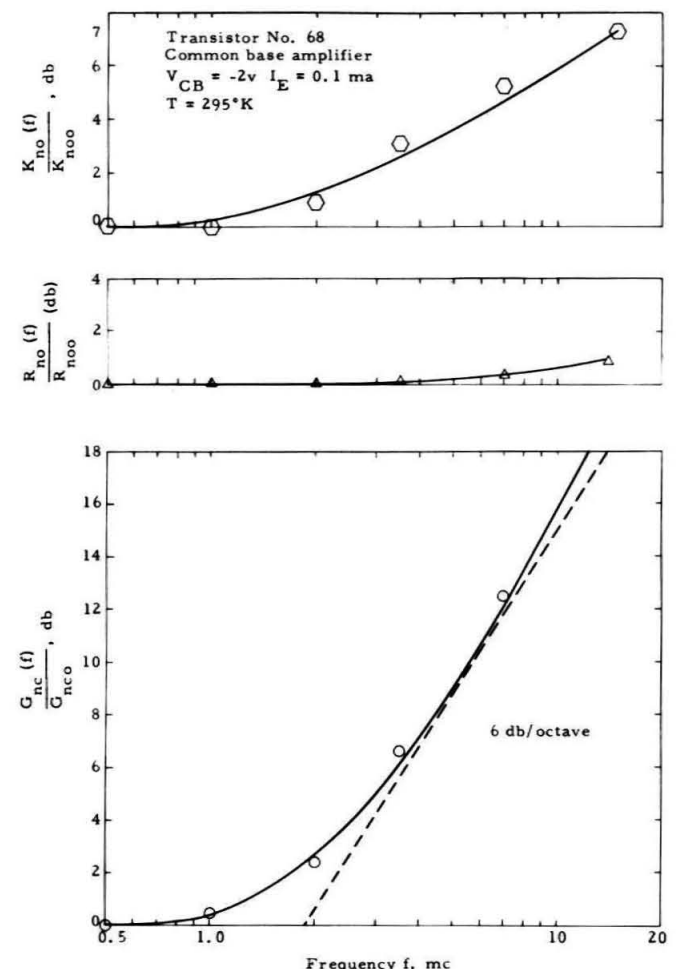


(b)

Figure 28. (a) F vs. R_s , (b) $K_o(f)$, $R_{no}(f)$, $G_{nc}(f)$ vs. f , (c) F_{min} and R_{so} vs. f .



(a)



(b)

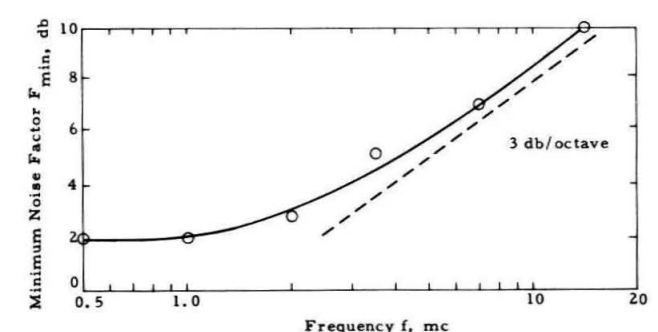
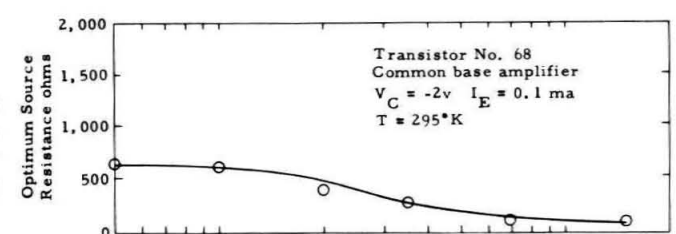


Figure 29. F vs. R_s , (b) $K_{no}(f)$, $R_{no}(f)$, $G_{nc}(f)$ vs. f , (c) F_{min} and R_{so} vs. f .

CONCLUSIONS

This section has been concerned with an analytical and experimental study of the noise performance of the high-frequency transistor amplifier. Its purpose has been to obtain an analytical solution to the noise optimization problem in which the source impedance is the only controllable parameter. The solution acquired gives the optimization parameter $R_{so}(f)$ as an explicit function of small signal transistor parameters:

β , the common-emitter current gain

r_e , the small-signal, emitter-junction resistance

$r_{b'b}$, the extrinsic base resistance

Corroboration through the experimental study shows that the high-frequency noise model (and the equations derived therefrom) form a valid basis from which to determine the noise performance of the high-frequency transistor amplifier.

The results of both the analytical and the experimental studies reveal that the source resistance becomes a critical parameter at high frequencies. With control of this parameter, it has been found possible to obtain reasonably low noise factors up to the α cutoff frequency. This result differs from other analytical studies (Ref. 29) which propose that the critical noise frequency, i.e., the high-frequency cutoff frequency, is $\sqrt{\alpha_o(1-\alpha_o)}f_c$.*

*This frequency corresponds to the break frequency f_8 given in equation 3-16c; hence, for larger values of source resistance, the critical noise frequency does become $\sqrt{\alpha_o(1-\alpha_o)}f_c$.

4. TRANSFORMER COUPLING

This section concerns the mean-frequency optimization problem in which the source resistance is an uncontrollable parameter, but in which transformer coupling is used at the input of the amplifier. The solution entails finding values for the emitter current, I_E , and the turns ratio, N , which satisfy the equations

$$\frac{\partial F}{\partial I_E} = 0 \quad (4-1)$$

$$\frac{\partial F}{\partial N} = 0 \quad (4-2)$$

TRANSFORMER-COUPLED COMMON-BASE AND COMMON-EMITTER AMPLIFIER

If it is assumed that the leakage and magnetizing inductances of the transformer are negligible and that only thermal noise is generated in the transformer windings, the noise factor parameters of the common-base and common-emitter amplifier become

$$K_o = 1 + \frac{1}{\beta r_e} \left(\frac{R_1}{N^2} + R_2 + r_{b'b} + r_e \right) \left(1 + \Gamma \right) \quad (4-3)$$

$$R_{no} = N^2 \left[r_e / 2 + r_{b'b} + \frac{R_1}{N^2} + R_2 + \frac{1}{2\beta r_e} (1 + \Gamma) \left(\frac{R_1}{N^2} + R_2 + r_{b'b} + r_e \right)^2 \right] \quad (4-4)$$

$$G_{nc} = \frac{1}{N^2} \left(\frac{1 + \Gamma}{2\beta r_e} \right) \quad (4-5)$$

Here, R_1 and R_2 are the resistances of the primary and secondary windings; N is the primary to secondary turns ratio,

$$\Gamma = \frac{\beta_o I_{CO}}{\alpha_o^2 I_E}$$

and

$$\beta_o = \frac{\alpha_o}{1 - \alpha_o}$$

Equation 4-3 shows that, with typical values of β_o , r_e , R_1 and R_2 , transformer coupling does not significantly alter the value of the noise factor parameter, K_o . From equations 4-4 and 4-5 it is found that R_{no} is multiplied by approximately the turns ratio squared while G_{nc} is divided by N^2 . Thus the minimum noise factor, which in terms of the noise factor parameters is written

$$F_{min} = K_o + 2(R_{no}G_{nc})^{1/2}$$

is not affected to any degree by transformer coupling. However, the optimum source resistance

$$R_{so} = \left(\frac{R_{no}}{G_{nc}} \right)^{1/2}$$

is multiplied by approximately the turns ratio squared.

Comparing the mean frequency noise model without transformer coupling (part b of figure 6) to the noise model with transformer coupling (figure 30), they become identical if

$r_{b'b}$ is replaced by $r_{b'b} + R_1/N^2 + R_2$

e_{nb} is replaced by $e_{nb} + e_{nT}$

e_{ns} is replaced by e_{ns}/N

R_s is replaced by R_s/N^2

As a result, the optimization problem given by equations 4-1 and 4-2 can be solved by using equations 1-21 and 1-24 which were derived in

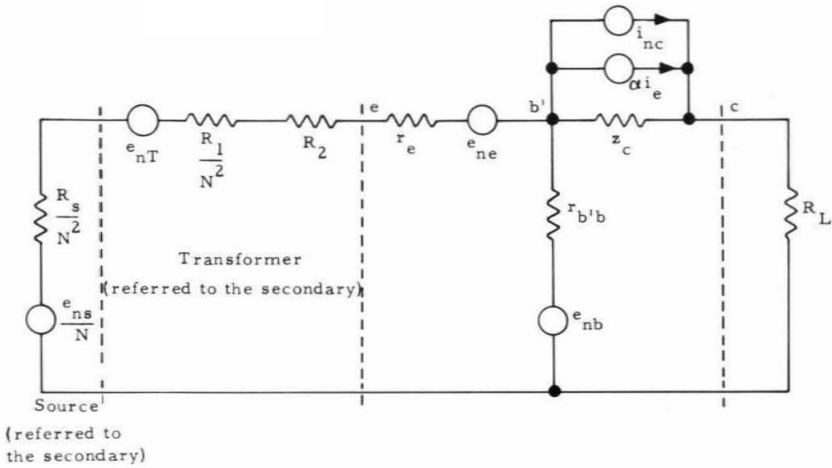


Figure 30. Noise Model of Transformer-Coupled Transistor Amplifier Connected in Common-Base Configuration.

Section 1. These are

$$I_{E0} = \left(\frac{kT_B I_{CO}}{2e r_{b'b}} \right)^{1/2} \quad (1-21)$$

$$(R_{so})_o = \frac{2r_{b'b}}{\Gamma} \beta_0^{1/2} \quad (1-24)$$

If, in equation 1-21, $r_{b'b} + R_1/N^2 + R_2$ is substituted for $r_{b'b}$,

the optimum emitter current of the transformer coupled amplifier becomes

$$I_{E0} = \left[\frac{kT_B I_{CO}}{2e(r_{b'b} + R_1/N^2 + R_2)} \right]^{1/2} \quad (4-6)$$

If, in equation 1-24, $\frac{1}{N^2}(R_{so})_o$ and $r_{b'b} + R_1/N^2 + R_2$ are substituted for $(R_{so})_o$ and $r_{b'b}$, the optimal source resistance of the transformer coupled amplifier becomes

$$(R_{so})_o = \frac{2N^2 \beta_0^{1/2}}{\Gamma} \left(r_{b'b} + R_1/N^2 + R_2 \right) \quad (4-7)$$

However, in the optimization problem given by equation 4-2, the turns ratio is the controllable parameter and the source resistance is the uncontrollable parameter. Substituting R_s for $(R_{so})_o$ and solving equation 4-7 for N , the optimum turns ratio of the transformer coupled amplifier becomes

$$N_o = \left[\frac{R_s - 2R_1/\Gamma}{2\beta_o^{1/2}(r_{b'b} + R_2)} \right]^{1/2} \quad (4-8)$$

In typical commercial transformers and transistors, the values of R_1 , R_2 , , and $r_{b'b}$ are such that

$$R_s \gg 2R_1/\Gamma$$

$$r_{b'b} \gg R_2$$

Therefore, the optimum turns ratio can be approximated as

$$N_o = \left(\frac{R_s}{2\beta_o^{1/2}r_{b'b}} \right)^{1/2} \quad (4-9)$$

Equations 4-6 and 4-9 form the solution to the transformer-coupled transistor amplifier noise optimization problem in which the controllable parameters are the emitter current and the transformer turns ratio. Comparison of equation 4-6 with equation 1-21 shows that transformer coupling does not significantly alter the value of the optimum emitter current. Equation 4-9 shows that an optimum transformer turns ratio exists for any arbitrary value of source resistance. N_o can be found by making d.c. and small signal measurements on the transistor.

TRANSFORMER COUPLED COMMON COLLECTOR AMPLIFIER

From an analysis similar to that carried out for the common base and common emitter amplifier, it is found for the common collector amplifier, that

$$I_{EO} = \frac{1}{\alpha_o} \left(\frac{kT_B I_{CO}}{2er_{b'b}} \right)^{1/2} \quad (4-10)$$

$$N_o = \left(\frac{\alpha_o R_s}{\beta_o^{1/2} 2r_{b'b}} \right)^{1/2} \quad (4-11)$$

EXPERIMENTAL VERIFICATION OF THE DERIVED RESULTS

To verify the results in equations 4-3 to 4-9, noise factor measurements were made on the transformer coupled common base and common emitter transistor amplifiers. The transformers used were commercial units with turns ratios varying from 1.4 to 14. To minimize the effects of the magnetizing inductance of the transformer, a variable capacitor was placed across the primary winding. The effect of the optimum value of capacity on the noise performance of the amplifier is shown in figure 31.

To insure that noise generated in the preamplifier could be neglected (figure 32), one set of noise factor versus source resistance measurements was made with the transistor connected in both the common base and common emitter configurations. If noise from the preamplifier is not negligible, this would be indicated by higher noise factor readings for the common base amplifier. The results of the test are shown in figure 33.

One solution to the optimization problem given by equations 4-1 and 4-2 is contained in figure 34. The turns ratio, N , was dictated by transformer availability; as a result, equation 4-7 rather than equation 4-9 was

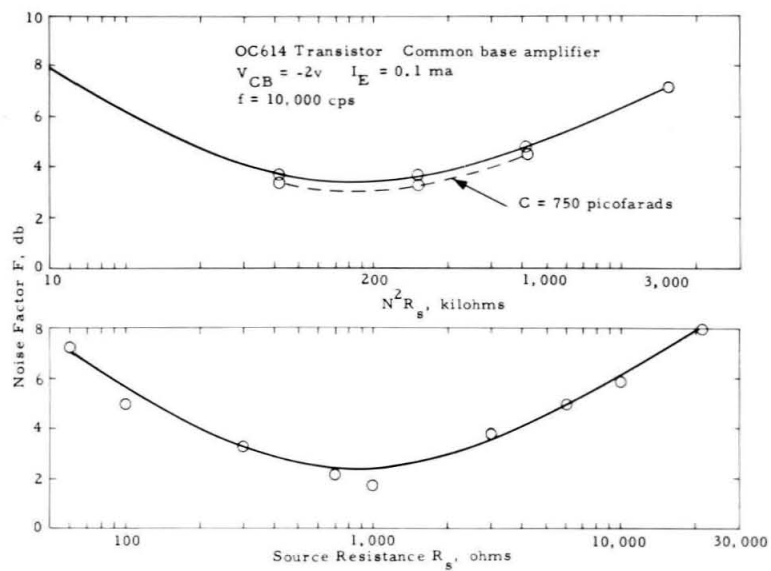


Figure 31. Noise Factor as a Function of Source Resistance (with and without Transformer Coupling). $N = 14.1$.

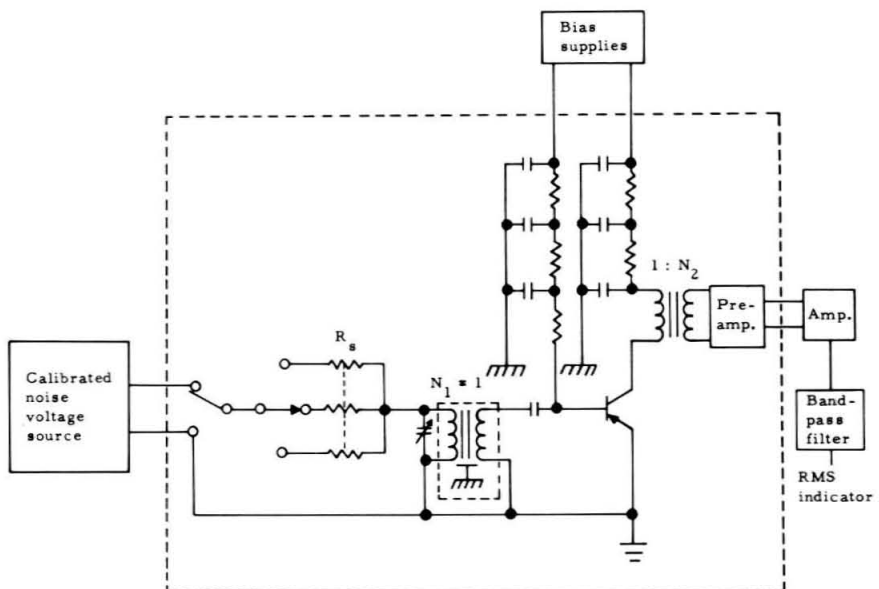


Figure 32. Apparatus for Experimental Noise Measurements of Transformer-Coupled Transistor Amplifier.

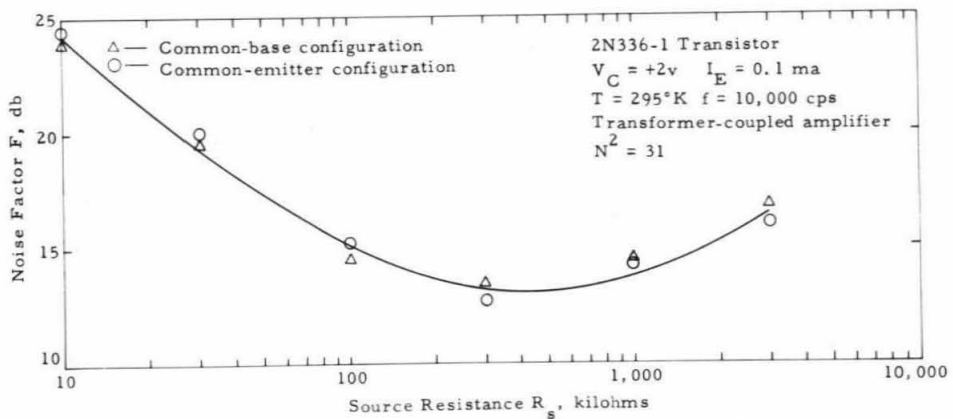


Figure 33. Noise Factor of Transformer-Coupled Common-Base and Common-Emitter Amplifier as a Function of Source Resistance.

used in the solution. For the OC 614 transistor, the theoretical optimization parameters (when $N = 14.1$) are

$$I_{E0} = 0.4\text{ma}$$

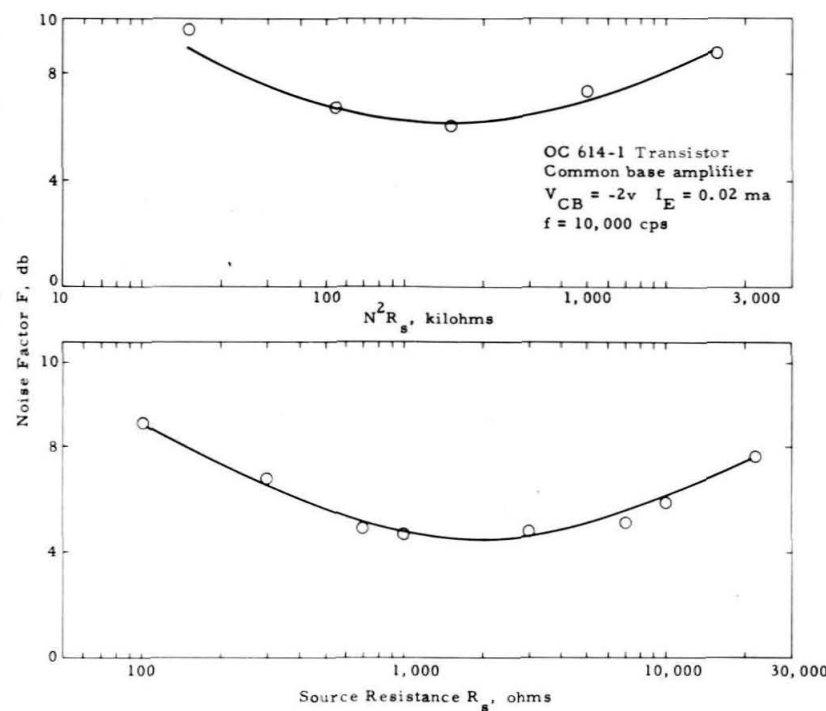
$$(R_{so})_0 = 200,000 \text{ ohms}$$

The experimental solution is

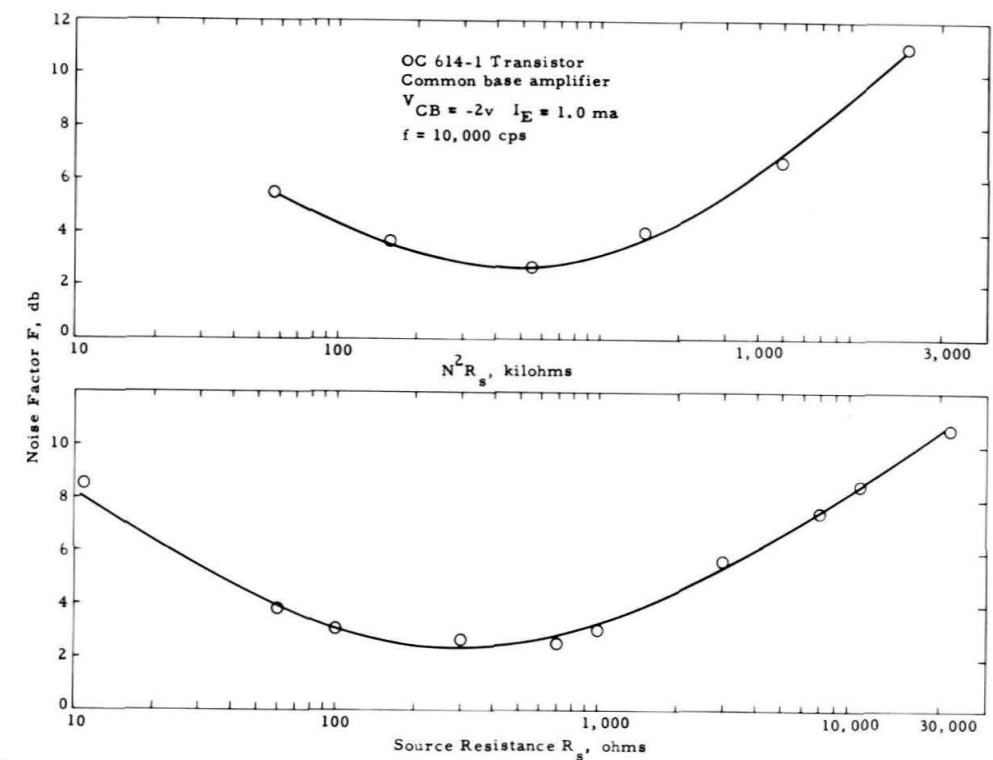
$$I_{E0} = 0.8\text{ma}$$

$$(R_{so})_0 = 100,000 \text{ ohms}$$

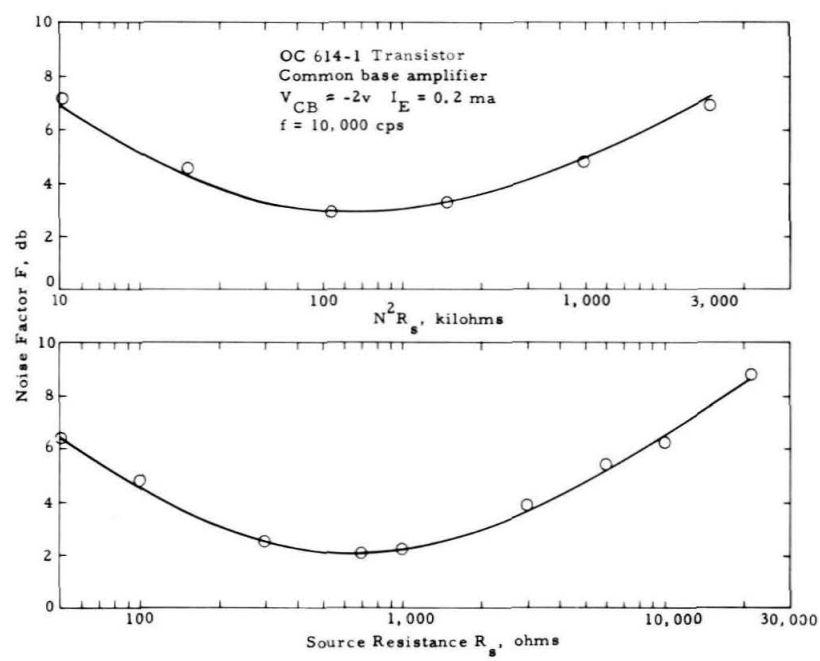
Although it was assumed that $1/f$ noise was negligible in the derivation of the equations in this section, this assumption was made only to obtain an analytical solution to the optimization problem. The results which show that the minimum noise factor is not affected, to any degree, by transformer coupling and that the optimum source resistance is multiplied by the turns ratio squared are not predicated on this assumption. This can be shown by carrying out an analysis similar to that shown here in terms of two frequency dependent noise generators. Experimentally, this is shown in figure 35.



(a)



(c)



(b)

Figure 34. Noise Factor as a Function of Source Resistance With and Without Transformer-Coupling, $N = 14.1$:
(a) $I_E = 0.02 \text{ ma.}$, (b) $I_E = 0.2 \text{ ma.}$, (c) $I_E = 1.0 \text{ ma.}$

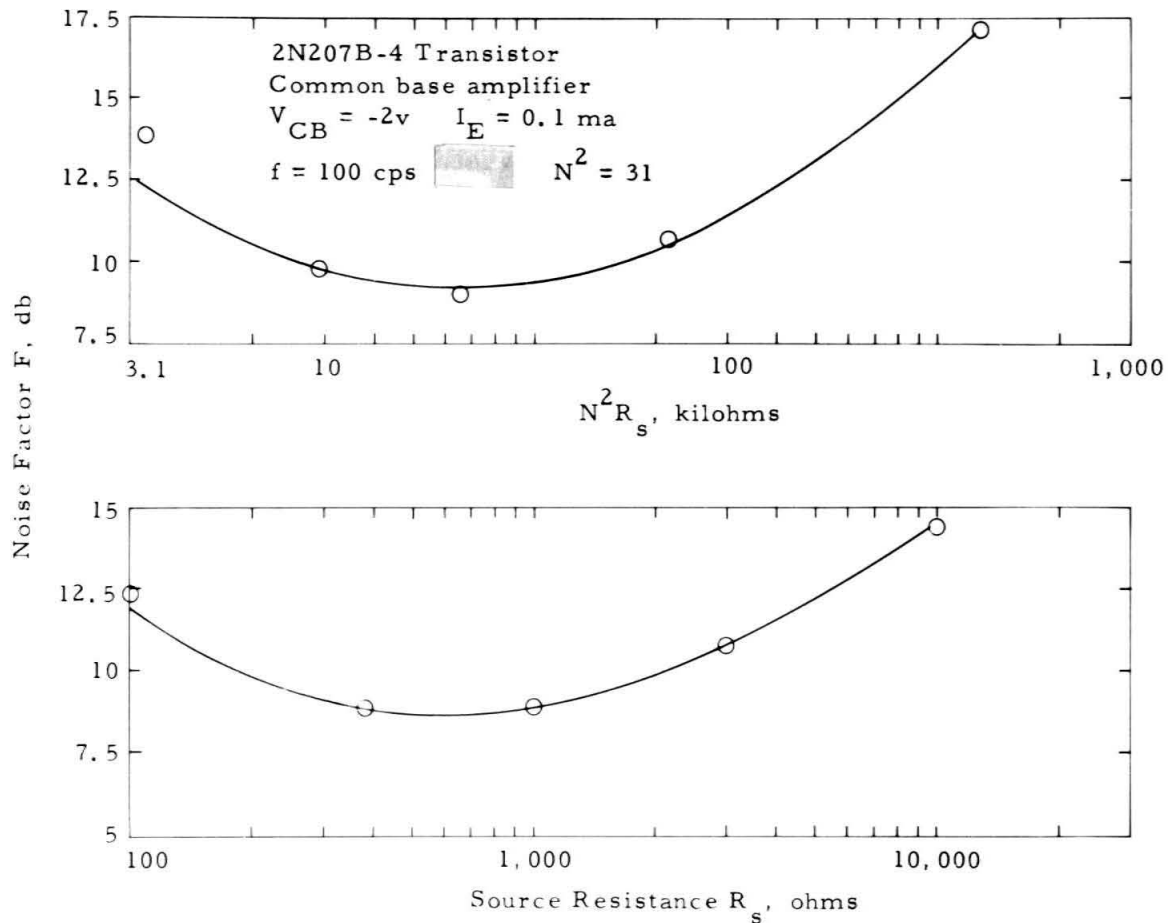


Figure 35. F vs. R_s with and without Transformer-Coupling,
 $N^2 = 31$, $f = 100$ cps.

5. TEMPERATURE

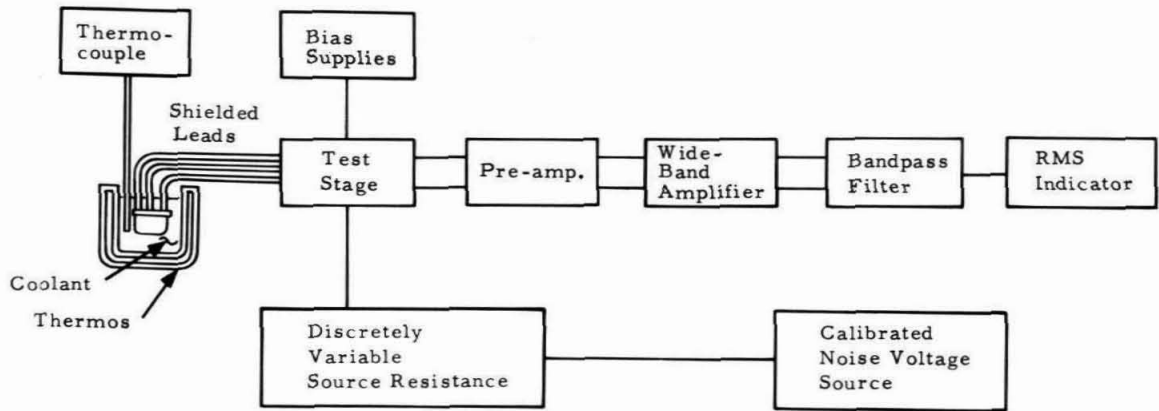
This section discusses an experimental study of the effect of temperature on the noise performance of a transistor amplifier. It differs from previous investigations in that a diverse set of source resistances is used. As a result, it is possible to determine from the experimental observations how this uncontrollable parameter affects the optimum source resistance and the minimum noise factor of the amplifier.

Also included is a description of a theoretical study of temperature and its effect on noise performance. However, owing to the complexity of the problem, the theoretical investigation is limited to the mean-frequency region.

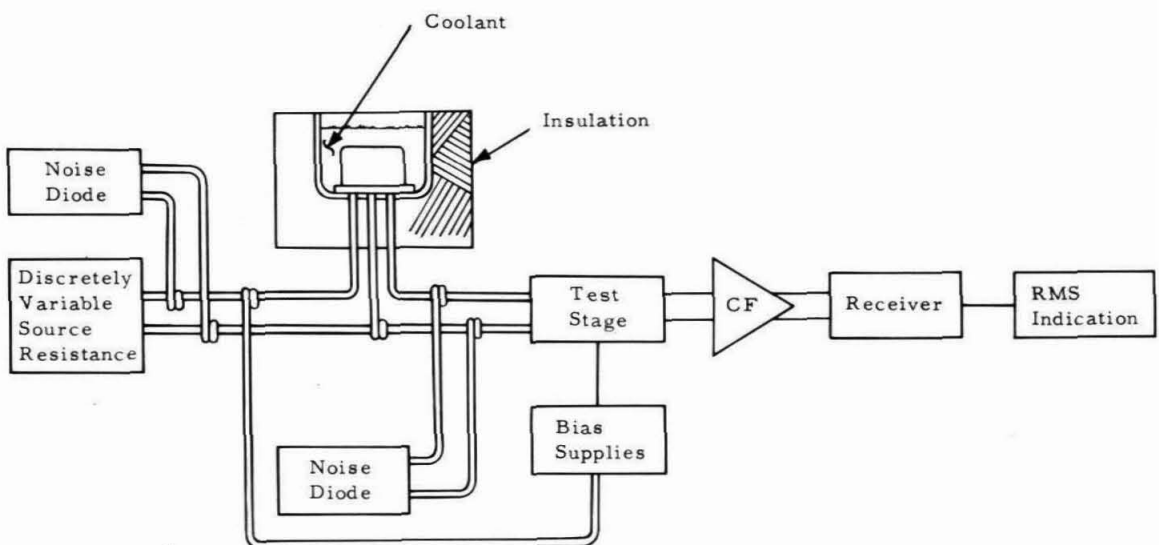
EXPERIMENTAL STUDY

The apparatus used to obtain the experimental results is shown in figure 36. For measurements at audio frequencies, extensive shielding was necessary to avoid erroneous readings caused by the 60 cycle field; at radio frequencies it was necessary to minimize the shunting effect of stray capacities. Liquid nitrogen was the coolant used to obtain readings at 77^0k ; a dry-ice alcohol mixture was utilized to obtain temperatures from 194^0k to room temperature; a thermostatically controlled hot water bath was used in the range from 330 to 300^0k . In order to facilitate switching of the source resistance, this parameter was maintained at room temperature throughout the experimental procedure.

A partial compilation of the experimental results can be seen in figures 37 to 42. These results show that in most instances, $1/f$ noise increases significantly as the transistor is cooled. This is



(a)



(b)

Figure 36. (a) Apparatus for Low-Frequency Study of Temperature Effects on Noise Performance. (b) High-Frequency Measurement Apparatus.

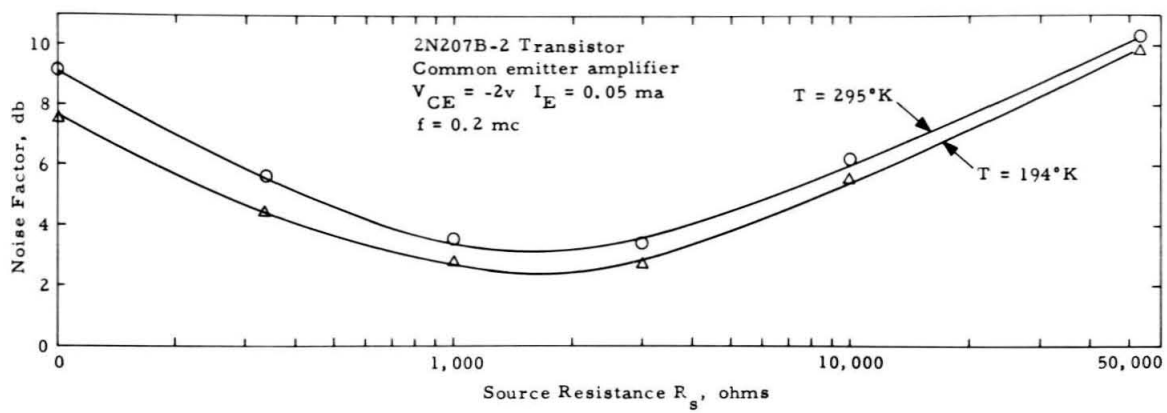


Figure 37. F vs. R_s , $T = 295^{\circ}\text{K}$ and $T = 313^{\circ}\text{K}$.

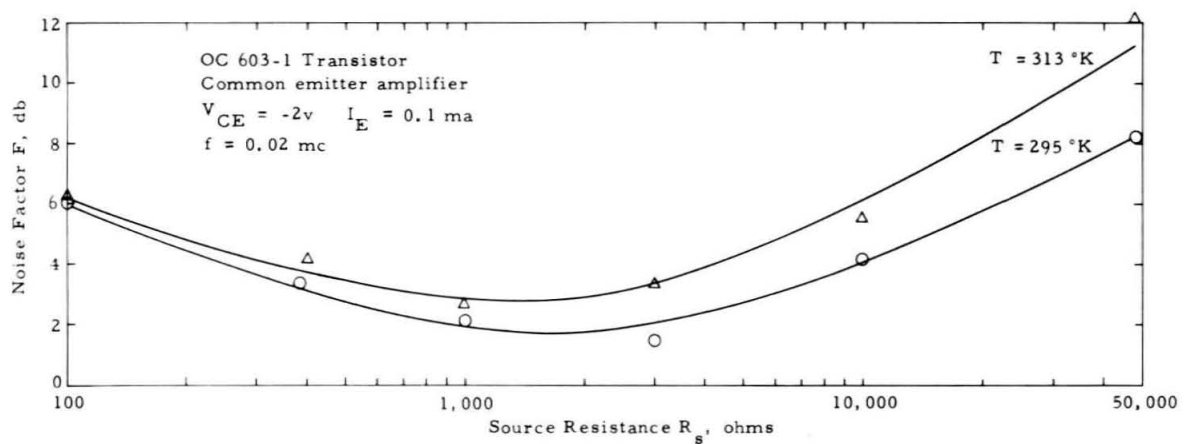


Figure 38. F vs. R_s , $T = 295^{\circ}\text{K}$ and $T = 194^{\circ}\text{K}$.

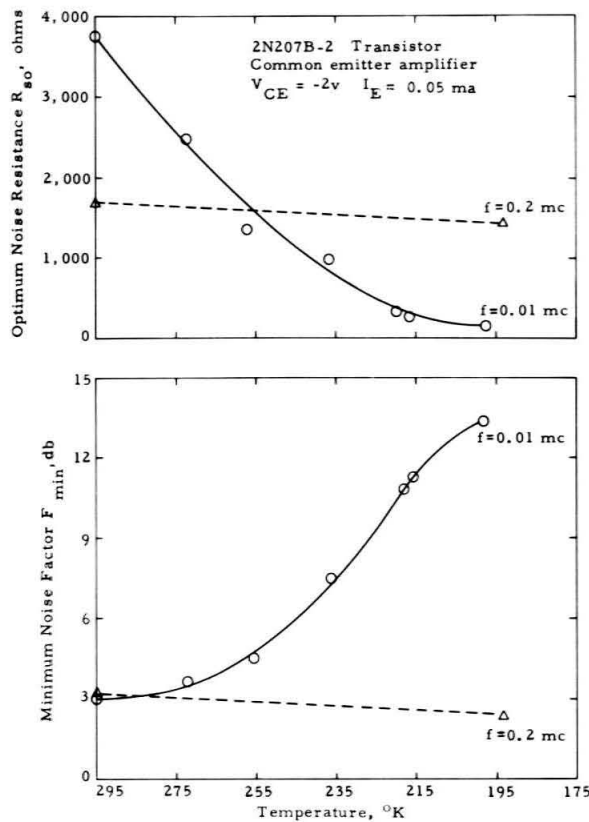


Figure 39. F_{min} and R_{so} vs. T, $f = 0.01$ and 0.2 mc.

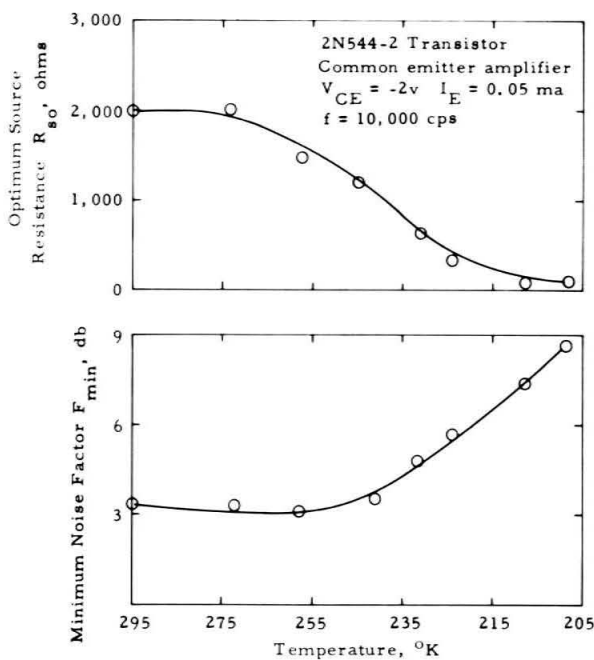


Figure 40. F_{min} and R_{so} vs. T, $f = 0.01$ mc.

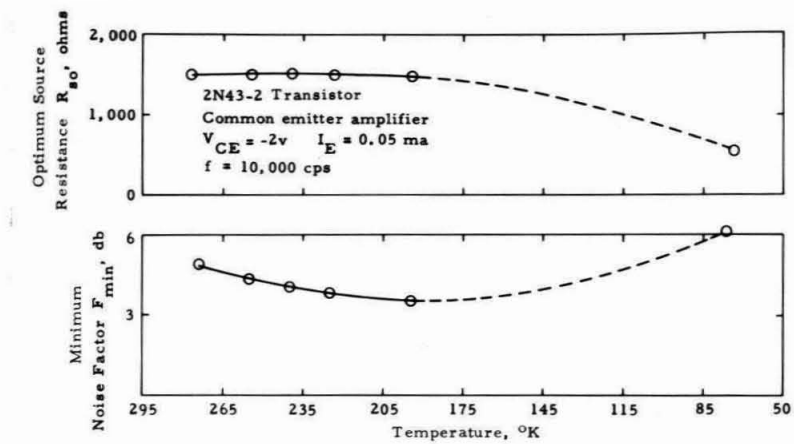


Figure 41. F_{min} and $R_{so'}$ vs. T , $f = 0.01$ mc.

especially true of the diffused base transistor (figure 42). Here, at 77°K , $1/f$ noise is visible in the megacycle region.

Although the majority of alloy junction transistors tested also exhibited an increase in $1/f$ noise as the transistor was cooled, the increase was not nearly as pronounced. For the 2N43 transistor, $1/f$ noise was negligible above a few kilocycles at liquid nitrogen temperature.

It is apparent from the marked decrease in the magnitude of the optimization parameter, R_{so} , that the $1/f$ noise observed at low temperatures is generated in the collector-base region of the transistor. An explanation of this phenomenon can perhaps be found in the adverse temperature dependence of the common-base current gain, α .

MEAN-FREQUENCY THEORETICAL STUDY

If the validity of van der Ziel's mean-frequency theory is assumed, and if it is assumed that the small-signal emitter junction resistance retains a temperature dependence given by

$$r_e = \frac{KT}{eI_E}$$

and if the source resistance is maintained at room temperature, T_o , the noise factor parameters of the common-base and common-emitter amplifiers become

$$K_o(T) = 1 + C_1 \left(\frac{r_{b'b} + r_{eo} T/T_o}{r_{eo}} \right) \quad (5-1)$$

$$R_{no}(T) = (1 + C_1) (T/T_o) \left[r_{b'b} + r_{eo}(T/T_o) \right] \quad (5-2)$$

$$G_{nc}(T) = \frac{C_1}{2r_{eo}} \quad (5-3)$$

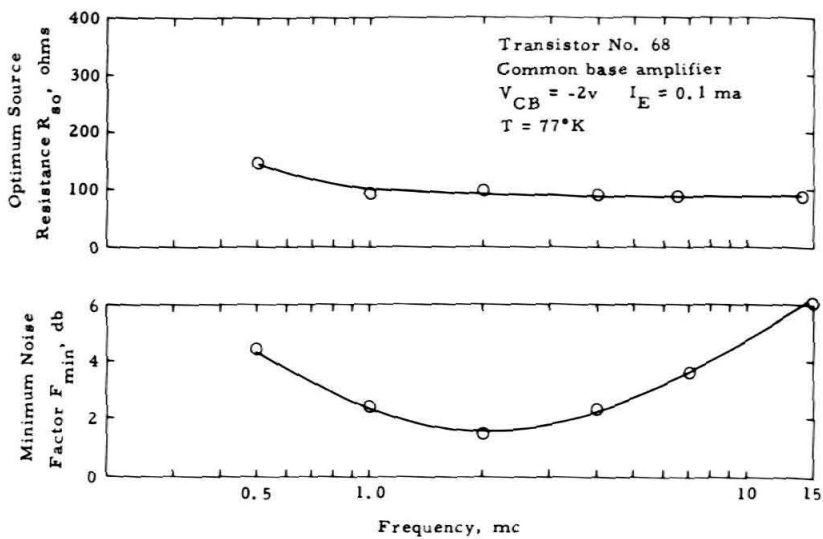


Figure 42. F_{min} and R_{so} vs. f , $T = 77^{\circ}\text{K}$.

Here

$$C_1 = \frac{1 + \frac{\beta I_{CO}}{\alpha_0^2 I_E}}{\beta}$$

$$r_{eo} = \frac{KT_0}{eI_E}$$

and

$$\beta = \frac{\alpha_0}{1-\alpha_0}$$

The common-emitter current gain, β , and the collector cutoff current, I_{CO} , in the preceding equations are implicit functions of temperature. In order to formulate the noise-factor parameters as explicit functions of T , it is necessary first to obtain equations that describe the temperature dependence of β and I_{CO} .

To obtain such a formulation for β , measurements of this parameter were made on a number of diffused base and alloy junction transistors. The results shown in figures 43 and 44 reveal that $\beta(T)$ can be written with reasonable accuracy as

$$\beta(T) = \beta(T_0)e^{\gamma(T-T_0)} \quad (5-4)$$

Here, γ is an empirical parameter that was found to vary from 7 to 11 $\times 10^{-3}/^{\circ}\text{K}$. Its average value, in those units tested, was $8 \times 10^{-3}/^{\circ}\text{K}$.

An experimental study by Hurtig (Ref. 30) shows that the collector cutoff current can be approximated by*

$$I_{CO}(T) = I_{CO}(T_0)e^{k_1(T-T_0)} \quad (5-5)$$

*The theoretical temperature dependence is given by

$$I_{CO}(T) = I_{CO}(T_0)e^{k_2\left(\frac{1}{T_0} - \frac{1}{T}\right)}$$

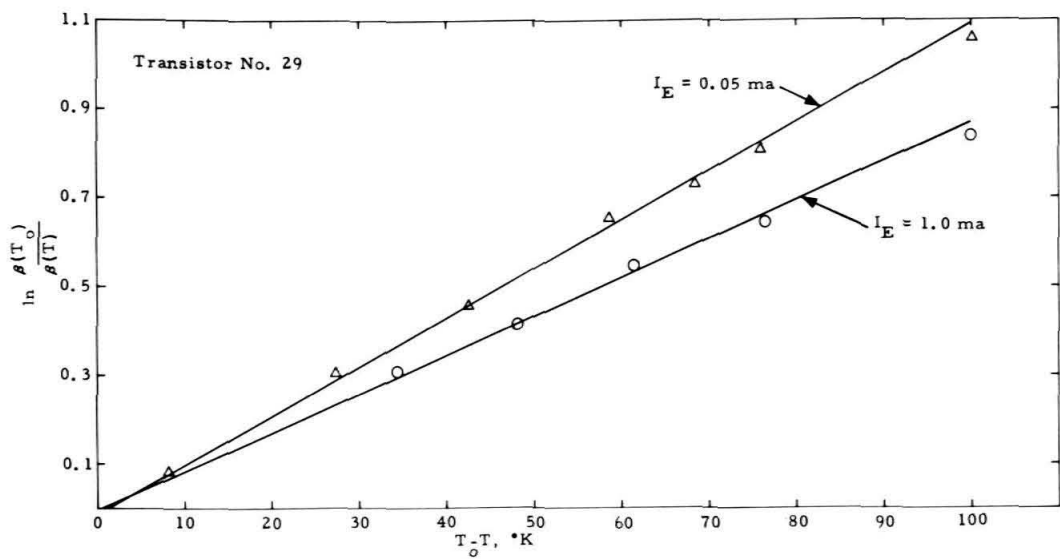


Figure 43. Common-Emitter Current Gain as a Function of Temperature, $I_E = 0.05 \text{ ma}$, $I_E = 1.0 \text{ ma}$.

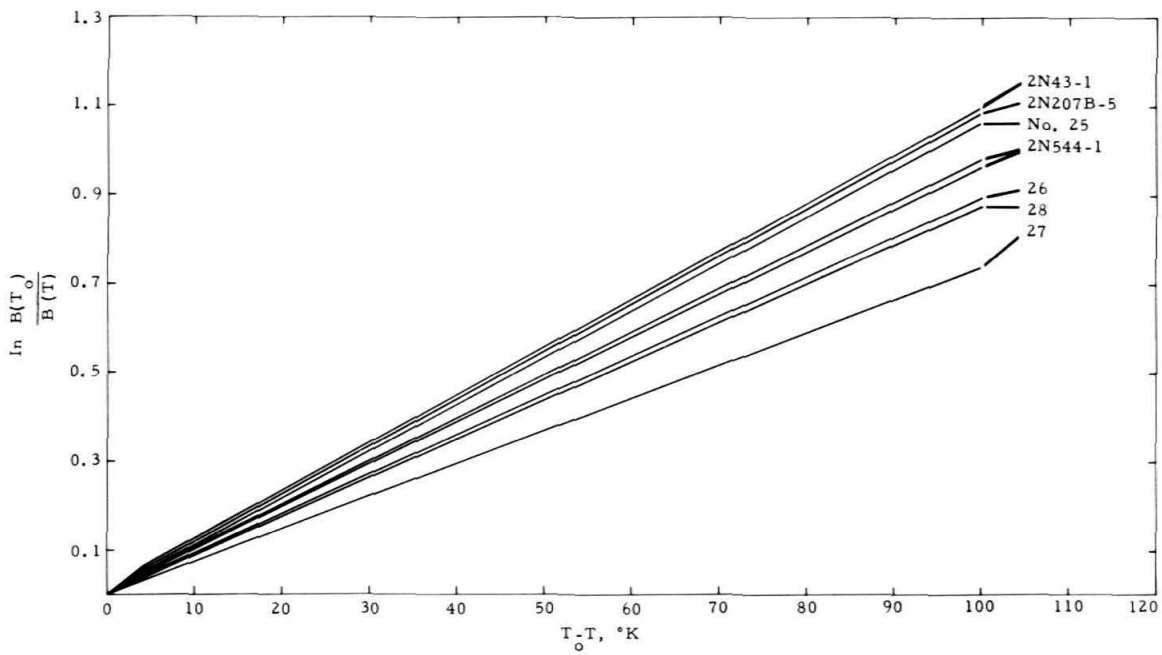


Figure 44. β vs. T , $I_E = 1.0 \text{ ma}$.

The parameter k_1 was found to vary from 6 to $9 \times 10^{-2}/^{\circ}\text{K}$; its average value was $8 \times 10^{-2}/^{\circ}\text{K}$.

Substituting the values for β and I_{C0} given by equations 5-4 and 5-5 into equations 5-1, 5-2, and 5-3, the temperature-dependent noise-factor parameters become

$$K_o(T) = 1 + c_1(T) \left[\frac{r_{b'b} + r_{eo}(T/T_o)}{r_{eo}} \right] \quad (5-6)$$

$$R_{no}(T) = 1 + c_1(T) (T/T_o) \left[r_{b'b} + r_{eo}(T/T_o) \right] \quad (5-7)$$

$$G_{nc}(T) = \frac{c_1(T)}{2r_{eo}} \quad (5-8)$$

Here,

$$c_1(T) = \frac{1 + \frac{\beta(T_o)I_{C0}(T_o)e^{(\gamma+k_1)(T-T_o)}}{\alpha_o^2}}{\frac{\beta(T_o)e^{\gamma(T-T_o)}}{\gamma(T-T_o)}}$$

It has been assumed in the formulation of $c_1(T)$ that temperature variations in α_o could be neglected. This is true for $\beta^2 \gg 1$.

Differentiating equation 5-6 with respect to temperature and substituting typical values for $\beta(T_o)$, $r_{b'b}$, r_{eo} , and I_{C0} into the resulting differential, it is found that for the temperature range considered (77 to 330°K)

$$\frac{\partial K_o(T)}{\partial T} \sim 0 \quad (5-9)$$

Owing to the difficulty in obtaining an experimental measure of $K_o(T)$, no attempt was made to directly verify the result shown in equation 5-9. However, it was indirectly verified by observing the temperature

dependence of the minimum noise factor.

It is found, by differentiating equation 5-7, that for temperatures above 77°K

$$\frac{\partial R_{\text{no}}(T)}{\partial T} > 0$$

This shows that R_{no} is a monotonically increasing function of temperature. Its rate of increase is a function of the emitter current I_E .

At larger values of emitter current, the generation-recombination and diffusion noise generated in the active base region of the transistor plays a more prominent role in determining the value of R_{no} . The adverse temperature dependence of β causes this noise to increase as the temperature is lowered, partially balancing the simultaneous decrease in the thermal noise generated in the base resistance. For small values of emitter current, R_{no} is determined principally by the shot-noise fluctuations in I_E . The influence of this noise on R_{no} is proportional to $\frac{1}{T^2}$.

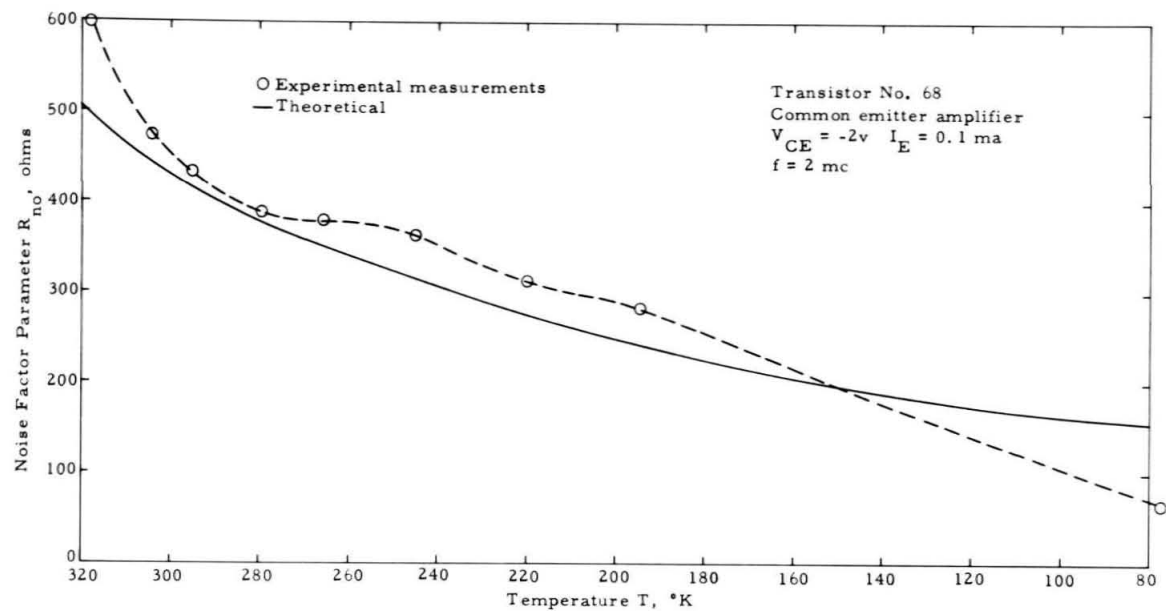
It is concluded from these observations that the parameter R_{no} is more sensitive to variations in temperature for small values of I_E (figure 45). This illustration shows both the experimental and theoretical values of R_{no} as a function of temperature.

Differentiation of equation 5-8 reveals that $G_{\text{nc}}(T)$ exhibits a minimum at a temperature T_1 for which

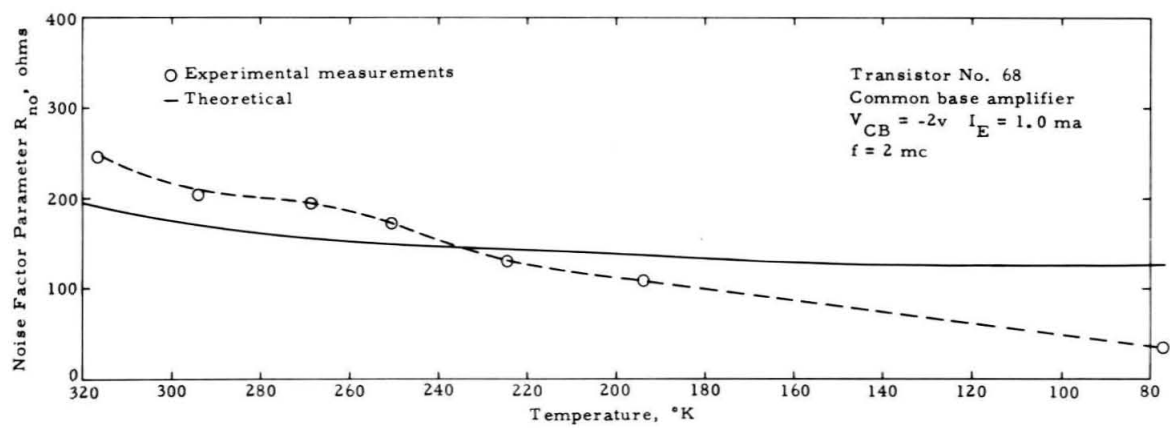
$$\frac{\beta(T_1) I_{C0}(T_1)}{\alpha_o^2 I_E} \sim 0.15$$

For typical values of the transistor parameters, T_1 is located in the range from 250 to 300°K .

With the transistor cooled to a temperature below T_1 , the parameter



(a)



(b)

Figure 45. Noise Factor Parameter $R_{no'}$ as a Function of Temperature:
 (a) $I_E = 0.1\text{ ma}$, (b) $I_E = 1.0\text{ ma}$.

G_{nc} increases at a rate of approximately 1% of its room temperature value per $^{\circ}\text{K}$. At temperatures above T_1 , it increases at an exponential rate given by

$$\frac{\partial}{\partial T} G_{nc}(T) \sim 0.04 \frac{e}{kT} I_{CO} e^{k_1(T-T_0)/^{\circ}\text{K}}$$

Figure 46 shows both the experimental and theoretical variation in G_{nc} as a function of temperature.

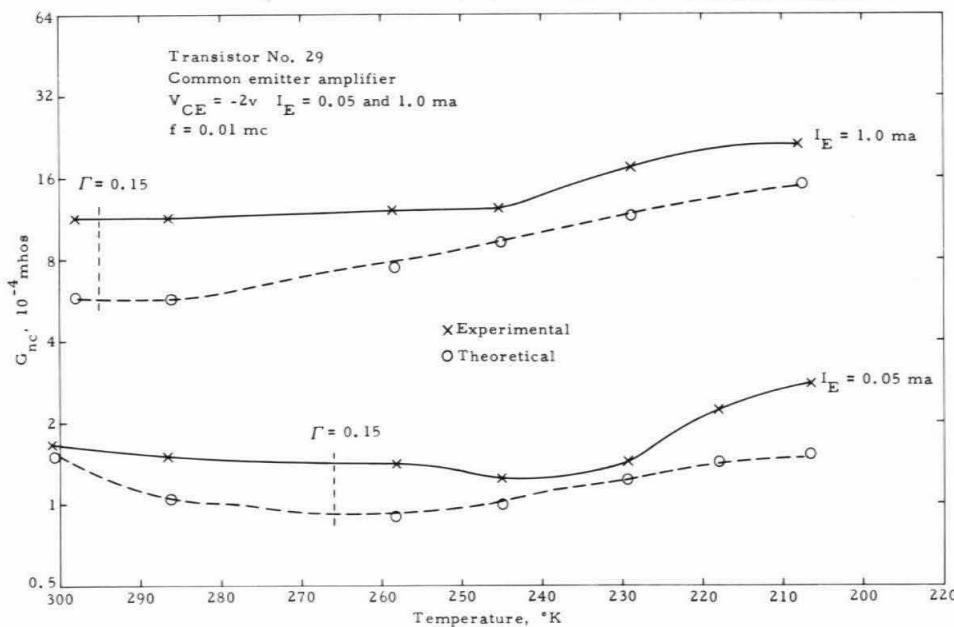


Figure 46. Noise Factor Parameter G_{nc} vs. T .

A further analysis of the preceding equations shows that the minimum noise factor which, in terms of the noise-factor parameters, is given by

$$F_{min}(T) = K_0(T) + 2 \left[R_{no}(T) G_{nc}(T) \right]^{1/2}$$

exhibits a minimum at a temperature approximately equal to T_1 . At higher temperatures, there is an exponential rise caused by the increase in I_{CO} . At lower temperatures,

$$\frac{\partial F_{min}(T)}{\partial T} \sim 0$$

Conversely, the optimizing parameter $R_{SO}(T)$ remains fairly constant from 320 to 194°k. At temperatures below 194°k, there is a sharp decline in this parameter. In all the units tested, the optimum source resistance was less than 100 ohms at a temperature of 77°k.

CONCLUSIONS

The results of the experimental and theoretical study indicate that the transistor can be used successfully as a low-level device at temperatures as low as 77°k. However, this success is predicated on restrictions concerning the magnitude of the driving-source resistance and the frequency of operation.

6. BIAS STABILIZATION AND EMITTER DEGENERATION

In the amplifier noise optimization problem, only the noise generated in the transistor itself has been considered. If this device is to be used as the active component in a low-level amplifier, extrinsic, noise-generating elements are usually added to stabilize the operating point of the transistor and the power gain of the amplifier. Middlebrook (Ref. 31) has shown these stabilizing elements affect both the minimum noise factor and the optimum source resistance of the transistor amplifier. In this section, utilizing van der Ziel's model, analytical expressions are derived which give the degradation in the minimum noise factor and the change in the optimum source resistance produced by bias stabilization and emitter degeneration.

EFFECT OF BIAS STABILIZATION ON NOISE PERFORMANCE OF TRANSISTOR AMPLIFIER

Bias stabilization (shown in figure 47a) is used to reduce temperature-induced variations in the collector current of the common-emitter amplifier.* However, this method of biasing also increases the noise factor. The extent of increase can be determined from an analysis of the noise model shown in figure 47b. From this model, if it is assumed that

1. Only thermal noise is generated in the bias stabilizing resistors
2. The correlation $\overline{e_{ne}^* i_{nc}} = 0$
3. $r_e^2 \ll \alpha_o (1 - \alpha_o) z_c^2$

*Without bias stabilization, i.e., with $R_1 = R_2 = \infty$ (figure 47a), the change in collector current, dI_C , induced by a change in temperature, dT , is given by

$$dI_C = \left[I_{CO} \frac{\partial B}{\partial T} + (B + 1) \frac{\partial I_{CO}}{\partial T} \right] dT$$

$$\sim (B + 1) dI_{CO}$$

Here, B is the direct-current, common-emitter current gain, and I_{CO} is the collector cutoff current. With bias stabilization, dI_C can be reduced to dI_{CO} .

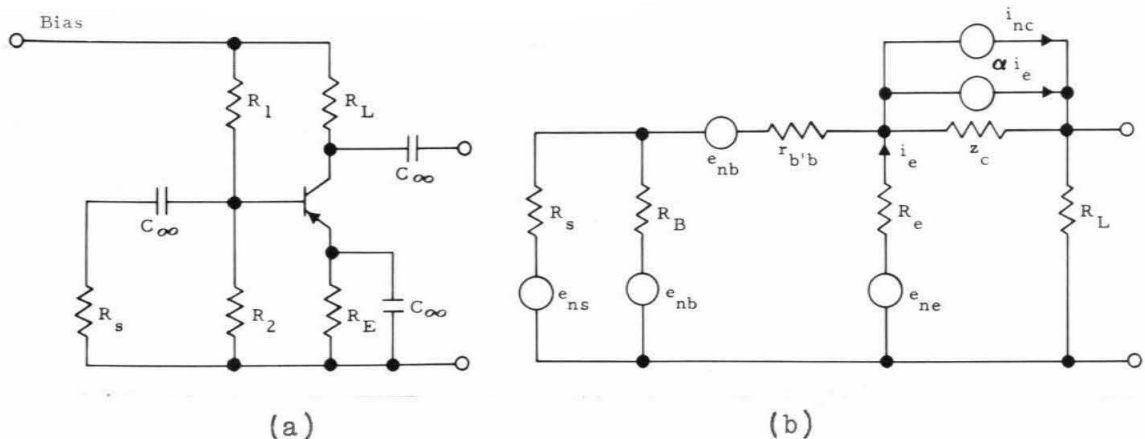


Figure 47. (a) Common-Emitter Transistor Amplifier With Bias Stabilization, (b) Noise Model of the Bias Stabilized Amplifier.

then the noise-factor parameters of the bias-stabilized amplifier become

$$K_0 = 1 + \frac{2(R_{ne} + R_{nb})}{R_B} + \frac{2g_{nc}}{R_B} (R_B + r_{b'b} + r_e)(r_{b'b} + r_e) \quad (6-1)$$

$$R_{no} = R_{ne} + R_{nb} + g_{nc}(r_{b'b} + r_e)^2 \quad (6-2)$$

$$G_{nc} = \frac{1}{R_B} + \frac{R_{ne} + R_{nb}}{R_B^2} + \frac{g_{nc}}{R_B^2} (R_B + r_{b'b} + r_e)^2 \quad (6-3)$$

Here

$$\overline{e_{ne}^2} = 4kT R_{ne} B$$

$$\overline{e_{nb}^2} = 4kT R_{nb} B$$

$$\overline{i_{nc}^2} = 4kT g_{nc} B |\alpha|^2$$

For values of R_B greater than a few thousand ohms, it can safely be assumed that

$$R_B \gg r_{b'b} + r_e$$

$$R_B \gg R_{nb} + R_{ne}$$

With these assumptions, equations 6-1, 6-2, and 6-3 become:

$$K_o = 2g_{nc}(r_{b'b} + r_e) \quad (6-4)$$

$$R_{no} = R_{ne} + R_{nb} + g_{nc}(r_{b'b} + r_e)^2 \quad (6-5)$$

$$G_{nc} = \frac{1}{R_B} + G_{nc} \quad (6-6)$$

To determine the increase in the noise-factor parameters produced by bias stabilization, only the terms containing R_B are retained in equations 6-4, 6-5, and 6-6. As a result:

$$\Delta K_o = 0 \quad (6-7)$$

$$\Delta R_{no} = 0 \quad (6-8)$$

$$\Delta G_{nc} = \frac{1}{R_B} \quad (6-9)$$

From equations 6-7, 6-8, and 6-9, as a first-order approximation for the change in the minimum noise factor and the optimum source resistance produced by bias stabilization, there is obtained

$$\Delta F_{min} = \frac{R_{so}}{R_B} \quad (6-10)$$

$$\Delta R_{so} = -\frac{R_{so}}{2G_{nc}R_B} \quad (6-11)$$

where R_{so} and G_{nc} are the values of these parameters for an amplifier with no stabilization.

Equation 6-10 shows that the degradation produced by bias stabilization is a function of the emitter current. This follows from the fact that R_{so} is a function of I_E . As the emitter current is lowered and the need for bias stabilization increases, the degradation produced by a fixed amount of biasing also increases.

Equation 6-11 shows that the optimum source resistance is lowered when bias stabilization is used. This effect is quite pronounced. For example, with $R_B = 20,000$ ohms and $I_E = 0.1$ ma, there is obtained for the 2N207B transistor, whose characteristics are given in Table 2-1, $\Delta R_{SO} = 1,100$ ohms and $\frac{\Delta R_{SO}}{R_{SO}} = 0.38$.

EMITTER DEGENERATION

The common-emitter stage, while offering the advantage of providing the largest power gain of the three configurations, is also found to give the poorest power gain stability. One method of improving the stability is to apply current feedback by means of an unbypassed emitter resistor (figure 48a). Although degeneration of this type has the added advantage of increasing the input impedance of the amplifier, it also degrades its noise performance. The extent of this degradation can be determined from an analysis of the noise model shown in figure 48b.

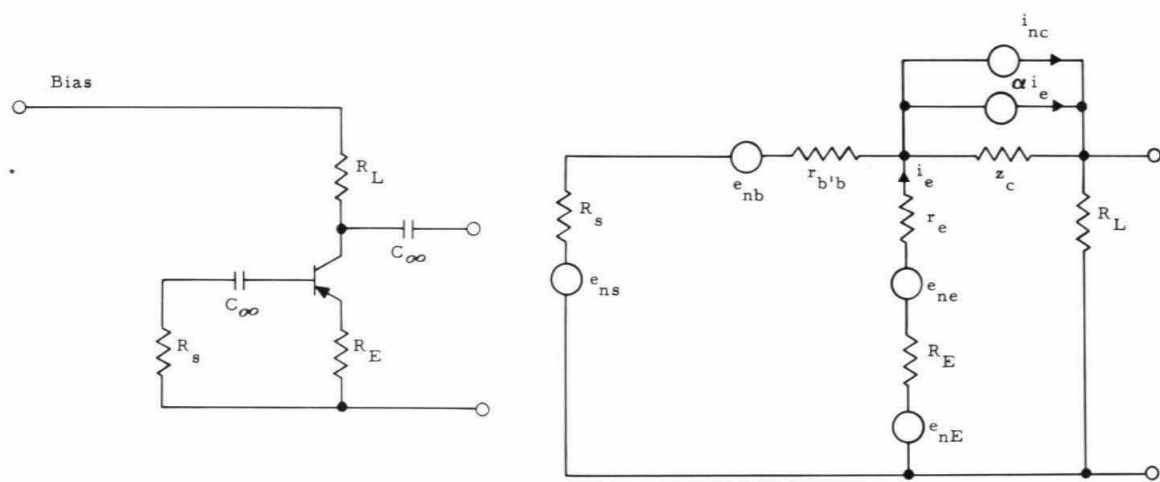


Figure 48. (a) Common-Emitter Transistor Amplifier with Emitter Degeneration, (b) Noise Model of Amplifier with Emitter Degeneration.

If it is assumed that

1. Only thermal noise is generated in the unbypassed emitter resistance
2. $\overline{e_{ne}^* i_{nc}} = 0$
3. $\frac{r_e^2}{\alpha_o(1-\alpha_o)} \ll |z_c|^2$

the noise-factor parameters of the stage with emitter degeneration become

$$K_o = 1 + 2g_{nc}(r_{b1b} + r_e + R_E) \quad (6-12)$$

$$R_{no} = R_{ne} + R_E + R_{nb} + g_{nc}(r_{b1b} + r_e + R_E)^2 \quad (6-13)$$

$$G_{nc} = g_{nc} \quad (6-14)$$

To determine the degradation in the noise-factor parameters introduced by bias stabilization, only those terms containing R_E are retained in equations 6-12, 6-13, and 6-14. It follows, from this procedure, that

$$\Delta K_o = 2g_{nc} R_E \quad (6-15)$$

$$\Delta R_{no} = R_E + g_{nc} R_E \left[R_E + 2(r_{b1b} + r_e) \right] \quad (6-16)$$

$$\Delta G_{nc} = 0 \quad (6-17)$$

As a first-order approximation, the changes in the optimum source resistance and emitter degeneration produced by bias stabilization become

$$\Delta F_{min} = \frac{R_E}{R_{so}} \quad (6-18)$$

$$\Delta R_{so} = \frac{R_{no} R_E}{R_{so}} \quad (6-19)$$

Equation 6-18 shows that the degradation produced by R_E is also a function of the emitter current. Here, as the current is raised and the need for emitter degeneration increases, the degradation in the noise performance produced by a fixed value of emitter resistance, R_E , also increases.

Unlike bias stabilization, emitter degeneration increases the optimum source resistance of the transistor stage.

CONCLUSIONS

The preceding analysis shows that both emitter degeneration and bias stabilization degrade the noise performance of the amplifier. The degradation produced by each is a function of the emitter current and the source resistance. For high values of source resistance and low values of emitter current, the effect of bias stabilization is more pronounced. With emitter degeneration, the converse is true.

7. LOAD RESISTANCE AND MULTISTAGING

In the preceding sections, only the single-stage transistor amplifier has been considered. It was assumed during these studies that thermal noise generated in the load resistance could be neglected. This section considers the multistage amplifier. Particular attention is focused on the degradation in noise performance produced by thermal noise generated in the load resistance of the first stage. Also derived is a noise figure for the multistage amplifier with resistive coupling between stages.

EFFECT OF LOAD RESISTANCE ON NOISE PERFORMANCE

In order to facilitate the analysis, each stage of the multistage system is treated as a noiseless Z parameter 4-pole. The noise generated in each stage is represented by two uncorrelated noise voltage generators.* Figure 49 shows the first two stages of the system to be analyzed. From this figure and the noise factor definition, the noise factor of the two stage amplifier becomes

$$\begin{aligned}
 F_{12} = F_1 + & \frac{|z_o|^2 |z_{11} + R_s|^2}{R_{L1} R_s |z_{21}|^2} + \frac{\overline{e_{n3}^2} |z_o + R_{L1}|^2 |z_{11} + R_s|^2}{4kT R_s B |z_{21}|^2 R_{L1}^2} \\
 & + \frac{\overline{e_{n4}^2} |z_o (R_{L1} + z_{33}) + R_{L1} z_{33}|^2 |z_{11} + R_s|^2}{4kT R_s B |z_{43}|^2 |z_{21}|^2 R_{L1}^2} \quad (7-1)
 \end{aligned}$$

Here, F_1 is the noise factor of the first stage

$$F_1 = 1 + \frac{\overline{e_{n1}^2}}{4kT R_s B} + \frac{\overline{e_{n2}^2} |z_{11} + R_s|^2}{4kT R_s B |z_{21}|^2}$$

*The solution becomes no less general with this assumption since correlation that may exist between the two noise generators is not a function of the input or output termination of the stage.

and

$$z_o = z_{22} - \frac{z_{21}z_{12}}{z_{11} + R_s}$$

In order to determine whether an optimum load resistance exists, equation 7-1 is differentiated with respect to R_{L1} . The result of this operation shows that for all values of R_{L1}

$$\frac{\partial F_{12}}{\partial R_{L1}} < 0 \quad (7-2)$$

Hence, the degradation in the noise performance of the two-stage system owing to the load resistance of the first stage is a monotonically decreasing function of R_{L1} .

Equation 7-1 further shows that the load resistance degrades the noise performance of the system in two ways. It introduces thermal noise (which is represented by the second term in equation 7-1) and it increases (by loading) the effects of the noise sources present in the second stage. This is evidenced by the presence of R_{L1} in the third and fourth terms of equation 7-1. In order to determine the degradation caused by R_{L1} , each of these effects are considered in turn.

With the first stage connected in the common-base configuration, the thermal noise can be neglected if the value of the load resistor

$$R_{L1} \gg \frac{2\beta r_e}{\alpha_o^2 (1 + \Gamma)} \quad (7-3)$$

Thermal noise with the first stage connected in the common-emitter configuration can be neglected if

$$R_{L1} \gg \frac{2r_e}{\beta\alpha_o^2 (1 + \Gamma)} \quad (7-4)$$

If the first stage is connected in the common-collector configuration, thermal noise can be neglected if

$$R_{L1} \gg 2r_e \quad (7-5)$$

To determine the effect on the noise performance produced by loading of the first stage, the common base-common base amplifier is considered first. Here, regardless of the value of R_{L1} , the noise generated in the second stage can never be neglected unless a step-up transformer is used between the first and second stage.

For the common emitter-common emitter amplifier, loading can be neglected if

$$R_{L1} \gg 2\beta r_e (r_e/2 + r_{b'b}) \quad (7-6)$$

The common collector-common collector (or Darlington) circuit will not be considered, since in this configuration a load resistance, R_{L1} , is not necessary.

From this analysis, it is found that in the cb-cb and ce-ce two stage amplifier, the degradation in noise performance produced by R_{L1} is due primarily to its loading effect on the second stage. For the cb-cb amplifier R_{L1} should be made as large as practicable; for the ce-ce amplifier it need only exceed the value given by equation 7-6.

MULTISTAGING

Extending the analysis to the multistage system, it is found that the noise factor of the m^{th} stage of the amplifier (figure 50b) can be written as

$$F_m = 1 + \frac{\overline{e_{n(2m-1)}^2}}{\overline{e_{nL(m-1)}^2}} + \frac{\overline{e_{n(2m)}^2} |z_{(2m-1), (2m-1)} + R_{L(m-1)}|^2}{\overline{e_{nL(m-1)}^2} |z_{(2m), (2m-1)}|^2} \quad (7-6)$$

The power gain of the m^{th} stage with conjugate matching at the input and output, becomes, from figure 50b

$$P_{gm} = \frac{|i_{(2m)}|^2 R_{L(m)}}{|i_{(2m-1)}|^2 R_{L(m-1)}} \quad (7-7)$$

or

$$P_{gm} = \frac{|z_{(2m), (2m-1)}|^2 R_{L(m)} R_{L(m-1)}}{|z_{(2m), (2m)} + R_{L(m)}|^2 |z_{(2m-1), (2m-1)} + R_{L(m-1)}|^2} \quad (7-8)$$

For the transistor amplifier operated at frequencies well below α cutoff, it is safe to assume that

$$z_{o(m)} \gg R_{L(m)}$$

With this assumption, and the further assumption that only thermal noise is generated in each of the load resistances, the noise factor of the n stage system becomes

$$F_{1 \dots n} = F_1 + \frac{F_2}{P_{g1}} + \dots + \frac{F_n}{P_{g1} \dots P_{g(n-1)}} \\ = \frac{\sum_{j=1}^n F_j}{\prod_{i=0}^{n-1} P_{gi}} \quad (7-8)$$

where, $P_{go} = 1.$

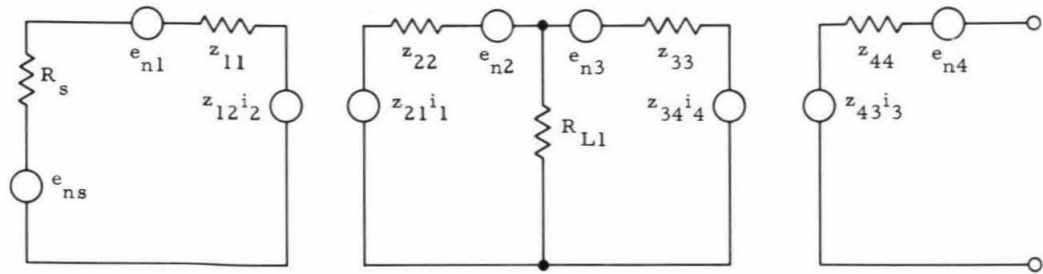
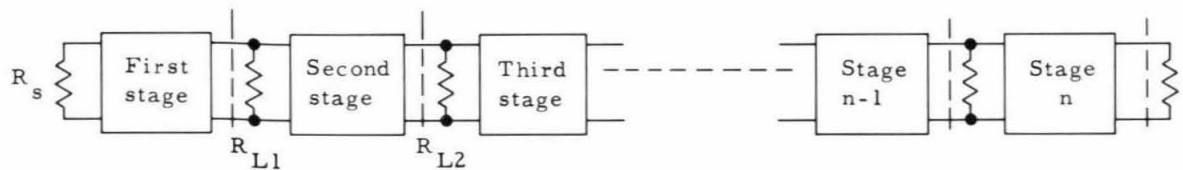
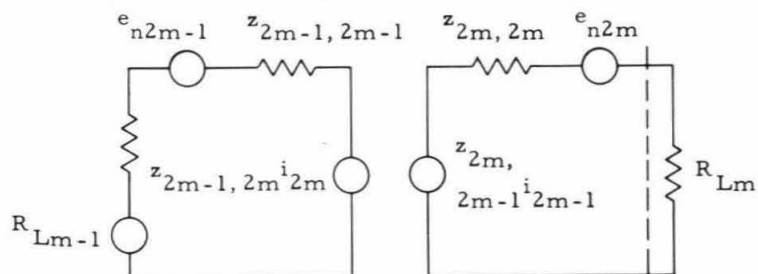


Figure 49. Z Parameter Noise Model of the Two Stage Amplifier.



(a)



(b)

Figure 50. Z Parameter Noise Model of the n Stage Amplifier,
(b) Noise Model of the m^{th} stage.

8. MEASURING METHODS

This section contains an analytical description of the methods used to obtain the noise-factor measurements found in the dissertation. As part of the measuring technique, a method of calculating the error introduced by noise generated in the measuring equipment is included.

TRANSISTOR NOISE-FACTOR MEASUREMENTS

Two methods were used to obtain the information necessary to quantify the noise factor of the transistor amplifier. Both involve increasing the power observed at the output of the system by injecting a voltage (or current) of known amplitude at the input. They differ, however, in the spectral properties of the injected signal.

The first method uses a continuous-wave (CW) voltage and requires, in addition to the amplitude of the injected signal, that B , the noise bandwidth of the system, be known.

The second method uses a noise current (or voltage) and requires a knowledge of the spectral properties of the added noise source.

CONTINUOUS-WAVE METHOD

Figure 51 is a block diagram of the system used to obtain the CW noise-factor measurements. When the CW voltage, $e_s(t)$, is reduced to zero, the mean-square output indication can be written as

$$\overline{e_{no}^2} = \int_0^{\infty} [S_{ns}(f) + S_{na}(f)] |A(f)|^2 df \quad (8-1)$$

where

$S_{ns}(f)$ = the unit-power spectral density of the driving source resistance, R_s

$S_{na}(f)$ = the unit power spectral density of the noise sources contained in the system when these sources are referred to the input

$A(f)$ = the voltage gain of the system when the input is terminated with R_s

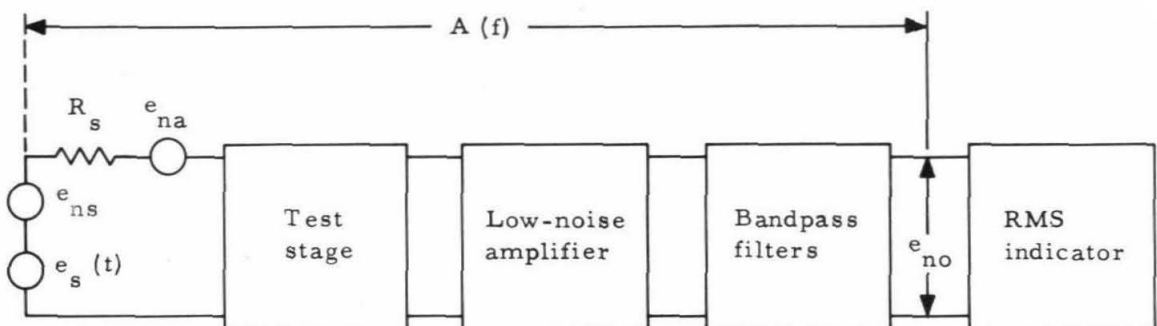


Figure 51. Block Diagram of Apparatus for CW Noise Measurement Method.

If B , the noise bandwidth of the system, is much less than f_o , the center frequency of the filters, equation 8-1 can be simplified to read

$$\overline{e_{no}^2} = \left[S_{ns}(f_o) + S_{na}(f_o) \right] |A(f_o)|^2 B \quad (8-2)$$

If the CW voltage, e_s , is increased until the mean-square meter indication becomes $N \overline{e_{no}^2}$, this increase, in terms of the spectral densities, can be written as

$$N \overline{e_{no}^2} = \overline{e_s^2} |A(f_o)|^2 + \left[S_{ns}(f_o) + S_{na}(f_o) \right] |A(f_o)|^2 B \quad (8-3)$$

Here, $\overline{e_s^2}$ is the mean-square CW voltage.

In terms of the spectral densities, the noise factor is given by

$$F(f_o) = \frac{S_{na}(f_o) + S_{ns}(f_o)}{S_{ns}(f_o)} \quad (8-4)$$

Therefore, from equations 8-2, 8-3, and 8-4,

$$F(f_o) = \frac{\overline{e_s^2}}{(N-1)S_{ns}(f_o)B} \quad (8-5)$$

With $N = 2$, and a resistive source at room temperature, equation 8-5 becomes

$$F(f_o) = \frac{\overline{e_s^2}}{1.6 \times 10^{-21} R_s B} \quad (8-6)$$

To determine the noise factor of the amplifier using the CW method, the noise bandwidth B must also be calculated. However, this part of the measurement procedure can be eliminated by utilizing a noise current (or voltage).

NOISE-INJECTION METHOD

The noise current source that was used to obtain the majority of the mean and high frequency measurements was the temperature limited diode. Its placement in the test stage is shown in figure 52. With this configuration, the noise factor as a function of diode plate current becomes

$$F = \frac{2eI_D R_s^2}{(N-1)S_{ns}(f_o)} \quad (8-7)$$

Here, N again signifies the increase in the output mean-square indication; I_D signifies the diode plate current necessary to produce this increase. With $N = 2$ and a resistive source at room temperature, equation 8-7 approximates to

$$F \sim 20I_D R_s \quad (8-8)$$

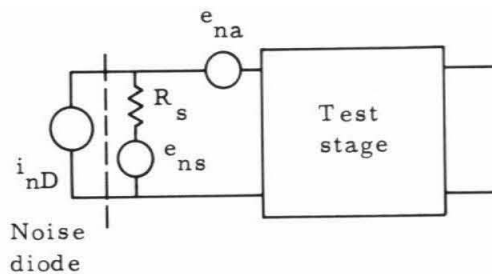


Figure 52. Placement of Diode for Measurements by Noise Current Method.

It is found from the preceding equation that large values of diode current are required when small values of source resistance are used. Under this condition it is desirable to use a noise source such as the Polaroid N-1 or the General Radio 1390. To make the device a near-perfect voltage generator,* its output can be modified as shown in figure 53.

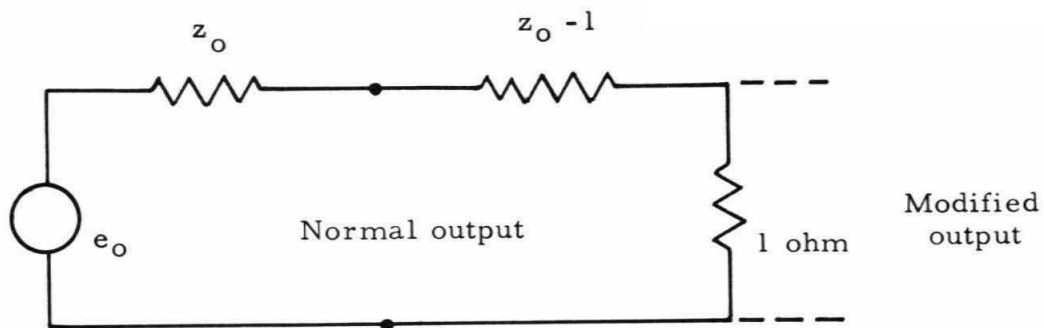


Figure 53. Method of Lowering Output Impedance of Noise Source.

The spectral density of the noise source can be calibrated in the following manner. If it is assumed that the spectral density of the noise source, S_{no} , is constant over some yet undetermined noise bandwidth, B_n , then the mean-square voltage measured at the output of the noise source

* This is a requisite in measurements of the noise-factor parameter, R_{no} .

becomes

$$\overline{e_n^2} = S_{no} B_n \quad (8-9)$$

The noise source is then used to drive a linear bandpass filter of known noise bandwidth, B_f , and insertion loss, A_f . In terms of these parameters, the output mean-square indication can be written as

$$\overline{e_o^2} = |A_f|^2 B_f S_{no} \quad (8-10)$$

Equations 8-9 and 8-10 yield B_n . With this value, S_{no} can be determined.

For noise-factor measurements, the noise voltage generator is placed in series with the driving source. With this configuration, the noise factor of the system is given by

$$\begin{aligned} F &= \frac{S_{no}}{(N-1) S_{ns}(f_o)} \quad (8-11) \\ &= \frac{\overline{e_n^2}}{(N-1) S_{ns}(f_o) B_n} \end{aligned}$$

Here, N signifies the increase in the mean-square output indication; $\overline{e_n^2}$ signifies the mean-square input noise voltage necessary to produce this increase. B_n is the noise bandwidth of the noise source.

With $N = 2$, and a resistive source at room temperature, this equation becomes

$$F = \frac{\overline{e_n^2}}{1.6 \times 10^{-21} R_s B_n} \quad (8-12)$$

EFFECTS OF EQUIPMENT NOISE ON NOISE-FACTOR MEASUREMENTS

In many of the noise measurements made (especially those at cryogenic temperatures) the noise added by the measurement equipment became a sig-

nificant part of the total noise observed. It therefore became necessary to derive a method of accurately determining the effect of noise generated in the measurement equation on a noise-factor measurement. The following is an analytical description of the derived method.

Figure 54 shows the test stage in terms of its admittance parameters and two uncorrelated noise current generators.* The transfer characteristics of the remaining system are represented by the admittances, y_{33} , y_{34} , y_{43} , and y_{44} ; its noise properties are represented by the noise current generator, i_{n3} . From figure 54, with sw_1 open, the mean-square noise current observed at the output is given by

$$\overline{i_{no1}^2} = \frac{|y_{43}|^2 \overline{i_{n3}^2}}{|y_{33} + y_L|^2} \quad (8-13)$$

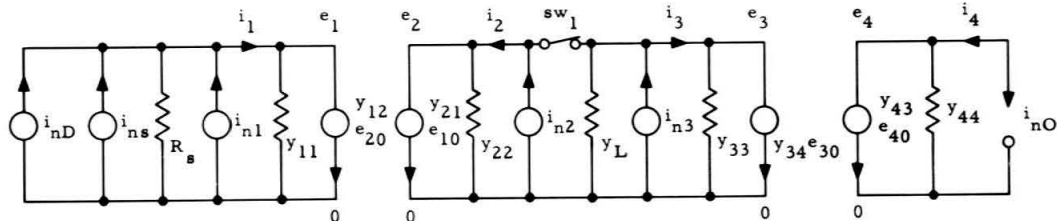


Figure 54. y Parameter Noise Model of Test Stage and Measurement Equipment.

With the switch closed, the mean-square noise current becomes

$$\overline{i_{no2}^2} = \frac{\left[(\overline{i_{ns}^2} + \overline{i_{nl}^2}) |y_{21}|^2 + (\overline{i_{n2}^2} + \overline{i_{n3}^2}) |y_{11} + y_s|^2 \right] |y_{43}|^2}{|\Delta|^2} \quad (8-14)$$

Here,

$$|\Delta|^2 = |(y_{11} + y_s)(y_{22} + y_{33} + y_L) - y_{12}y_{21}|^2$$

* Although the analysis was carried out assuming uncorrelated noise sources in the test stage, a similar analysis, made without this assumption, yields identical results.

With noise diode current, $\overline{i_{no_2}^2}$ is multiplied by a yet undetermined constant K for which the noise factor of the test stage, F_1 , can be written

$$F_1 = \frac{(K-1) \overline{i_{no_2}^2}}{(\overline{i_{ns}^2})^*} \quad (8-15)$$

Here, $(\overline{i_{ns}^2})^*$ is the contribution to $\overline{i_{no_2}^2}$ from noise generated in the driving source.

Since F_T , the noise factor of the system (including the test stage), can be written as

$$F_T = \frac{\overline{i_{no_2}^2}}{(\overline{i_{ns}^2})^*} \quad (8-16)$$

it follows, from equations 8-15 and 8-16, that

$$F_1 = (K-1)F_T \quad (8-17)$$

Writing the noise factor of the test stage in terms of the admittance parameters,

$$F_1 = 1 + \frac{\overline{i_{n1}^2}}{\overline{i_{ns}^2}} + \frac{\overline{i_{n2}^2} |y_{11} + y_s|^2}{\overline{i_{ns}^2} |y_{21}|^2} \quad (8-18)$$

For the transistor amplifier, it can safely be assumed that

$$y_{33} + y_L \gg y_{22}$$

and

$$(y_{11} + y_s)(y_{22} + y_{33} + y_L) \gg y_{12}y_{21}$$

With these assumptions, and equations 8-13, 8-14, and 8-18, the noise factor of the test stage becomes

$$F_1 = \frac{\overline{i_{no_2}^2} - \overline{i_{no_1}^2}}{\overline{(i_{ns}^2)}^*} \quad (8-19)$$

It follows, from equations 8-15 and 8-19, that

$$K-1 = \frac{\overline{i_{no_2}^2} - \overline{i_{no_1}^2}}{\overline{i_{no_1}^2}}$$

Therefore,

$$K = 2 - \frac{\overline{i_{no_1}^2}}{\overline{i_{no_2}^2}} \quad (8-20)$$

A diode current and a mean-square current indicating device were assumed in the preceding analysis for convenience only. The final results are not predicated on these assumptions.

Figure 55 illustrates the error incurred in a noise-factor measurement as a function of the logarithmic ratio of output noise currents. An example will illustrate the use of the graph.

If it is assumed the mean-square output indication is -7 decibels with SW-1 open and +12 decibels with SW-1 switch closed, the error incurred in this noise-factor measurement is 0.5 db.

INDICATING DEVICE ERROR

Another source of error encountered in time-averaged noise measurements is the finite time constant of the indicating device. That is, in order to obtain a true measure of the mean-square noise current (or voltage)

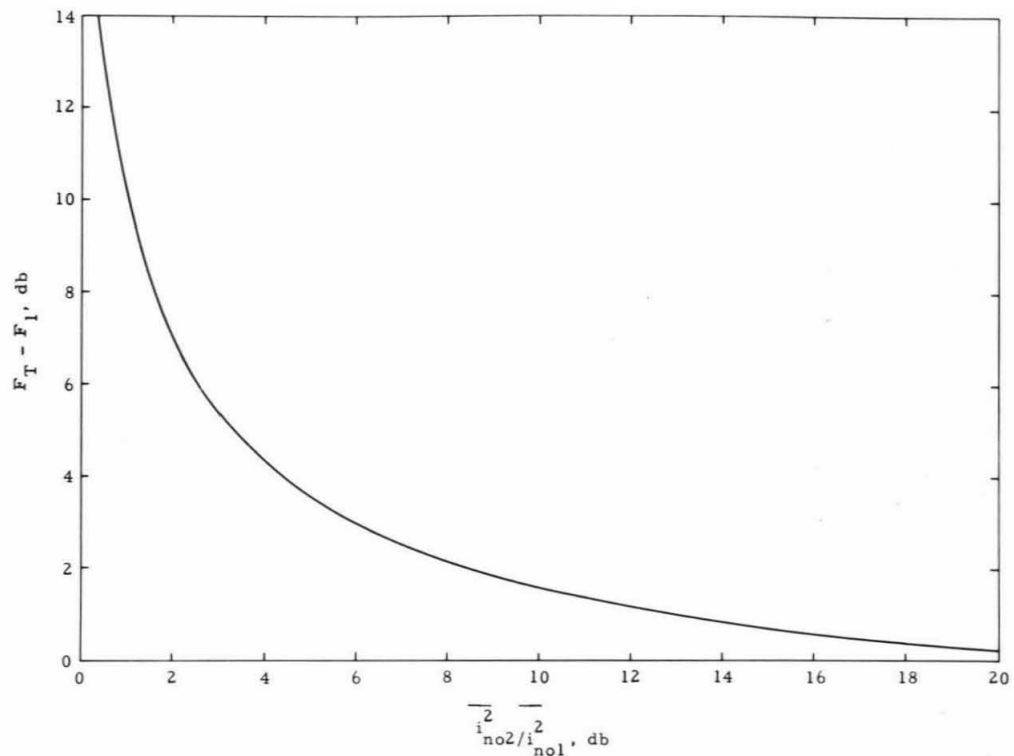


Figure 55. Error in Noise Factor Measurement as a Function of Output Noise Power Ratios.

given by

$$\bar{i_n^2} = \int_0^{\infty} |i_n(t)|^2 dt$$

the device must have an infinite time constant. Therefore, an error will be incurred since the actual integration is performed over a finite time interval. The probable error in a reading owing to the finite integration period is shown by van der Ziel (Ref. 32) to be

$$P. E. = \frac{1}{2(B\tau)^{1/2}} \%$$

Here, B is the noise bandwidth of i_n^2 and τ is the time constant of the indicator.

Applying the sampling theorem to van der Ziel's result, it is found that the probable error of the mean of M readings is given by

$$P.E. = \frac{1}{2(MB\tau)^{1/2}} \%$$

A numerical example will illustrate the difficulties encountered in obtaining accurate noise measurements when the noise is limited to very narrow bandwidths. If it is assumed that the noise bandwidth $B = 4$ cps and that the time constant of the indicating device is $\tau = 15$ seconds, the probable error in a reading is 11% or 0.4 db. To reduce the error to 0.1 db requires 25 readings or an integration time of 375 seconds.

CONCLUSIONS

Van der Ziel's transistor noise model formed the basis for the theoretical study conducted at mean and high frequencies. From this model, expressions for the noise factor of the transistor amplifier in each of its configurations were derived. An investigation of the noise-factor formulas reveals that in the unconstrained amplifier, i.e., one in which the source resistance is not a fixed parameter, two quantities are of importance in determining the noise performance of the amplifier. These are the magnitudes of the source resistance and the emitter current. Partial differentiation of the noise-factor equations with respect to these two parameters reveals that a unique value of source resistance, $(R_{so})_o$, and emitter current I_{EO} exist, which will minimize the effects of internally generated transistor noise. The formulas that describe these two quantities were found to be functions of easily measurable transistor parameters.

In applications where the value of source resistance is constrained, the noise-factor formulas can be differentiated directly to obtain an equation that describes the optimum emitter current.

At frequencies where $1/f$ noise predominates, it was found that a two generator empirical noise model would suffice to describe the amplifier's noise performance. Utilizing this model, an experimental procedure was derived for obtaining the optimization parameters $(R_{so})_o$ and I_{EO} . From an experimental study made to substantiate the procedure, it was found that the collector noise generator contained in the noise model was the predominant noise source at $1/f$ frequencies. Utilizing this fact, it was found that analytical expressions could be derived for $(R_{so})_o$ and I_{EO} .

These formulas are functions only of the extrinsic base resistance.

At frequencies approaching alpha cutoff, the noise-factor formulas exhibit an f^2 frequency dependence similar to that found to exist in vacuum tube amplifiers. However, the high-frequency noise cutoff point was observed to be a function of the source resistance. By decreasing the value of R_s , it was found possible to obtain reasonably low noise factors up to the alpha cutoff frequency.

In the constrained amplifier, it is sometimes possible to interpose a transformer between the driving source and the input to the amplifier. With this configuration, it was found possible to obtain reasonable noise figures from the transistor amplifier with values of source resistance exceeding 1,000,000 ohms. An investigation of the equations that pertain to the transformer-coupled amplifier revealed that a turns ratio existed which, for any given value of R_s , minimized the effects of internally generated transistor noise.

In a study conducted to determine the effect of temperature on the noise performance of a transistor amplifier, it was found

1. that at temperatures above 300°K the principal source of transistor noise is shot noise fluctuations in the collector cutoff current, I_{C0} . The mean-square magnitude of these fluctuations increases exponentially with temperature and noise produced by these fluctuations masks, at temperatures only a few degrees above room temperature, noise caused by diffusion and recombination-regeneration

2. that at liquid nitrogen temperature it becomes possible to obtain extremely low noise resistances in a transistor amplifier. This phenomenon, which is predicted by theory, introduces the possibility of utilizing a transistor amplifier in conjunction with a low impedance detector in

cryogenic infra-red applications. Also, the very low input impedance of the cryogenically-cooled transistor amplifier in conjunction with its low noise resistance makes it ideally suited as the R.F. stage of an ultra-sensitive radio receiver.

It has been shown that bias stabilization and emitter degeneration affect the optimum source resistance and the minimum noise factor of a transistor amplifier. In a theoretical study, using van der Ziel's model, analytical expressions were derived which give the degradation in noise performance and the change in source resistance caused by these stabilizing elements.

Previous investigations have concluded that, in the two-stage r-c coupled transistor amplifier, the value of the load resistance of the first stage should optimize the noise factor of the second stage. For typical applications, this value is a few thousand ohms. However, by differentiating the noise factor, F_{12} , of the two-stage amplifier with respect to the load resistance, it was found that F_{12} is a monotonically decreasing function of this parameter. Hence, for noise optimization, the load resistance should be as large as practicable.

It was found, in obtaining analytical expressions for the measurements required to attain noise factor readings, that the noise diode method would be the most convenient to be used. Here, F is a linear function of I_D , the d.c. diode current, and R_s , the source resistance. However, with low values of source resistance, this method becomes impractical owing to the large values of diode current required. In this case, it was found necessary to use either a continuous-wave or noise voltage.

Owing to the small power gains obtainable from cryogenically-cooled transistors, it was found necessary to derive a procedure that would permit

noise measurements when equipment noise was not negligible. The method derived gives the error incurred as a function of two r.m.s. readings.

APPENDIX

Friis defines the noise factor in terms of available signal-to-noise power ratios. By this definition, conjugate matching must be used at the input and output of an amplifier whenever noise factor measurements are made. However, this restriction does not apply to spot noise factor measurements.

Any linear noisy 4 pole can be represented as a noiseless 4 pole and two noise voltage generators which describe its noise properties. Such a representation is shown in figure 56a. Here, e_s signifies the input signal, e_{ns} signifies the noise generated in the driving source impedance z_s , and e_{n1} and e_{n2} represent the noise generated in the amplifier. If the mutual impedance z_{21} is not zero or infinite, then the two-generator noise model can be replaced by the one-generator model shown in figure 56b. The magnitude of e_{na} is given by

$$e_{na} = e_{n1} + \frac{e_{n2}(z_{11} + z_s)}{z_{21}} \quad (A-1)$$

The amplifier is noiseless beyond the points 1-1' (figure 56b); therefore the signal-to-noise ratio at the output is equal to that obtained at 1-1'. This ratio is not a function of the output termination.

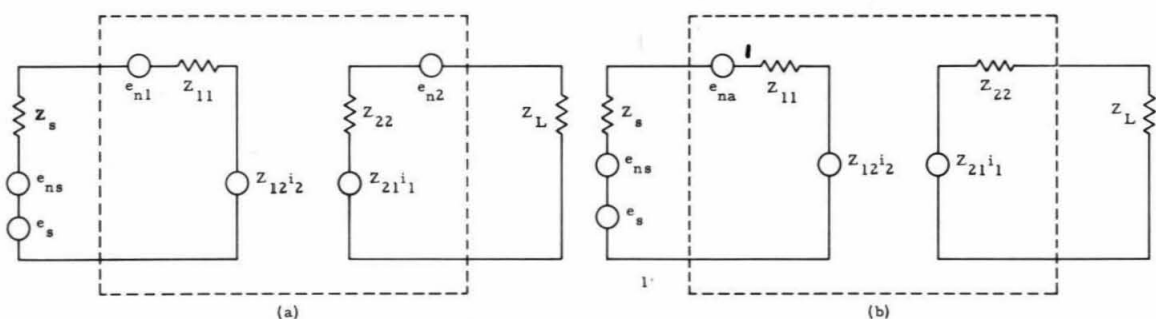


Figure 56. Z Parameter Noise Model, (b) Equivalent One Generator Noise Model.

With conjugate matching at the input, the signal-to-noise ratio at $1-1'$ is given by

$$(S/N) \Big|_{1-1'} = \frac{\frac{1}{4R_s} \int_0^{\infty} S_s(f) df}{\frac{1}{4R_s} \int_0^{\infty} [S_{ns}(f) + S_{na}(f)] df} \quad (A-2)$$

Here, $S_s(f)$, $S_{ns}(f)$, and $S_{na}(f)$ are the unit power spectral densities of the signal voltage, e_s , the source noise voltage, e_{ns} , and the amplifier noise voltage, e_{na} .

Without conjugate matching at the input,

$$(S/N) \Big|_{1-1'} = \frac{\int_0^{\infty} S_s(f) \frac{r_{11}}{|z_{11} + Z_s|^2} df}{\int_0^{\infty} (S_{ns}(f) + S_{na}(f)) \frac{r_{11}}{|z_{11} + Z_s|^2} df} \quad (A-3)$$

where r_{11} signifies the real part of z_{11} .

In order to obtain the same noise-factor measurement with and without conjugate matching, an equality must be established between equations A-2 and A-3. They become equal if B , the noise bandwidth of the measuring system, is much less than f_o , the frequency at which the measurements are made. This can be shown by writing r_{11} , z_{11} , and Z_s in a Taylor series about f_o . This gives

$$\begin{aligned} r_{11}(f) &= r_{11}(f_o) + r_{11}'(f_o)(f-f_o) + r_{11}''(f_o) \frac{(f-f_o)^2}{2!} \dots \\ z_{11}(f) &= z_{11}(f_o) + z_{11}'(f_o)(f-f_o) + z_{11}''(f_o) \frac{(f-f_o)^2}{2!} \dots \quad (A-4) \\ Z_s(f) &= Z_s(f_o) + Z_s'(f_o)(f-f_o) + Z_s''(f_o) \frac{(f-f_o)^2}{2!} \dots \end{aligned}$$

With spot noise-factor measurements, the frequency band is limited to the incremental range $f \pm df$. When these limits are placed on the integrals of equation A-3, the second and subsequent terms of the series can be neglected.* As a result, this equation can be written

$$\frac{\int_{f_o-df}^{f_o+df} S_s(f) df}{\int_{f_o-df}^{f_o+df} [S_{ns}(f) + S_{na}(f)] df} \quad (A-5)$$

If the same limits are placed on the integrals of equation A-2, it becomes identical to equation A-5. From this, it is concluded that the same noise-factor measurement is obtained with and without conjugate matching.

*Assuming no poles of $r_{11}(f)$, $z_{11}(f)$, and $Z_s(f)$ exist in the incremental frequency band $f_o \pm df$.

REFERENCES

1. van der Ziel, A., Proceedings of the I.R.E., vol. 46 (June, 1958), pp. 1019-1038.
2. Guggenbuehl, W., and Strutt, M. J. O., Proceedings of the I.R.E., vol. 45 (June, 1957), pp. 839-857.
3. Johnson, J. B., Physical Review, vol. 32 (July-December 1928), pp. 97-109.
4. Schottky, W., Annalen der Physik, vol. 57 (Sept. 1918-Jan. 1919), pp. 541-567.
5. Fonger, W. H., Transistors I, R.C.A. Laboratories, Princeton, N.J. (1956).
6. Yajimi, T., Journal of the Physical Society (Japan), vol. 11 (Oct. 1956), pp. 1126-1127.
7. North, D. O., R.C.A. Review, vol. 6 (Jan. 1942), pp. 332-344.
8. Friis, H. T., Proceedings of the I.R.E., vol. 32 (July, 1944), pp. 419-422.
9. Peterson, L. C., Proceedings of the I.R.E., vol. 35 (Nov. 1947), pp. 1264-1272.
10. Volkers, W. K. and Pedersen, N. E., Tele-Tech, vol. 14 (Dec. 1955), pp. 82-84, 156-158 and vol. 15 (Jan. 1956), p. 70.
11. Harris, E. J., et al, Telecommunications Research Establishment Report T2051.
12. Bunker, E. R., Aerojet Report 964.
13. Nielsen, E. C., Proceedings of the I.R.E., vol. 45 (July, 1957), pp. 957-963.
14. North, D. O. and Ferris, W. R., Proceedings of the I.R.E., vol. 29 (Jan. 1941), p. 49.
15. Talpey, T. E., Noise in Electron Devices, Smullin and Haus, eds., New York, John Wiley and Sons (1959).
16. Montgomery, H. C., Proceedings of the I.R.E., vol. 40 (Nov. 1952), pp. 1461-1471.
17. Nielsen, E.C., loc. cit.
18. Bess, L., Physical Review, vol. 91 (Sept. 1953), p. 1569.

19. du Pre, F. K., Physical Review, vol. 78 (June 1, 1950), p. 615.
20. McWhorter, A. L., Semiconductor Surface Physics, R. H. Kingston et al, eds., Philadelphia, University of Pennsylvania Press (1957).
21. North, D. O., "Theory of Noise in Diodes and Transistors." presented before the American Physical Society, Boulder, Colorado, (Sept. 1957).
22. van der Ziel, A., Physica, vol. 16 (April, 1950), pp. 359-372.
23. Baker, D., Journal of Applied Physics, vol. 25 (July, 1954), pp. 922-924.
24. Montgomery, H. C., Bell System Technical Journal, vol. 31 (Sept. 1952), pp. 950-975.
25. Rollin, R. V. and Templeton, I. M., Proceedings of the Physical Review, vol. B70 (March, 1957), pp. 331-332.
26. McWhorter, A. L., loc. cit.
27. North, D. O., loc. cit.
28. Petritz, R. L., Semiconductor Surface Physics, R. H. Kingston et al, eds., Philadelphia, University of Pennsylvania Press (1957), p. 226.
29. Nielsen, E. C., loc. cit.
30. Hurtig, C., Handbook of Semiconductor Electronics, L. P. Hunter, ed., New York, McGraw-Hill (1956).
31. Middlebrook, R. D., Semiconductor Products, vol. 7 (July-Aug. 1958), pp. 14-20.
32. van der Ziel, A., Noise, Englewood Cliffs, Prentice Hill Inc., (1954).